

Radiative Processes in Astrophysics

Observation

Up to cosmic size scale

C/2012S1
(comet)

Jupiter
(planet)

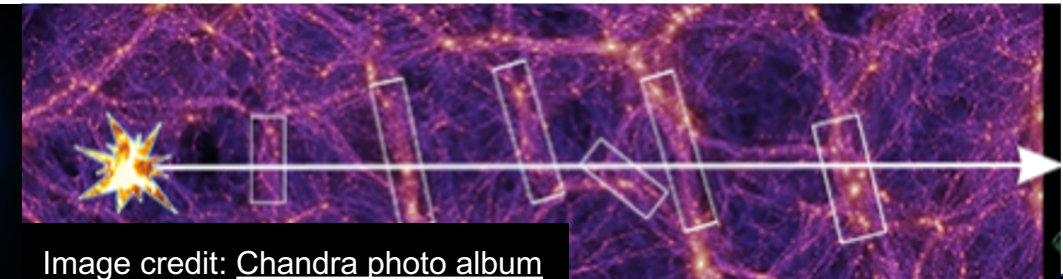
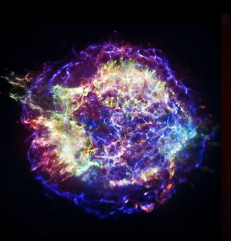
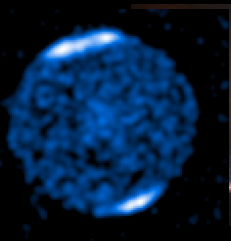
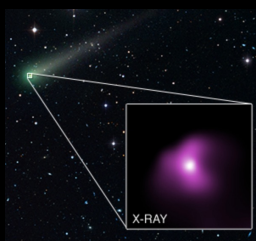
Sun
(star)

Cas A
(SNR)

M82
(galaxy)

Phoenix
(gal. cluster)

Cosmic web filament

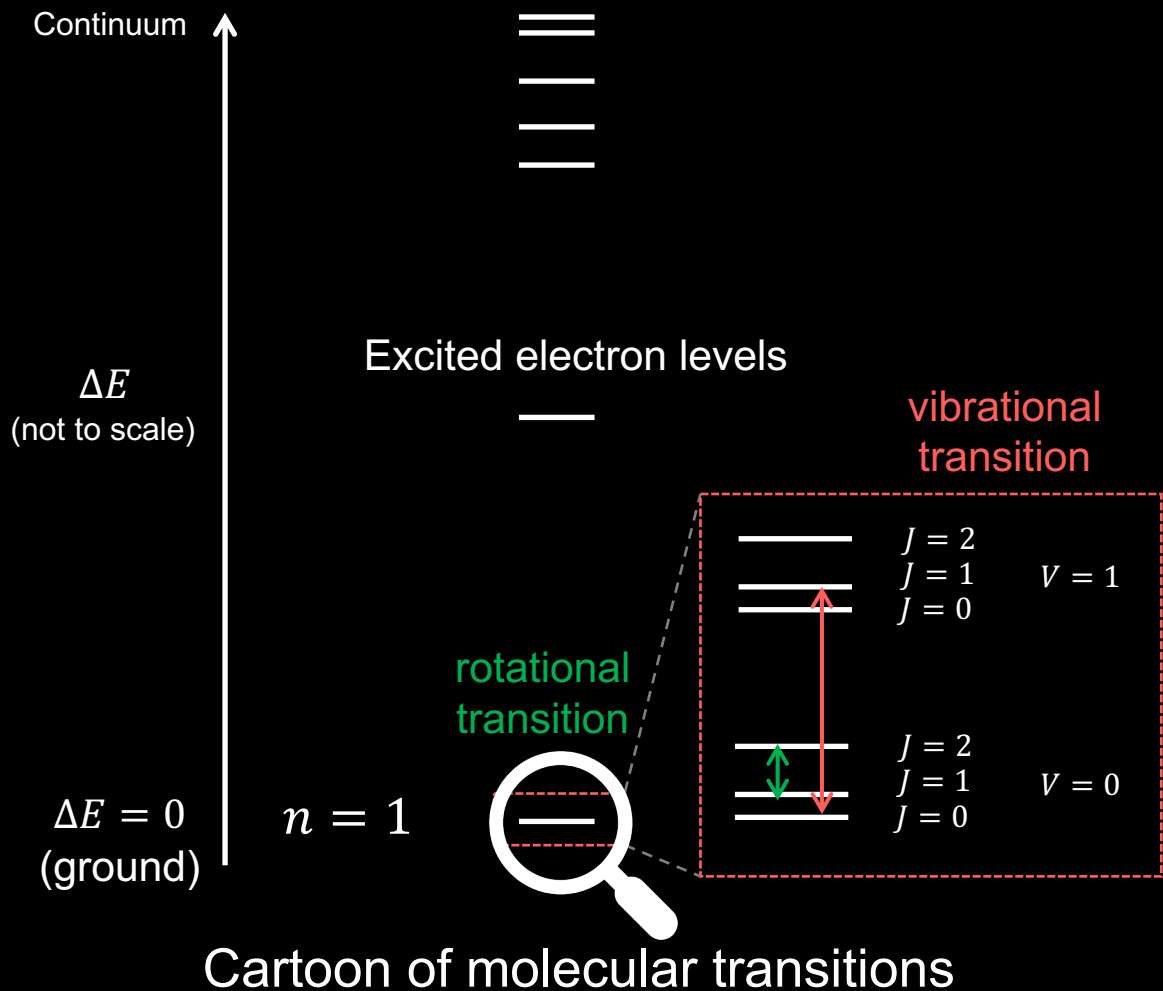


Chpt.6 Molecular and dust processes

Image credit: Junjie Mao

- 6.1 Molecular processes
- 6.1 The molecular Universe
- 6.1.1 Molecular structure
- 6.1.2 Molecular transitions
- 6.1.3 Chemical reactions
- 6.1.4 More about astrochemistry/ astrobiology

6.2 Dust processes



The molecular Universe

The essential subject of matter of **astrochemistry** is the formation, destruction, and excitation of molecules in astronomical environments and their influence on the structure, dynamics, and evolution of astronomical objects.

— Dalgarno (2008)

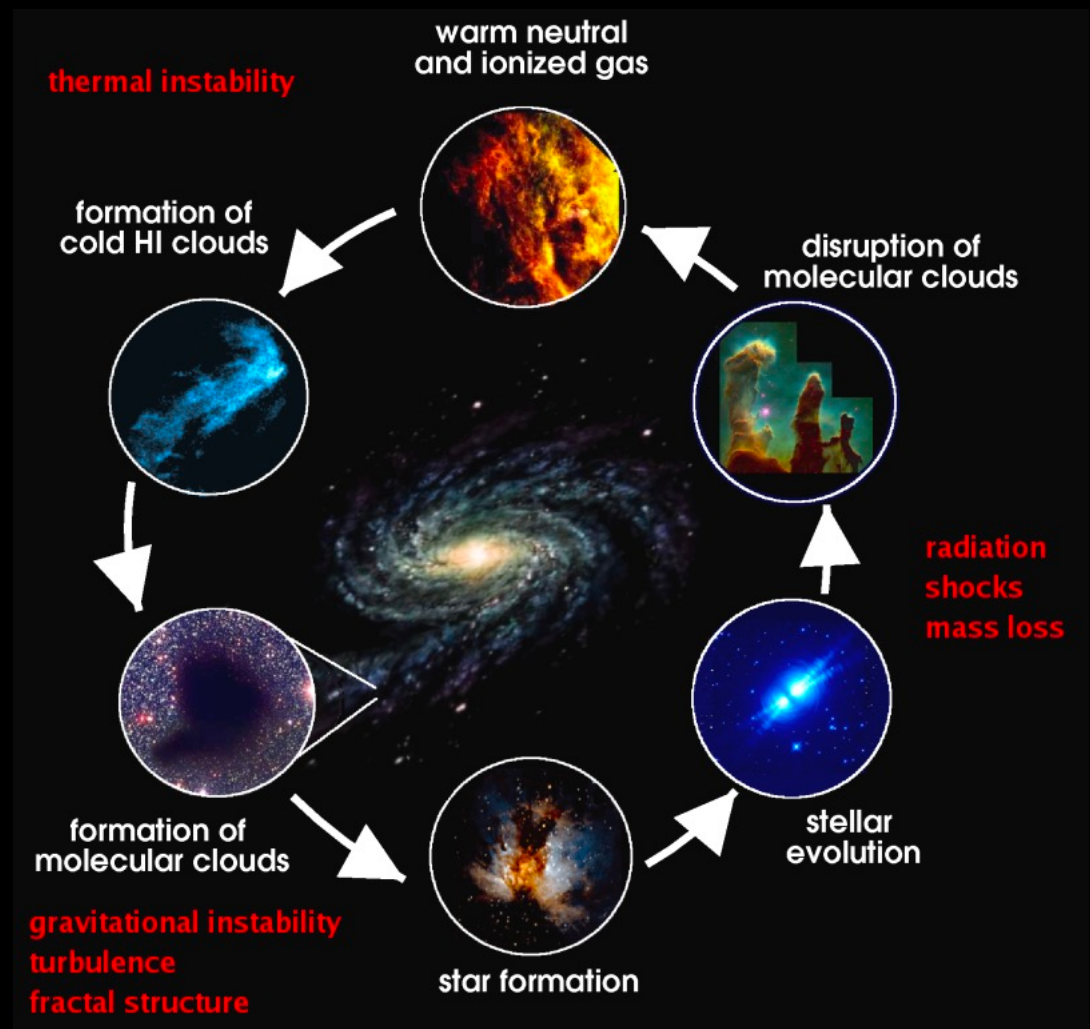


Image credit: Steward Observatory
Radio Astronomy Laboratory

Molecules in comet

Bieler et al. 2015

Comet 67P/C-G

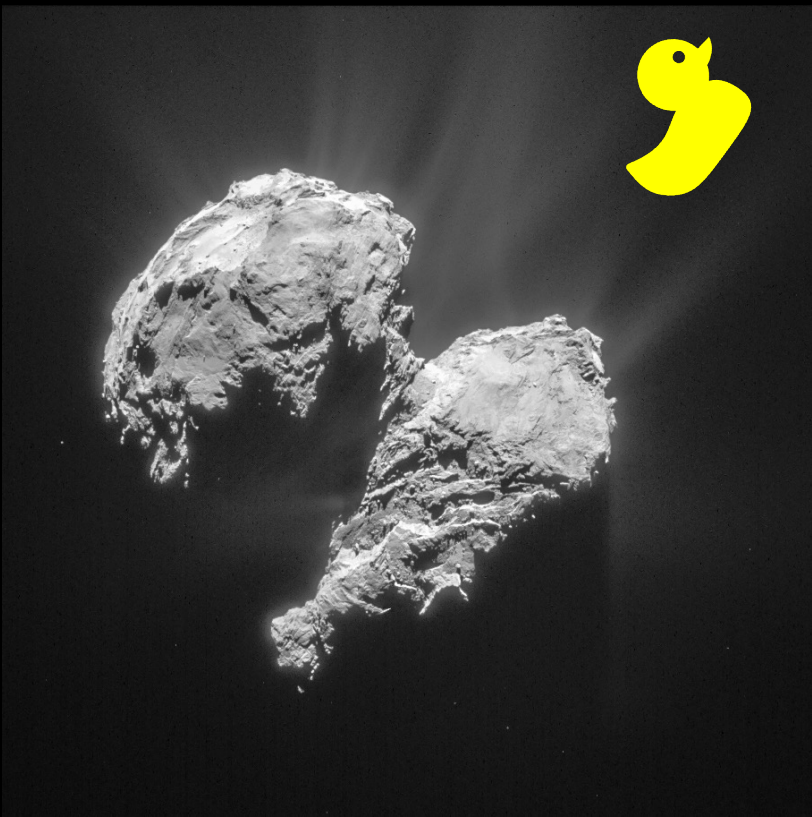
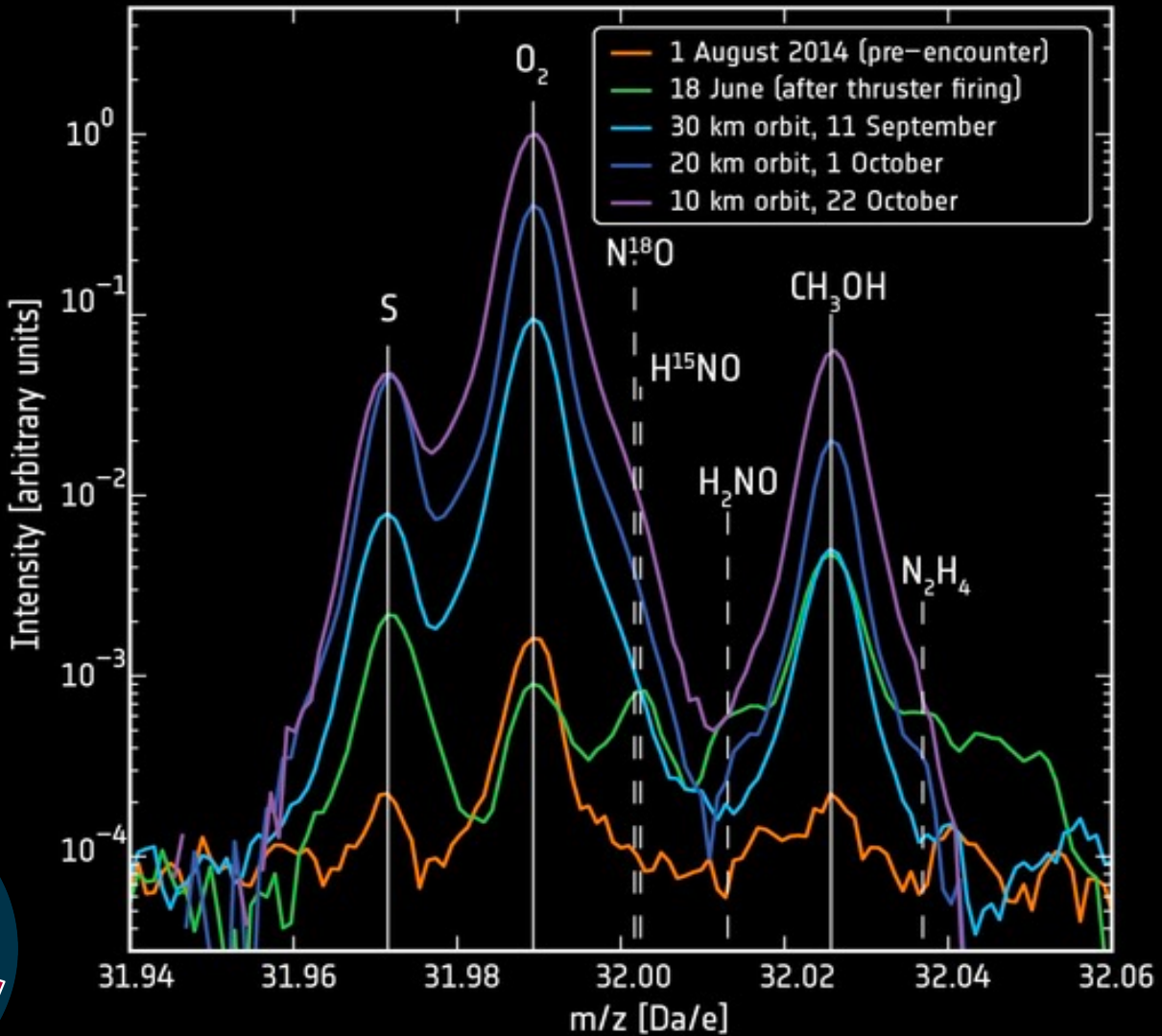


Image credit: ESA/Rosetta/NAVCAM



m/z: mass-to-charge, 1 Da = 1 atomic mass unit

Molecules in exoplanets (emission)

EXOPLANET VHS 1256 b EMISSION SPECTRUM

NIRSpec and MIRI | IFU Medium-Resolution Spectroscopy

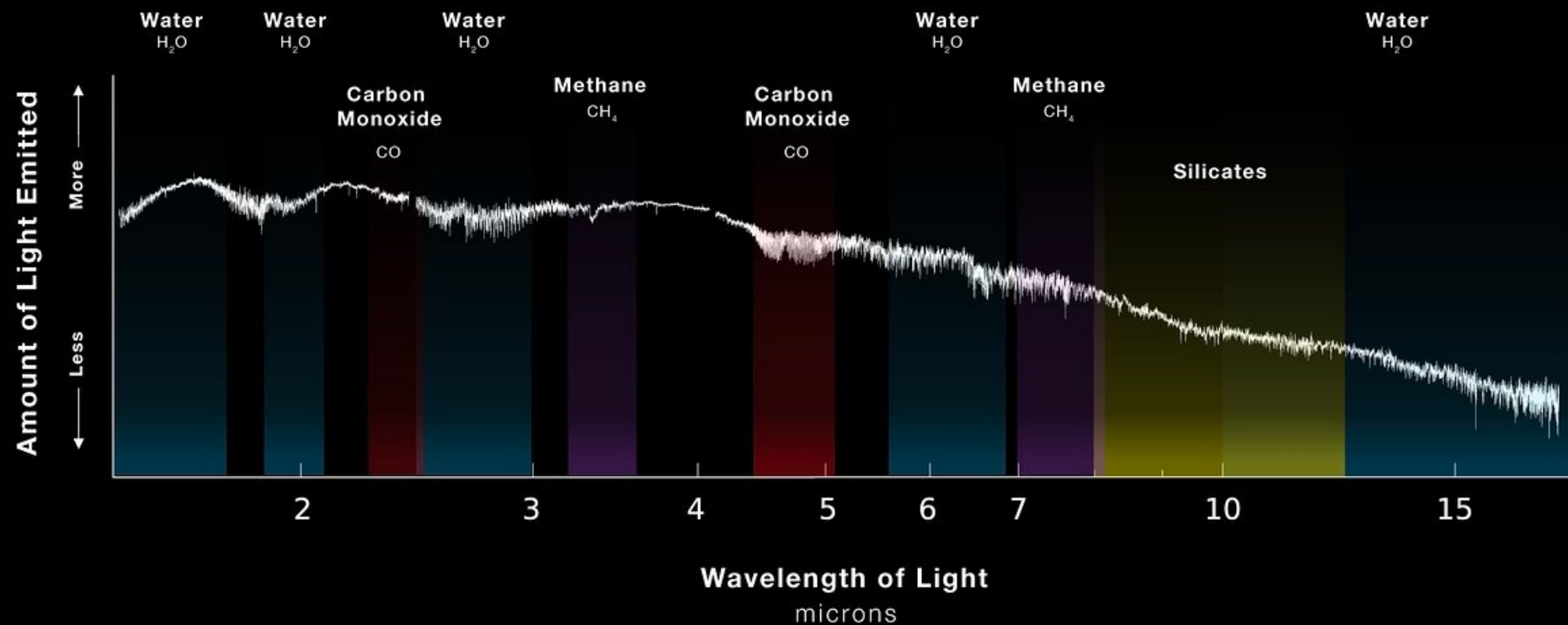
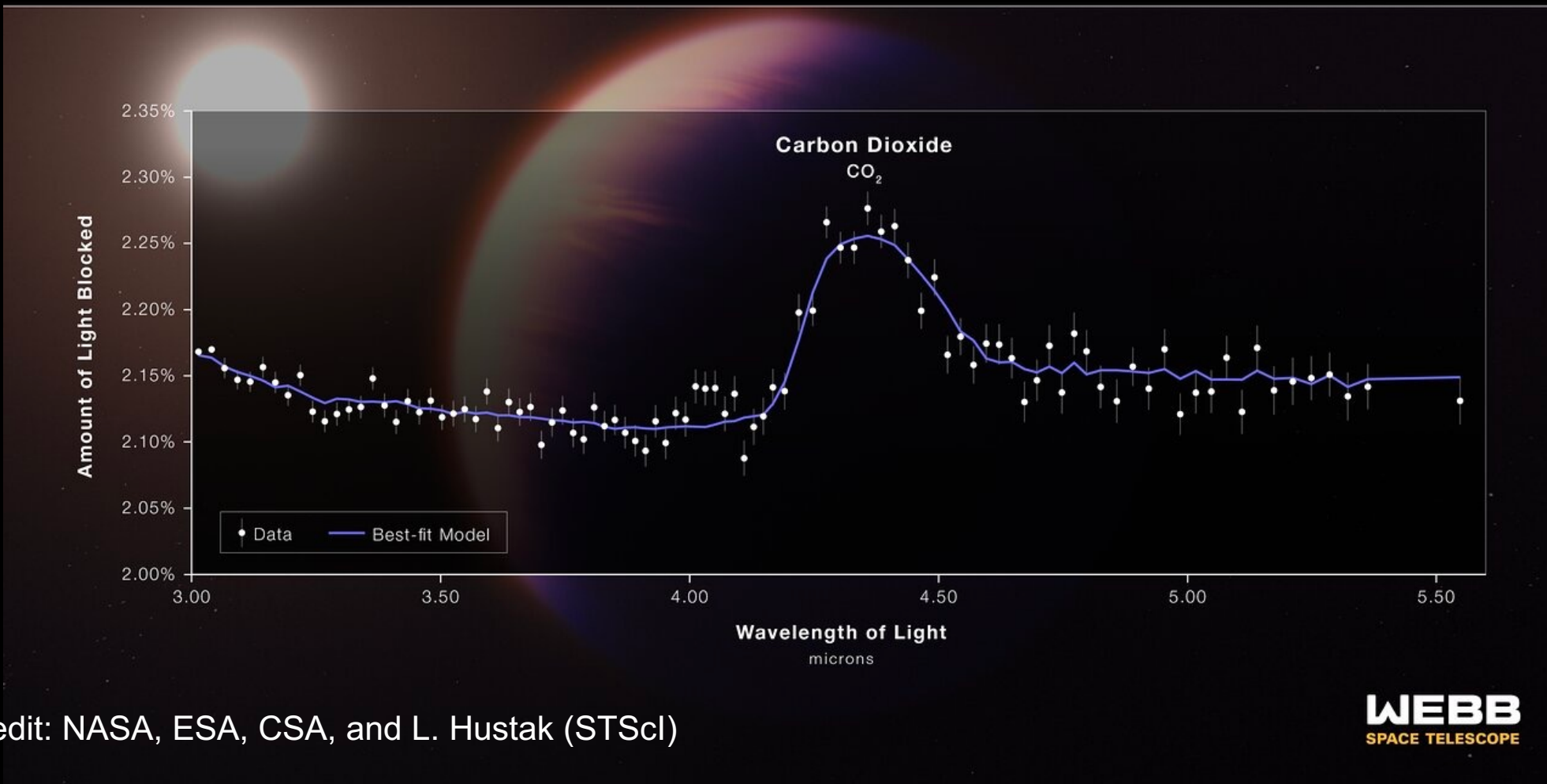


Image credit: NASA, ESA, CSA, J. Olmsted (STScI), B. Miles (University of Arizona), S. Hinkley (University of Exeter), B. Biller (University of Edinburgh), A. Skemer (University of California, Santa Cruz)

Molecules in exoplanets (absorption)

HOT GAS GIANT EXOPLANET WASP-39 b ATMOSPHERE COMPOSITION

NIRSpec | Bright Object Time-Series Spectroscopy



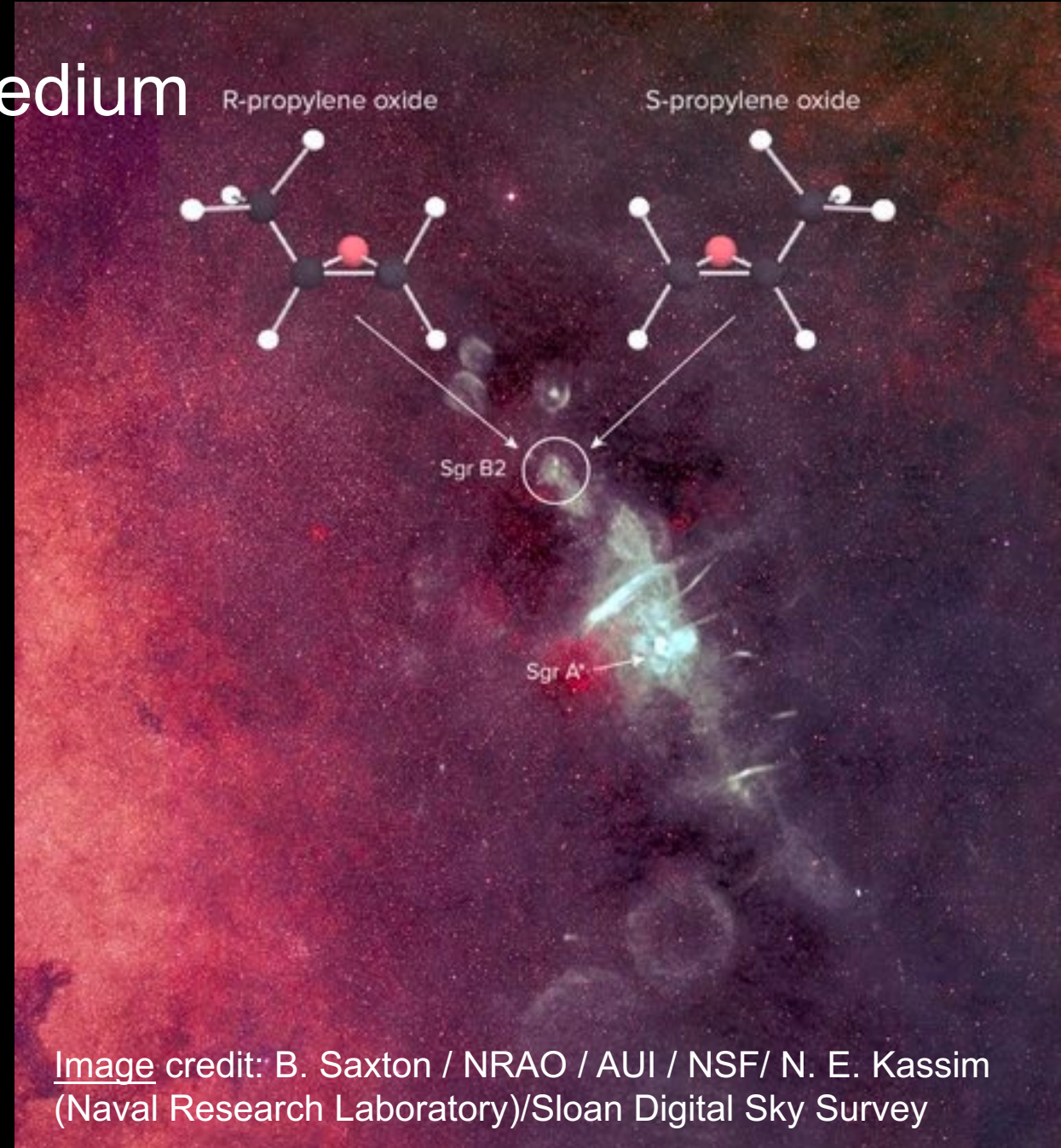
Chiral molecules in interstellar medium

Life on Earth relies on chiral molecules. Each living species uses only one handedness of many types of chiral molecules.

The first astronomical detection of a chiral molecule, propylene oxide $\text{CH}_3\text{CHCH}_2\text{O}$, was found in absorption toward the Galactic centre ([McGuire et al. 2015](#))

- ❖ S: sinister configuration
- ❖ R: rectus configuration

Need polarization measurement to constrain the left/right ratio.



Aromatic molecules in interstellar medium

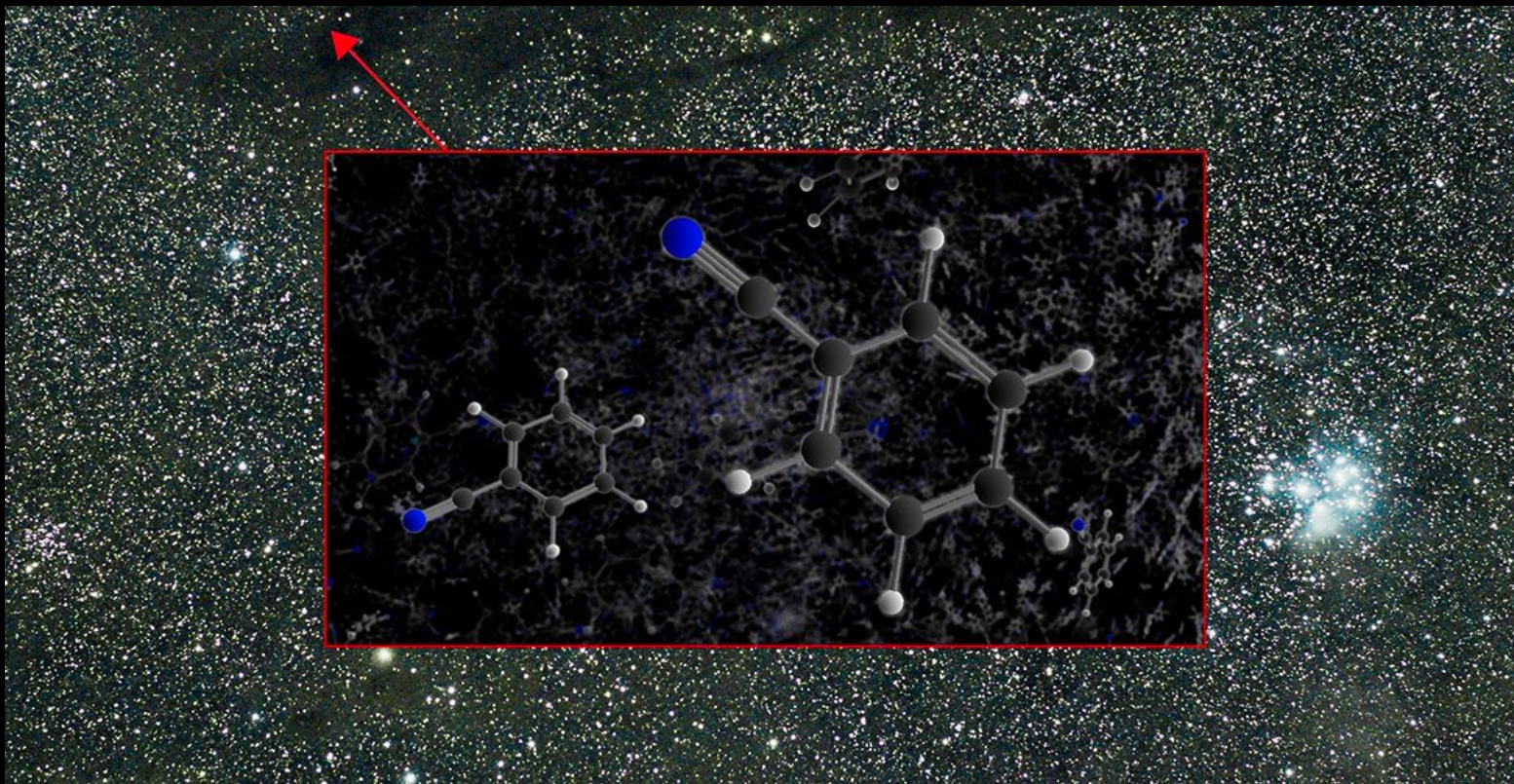


Image credit: B. McGuire, B. Saxton (NRAO/AUI/NSF)

McGuire et al. 2018:
Discovery of the first
aromatic molecule
(benzonitrile) in the ISM.

Benzonitrile $C_6H_5(CN)$ is an
aromatic organic.

Aromatic molecules have a stable structure.

- Three of the twenty amino acids forming protein are aromatic molecules.
- All five of the nucleotides forming DNA and RNA sequences are aromatic molecules.

Buckminsterfullerene in interstellar medium

Kroto et al. 1985 predicted to find long-chain carbon molecules like buckminsterfullerene in interstellar space and circumstellar shells.

Cami et al. 2010 detected C₆₀ and C₇₀ in a young planetary nebula Tc 1

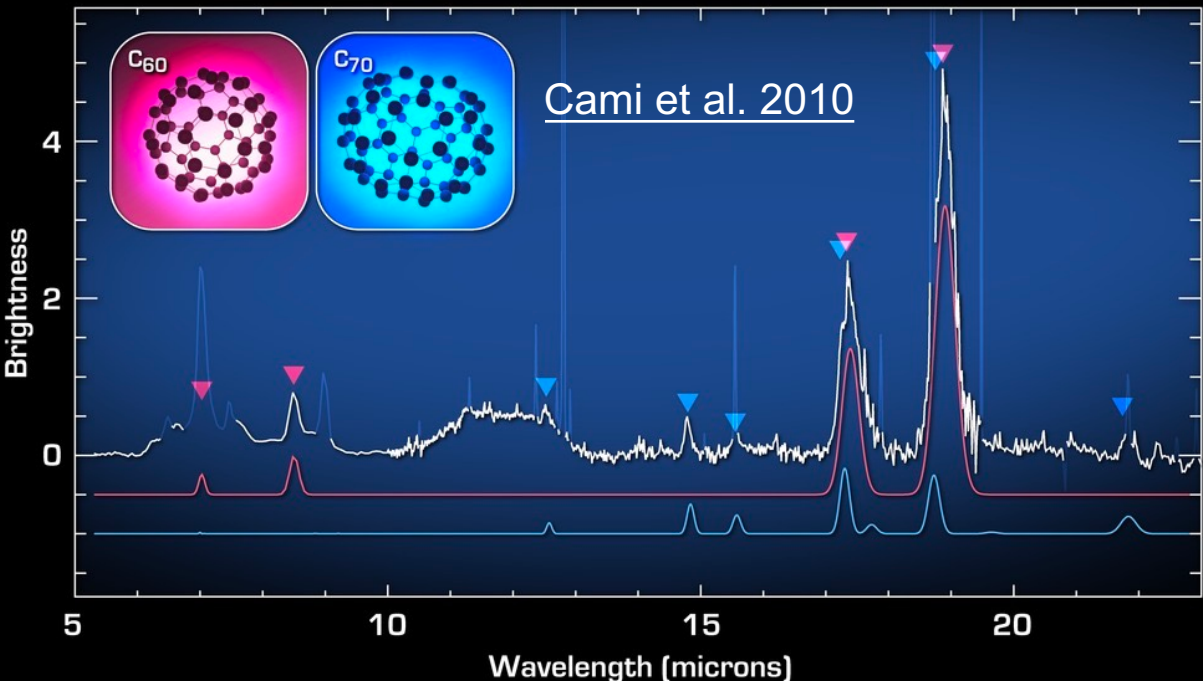


Image credit: NASA/JPL-Caltech/J. Cami (Univ. of Western Ontario/SETI Institute)

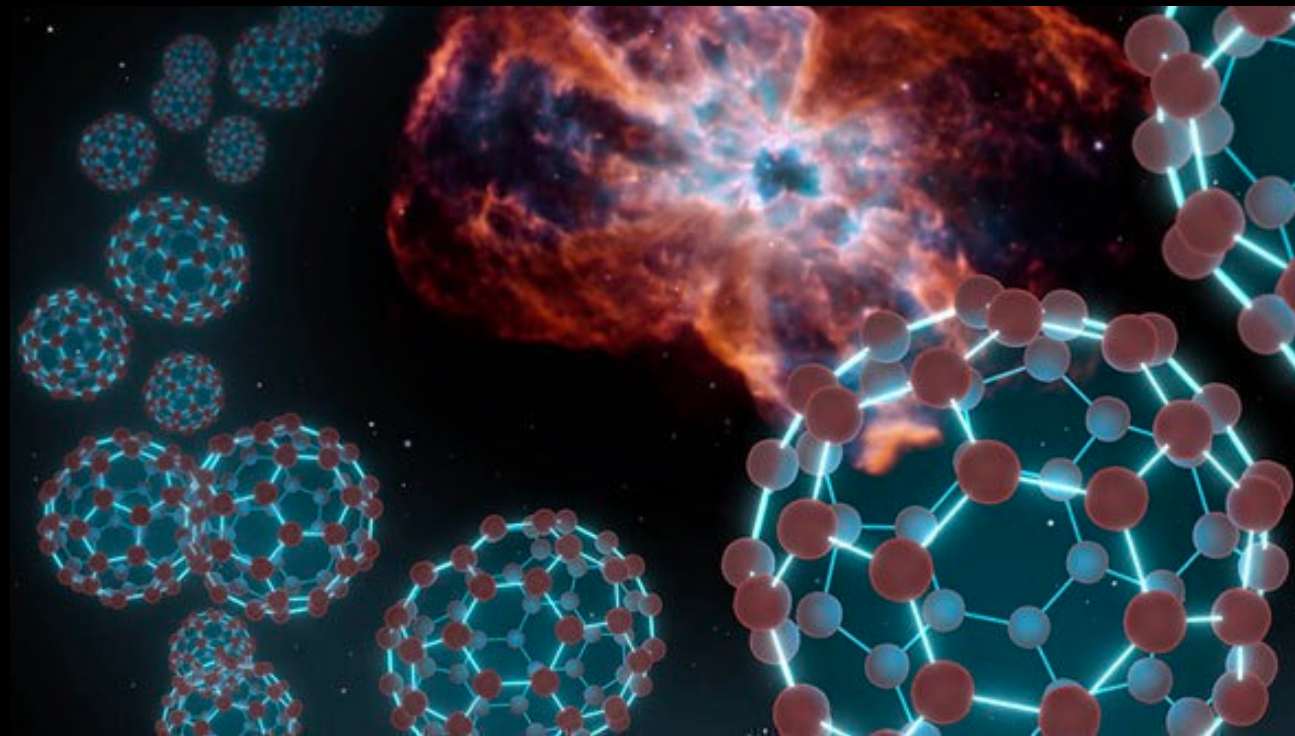


Image credit: NASA/JPL-Caltech/T. Pyle (SSC)

First noble molecule in interstellar medium

Barlow et al. 2013

Crab nebula ([Herschel](#) + HST view)

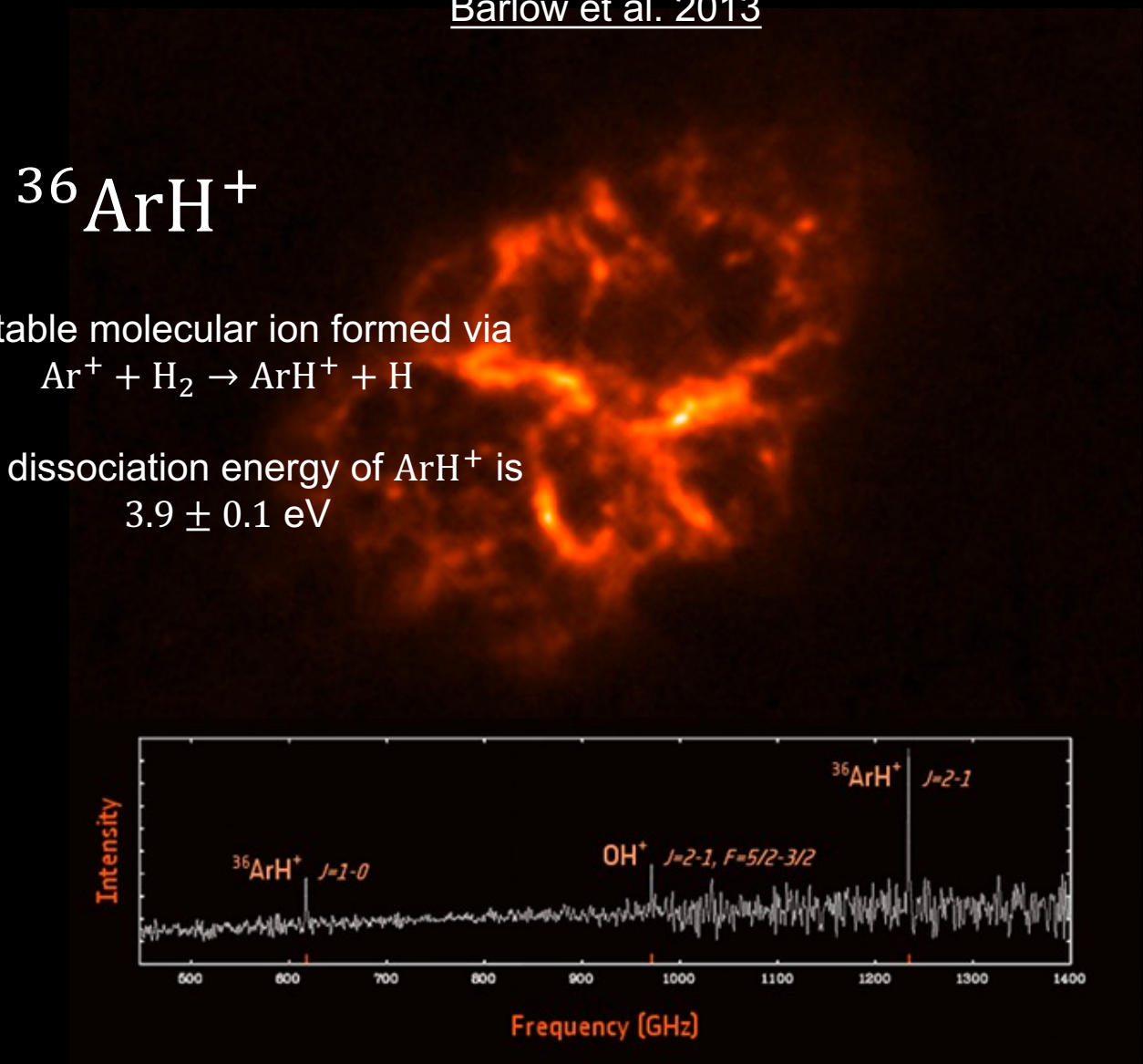
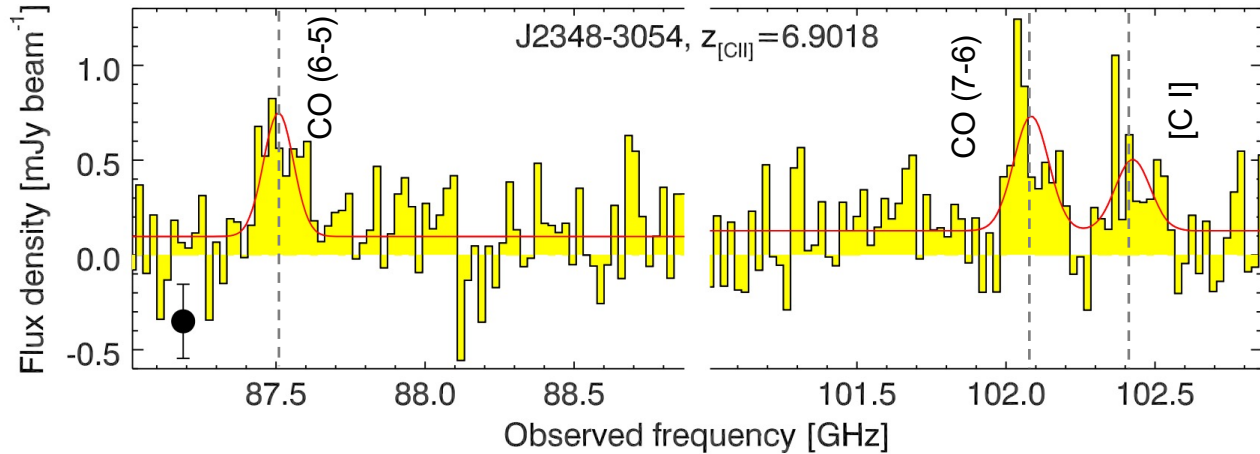


Image credit: ESA/Herschel/PACS/MESS Key Programme Supernova Remnant Team; NASA, ESA and Allison Loll/Jeff Hester (Arizona State University)

Molecules in distant galaxies

(lensed) dusty star-forming galaxies

Venemans et al. 2017

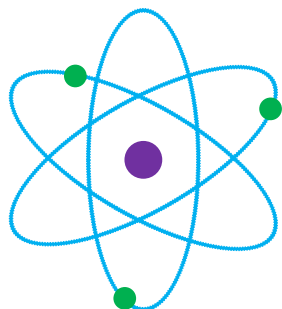


Source	z	T_{dust} (K)	Lines
Secure Redshifts			
SPT0103-45	3.0917(3)^a	33.3 ± 2.5	CO(3-2) & CO(4-3)
SPT0113-46	4.2328(5)	31.8 ± 3.1	CO(4-3), CI(1-0) & CO(5-4)
SPT0125-47	2.51480(7)	40.7 ± 4.2	CO(3-2)
SPT0243-49	5.699(1)	30.1 ± 4.9	CO(5-4) & CO(6-5)
SPT0345-47	4.2958(2)	52.1 ± 7.8	CO(4-3) & CO(5-4)
SPT0346-52	5.6559(4)	52.9 ± 5.3	CO(5-4), CO(6-5), H ₂ O & H ₂ O ⁺
SPT0418-47	4.2248(7)	52.9 ± 7.5	CO(4-3) & CO(5-4)
SPT0441-46	4.4771(6)	39.3 ± 3.9	CI(1-0) & CO(5-4)
SPT0452-50	2.0104(2)	20.9 ± 1.8	CO(3-2)
SPT0459-59	4.7993(5)	36.0 ± 3.7	CI(1-0) & CO(5-4)
SPT0529-54	3.3689(1)	31.9 ± 2.4	CO(4-3), CI(1-0) & ¹³ CO(4-3)
SPT0532-50	3.3988(1)	35.1 ± 3.0	CO(4-3), CI(1-0) & ¹³ CO(4-3)
SPT0551-50	2.1232(2)	26.3 ± 2.0	CO(3-2)
SPT2103-60	4.4357(6)	38.6 ± 3.5	CO(4-3) & CO(5-4)
SPT2132-58	4.7677(2)	37.8 ± 4.5	CO(5-4)
SPT2134-50	2.7799(2)	40.5 ± 4.6	CO(3-2)
SPT2146-55	4.5672(2)	38.7 ± 5.1	CI(1-0) & CO(5-4)
SPT2147-50	3.7602(3)	41.8 ± 4.1	CO(4-3) & CI(1-0)
SPT0538-50	2.783	31.2 ± 7.1	CO(7-6), CO(8-7), Si IV 1400 Å
SPT2332-53	2.738	32.9 ± 3.6	CO(7-6), Ly α , C IV 1549 Å

Weï et al. 2013

cf. atomic and molecular structures

- ❑ Simple symmetries of atom (e.g., complete rotational symmetry about the nucleus) are not valid for molecules → fewer quantum numbers to describe the molecular states
 - ✓ For diatomic molecules (e.g., H₂, CO), there is still a rotational symmetry about a line



- ✓ Rotation and/or vibration transitions (not occur in atoms) are much simpler than atomic transitions

Born-Oppenheimer approximation

The mass ratio of electrons to nuclei in molecule is typically $\sim 10^{-(4-5)}$
Electrons are much faster, thus have higher energies

Electron energy

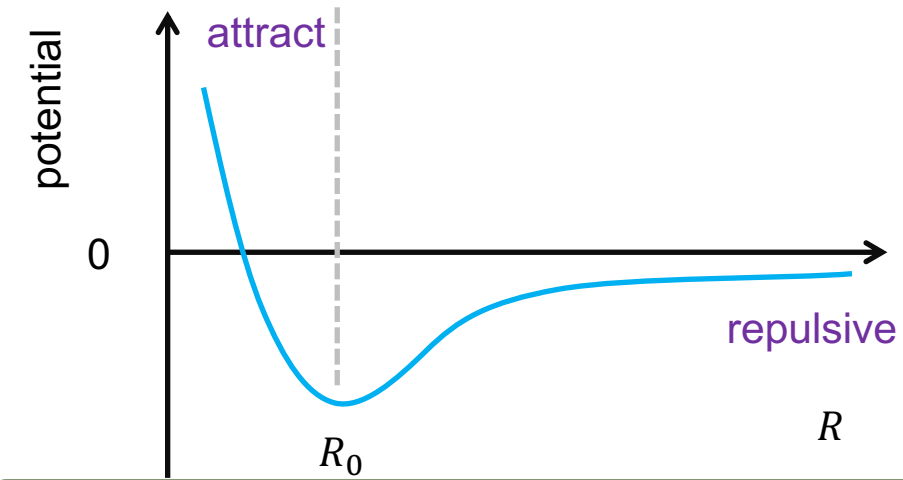
$$p_e \sim \frac{h}{2\pi a} \quad \text{molecular size, typically } \sim 10^{-8} \text{ cm}$$

$$E_e \sim \frac{(h/2\pi)^2}{m_e a^2}$$

$$\frac{E_e}{\text{eV}} \sim 7.62 \left(\frac{a}{10^{-8} \text{ cm}} \right)^{-2}$$

Sect. 11.1 of the REF book (p294-295) by Rybicki & Lightman

For stable molecules, the internuclear potential has a minimum at some point (R_0). Vibrations about the minimum can occur



Vibration energy

$$\frac{1}{2} M \omega^2 a^2 \sim \frac{(h/2\pi)^2}{2 m_e a^2}$$

vibration frequency

$$E_{\text{vib}} \sim h\nu \sim \left(\frac{m_e}{M} \right)^{\frac{1}{2}} E_e$$

Born-Oppenheimer approximation (cont.)

The nuclei in molecule can also rotate about each other. Assuming the angular momentum is $J\hbar$ ($J = 0, 1, 2, \dots$),

Rotation energy

$$E_{\text{rot}} \sim \frac{\hbar^2 J(J+1)}{2I} \sim \frac{\hbar^2 J(J+1)}{2 M a^2} \sim J(J+1) \frac{m_e}{M} E_e$$

momentum of inertia of
the molecule $\sim Ma^2$

Sect. 11.1 of the REF book (p294-295) by Rybicki & Lightman

prev. sl.

$$E_e \sim \frac{(h/2\pi)^2}{m_e a^2}$$

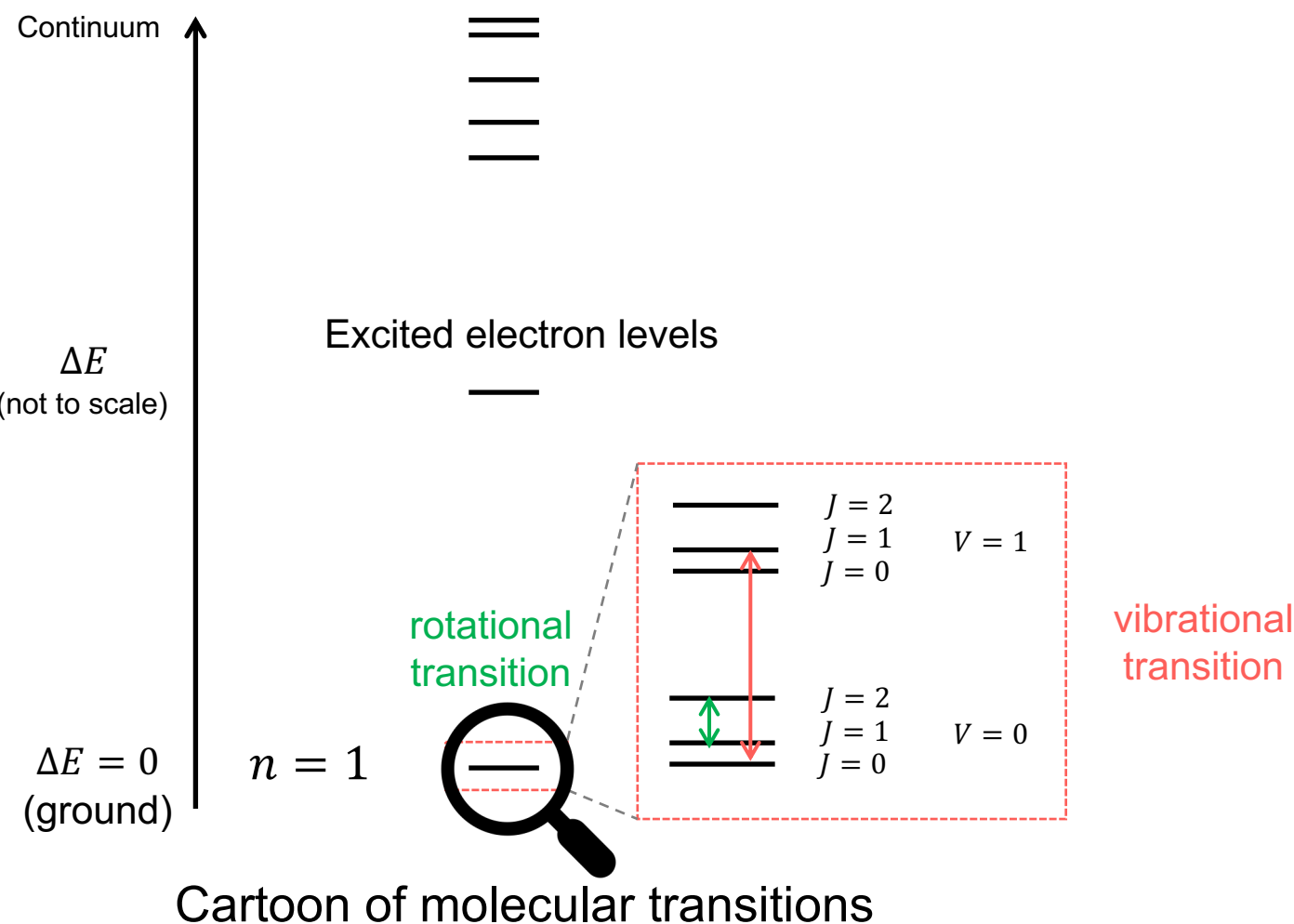
$$E_{\text{vib}} \sim \left(\frac{m_e}{M}\right)^{\frac{1}{2}} E_e$$

$$E_e : E_{\text{vib}} : E_{\text{rot}} \sim 1 : \sqrt{\frac{m_e}{M}} : \frac{m_e}{M}$$

Total energy

$$E = E_e + E_{\text{vib}} + E_{\text{rot}}$$

Rotation and vibration transitions



prev. sl.

$$E_e : E_{\text{vib}} : E_{\text{rot}} \sim 1 : \sqrt{\frac{m_e}{M}} : \frac{m_e}{M}$$

prev. sl.

$$\frac{E_e}{\text{eV}} \sim 7.62 \left(\frac{a}{10^{-8} \text{ cm}} \right)^{-2}$$

$$\frac{m_e}{M} \sim 3 \times 10^{-6} \text{ to } 5 \times 10^{-4}$$

$$\frac{\lambda}{\mu\text{m}} = 1.2398 \left(\frac{\text{eV}}{E} \right)$$

- vibration transitions:**
 - IR band
- rotation transitions:**
 - FIR and radio bands

Molecular transitions

Line	Reference
H I 21 cm	Ewen & Purcell 1951 Muller & Oort 1951
OH 18 cm	Weinreb et al. 1963
NH ₃ 1 cm	Cheung et al. 1968
H ₂ 1013 – 1108 Å	Carruthers 1970
CO 2.6 mm	Wilson et al. 1970

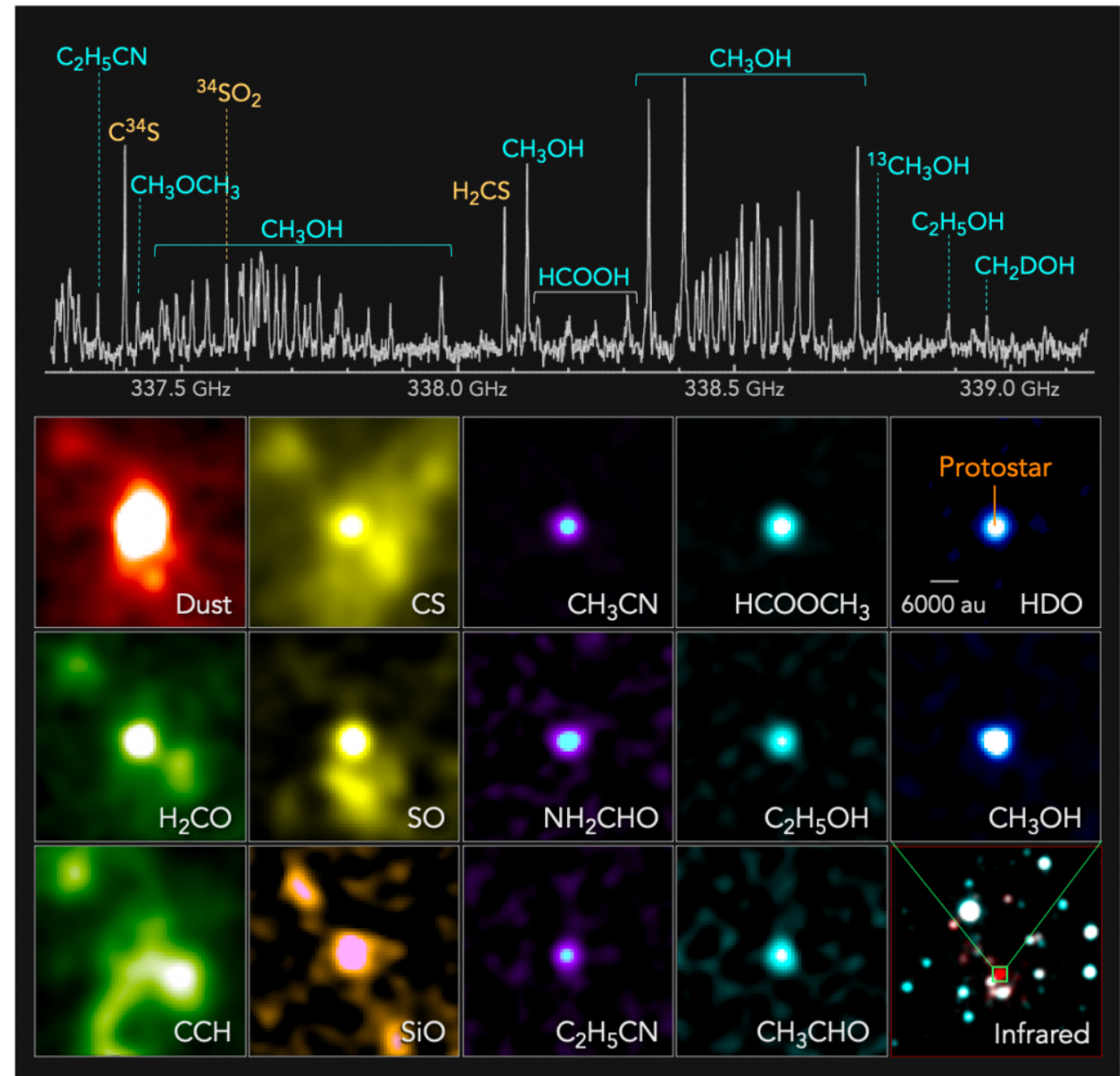
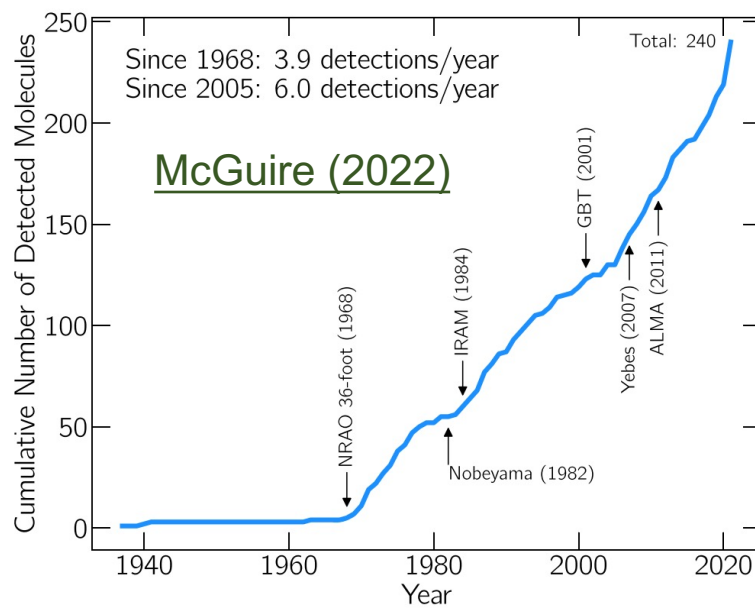
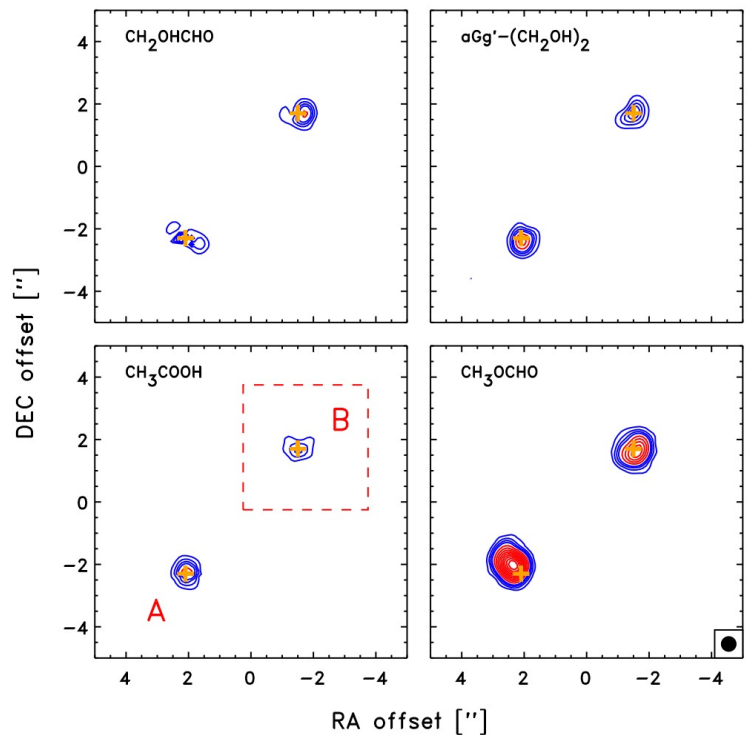
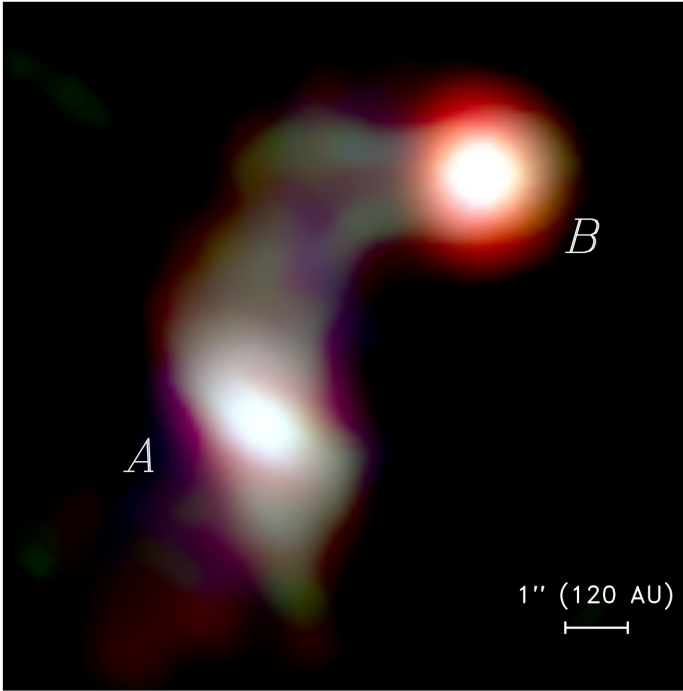


Image credit: ALMA (ESO/NAOJ/NRAO), T. Shimonishi (Niigata University)

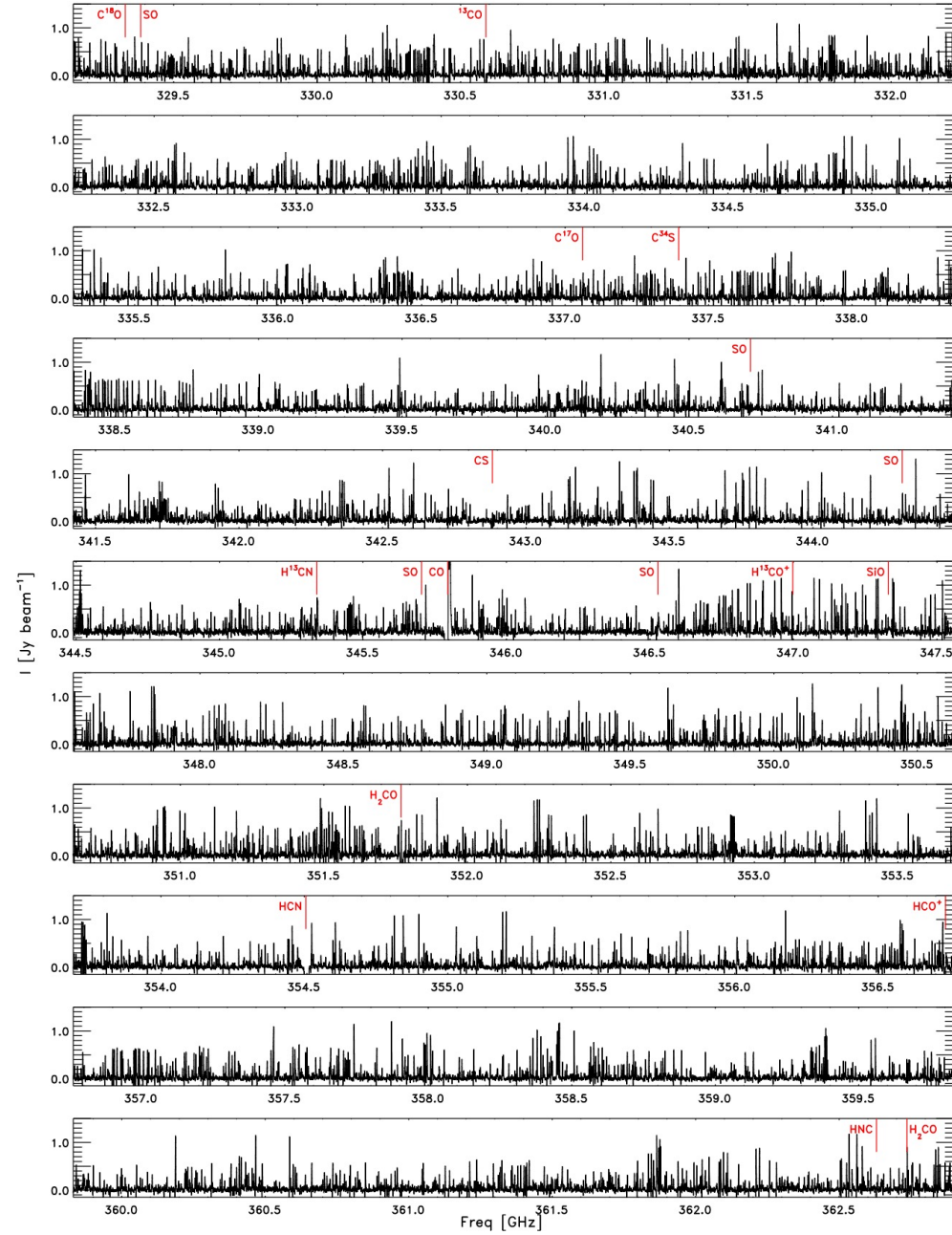
Molecular spectra



ALMA image of protostellar binary
IRAS 16293-2422

> 10^4 molecular transitions (lines), i.e.
approximately 1 line per 3 km/s

Jørgensen et al. 2016



Molecular transition database

<https://cdms.astro.uni-koeln.de/cdms/portal/>

CDMS

Cologne Database for Molecular Spectroscopy

HOME GENERAL CATALOG TOOLS CONTACT HELP

FILTER SPECIES LIST

Use regular expressions

include JPL data

Tag
e.g. 18501

Molecule
Hill notation, e.g. ${}^{\mathrm{A}}\mathrm{H}_3\mathrm{N}^{\mathrm{+}}$

Trivial Name
e.g. Ammonia

Isotopolog
Stoichiom. formula, e.g. ${}^{\mathrm{A}}\mathrm{CH}_3\mathrm{OH}$

State
e.g. $v=0$

SPECIES ISOTOPLOGS MOLECULES

Tag	Molecule	Isotopolog	State	
3501	H ₂	HD	$v=0,1$	doc
12501	C	C	3P Ground state	doc
13501	C	C-13	3P Ground state	doc
14501	CH ₂	CH ₂	$v=0$	doc
15501	HN	NH	$v=0$	doc
16501	H ₂ N	NH ₂	$v=0$	doc
16502	HN	ND	$v=0$	doc
18501	H ₃ N	NH ₂ D	$v=0$	doc
19501	H ₃ N	NHD ₂	$v=0$	doc
20501	H ₃ N	ND ₃	$v=0$	doc
24501	HNa	NaH	$v=0$	doc
25502	H _{Mg}	MgH	$v=0$	doc

HYDROGEN MOLECULE

HD
 $v=0,1$

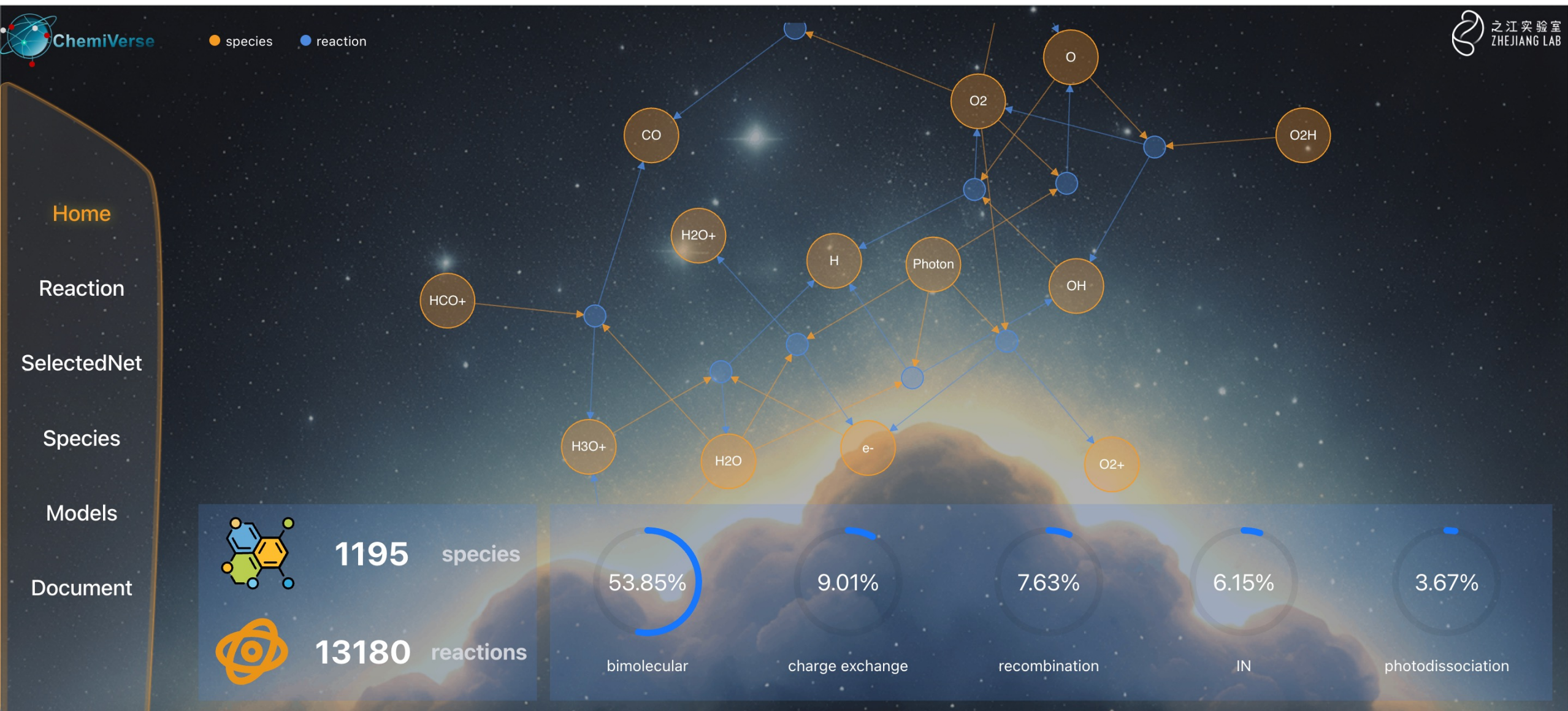
Tag: 3501
Version: 2*
Date of Entry: 2011-12-01
Contributor: H. S. P. Müller

https://spec.jpl.nasa.gov/

Molecular Spectroscopy
Jet Propulsion Laboratory
California Institute of Technology

ChemiVerse

<https://chemiverse.zero2x.org/>

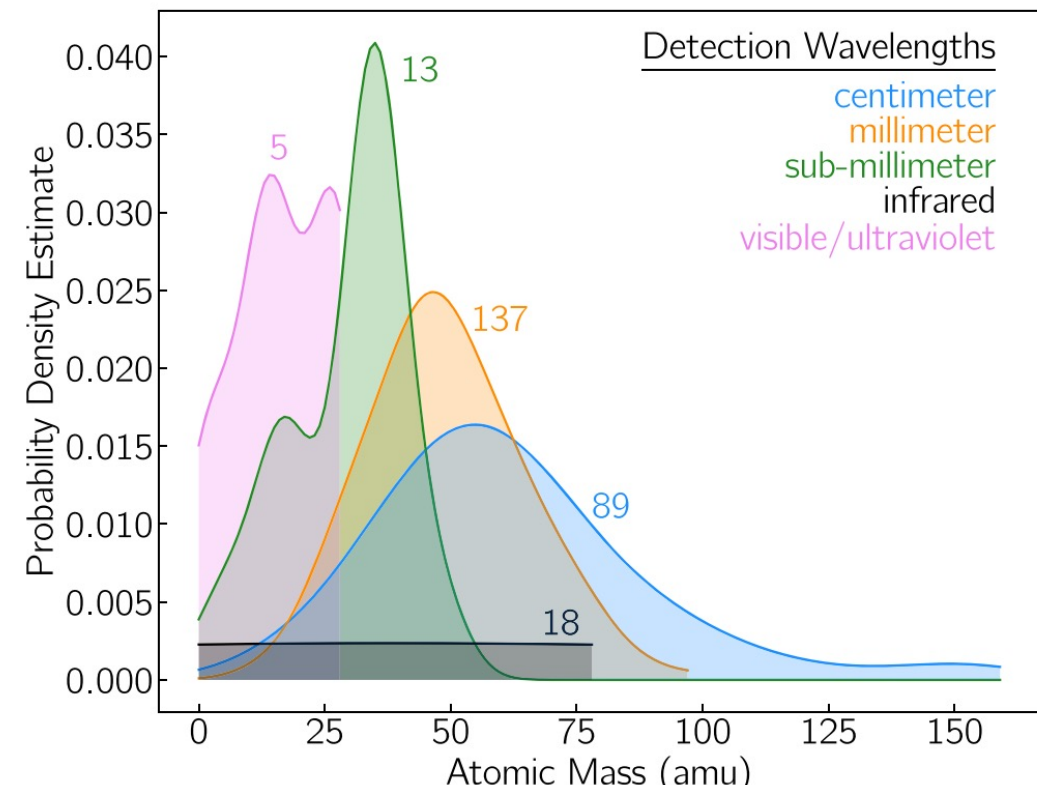


Molecular species found in space

2 Atoms		3 Atoms		4 Atoms		5 Atoms		6 Atoms		7 Atoms	
CH	NH	H ₂ O	MgCN	NH ₃	SiC ₃	HC ₃ N	C ₄ H ⁻	CH ₃ OH	CH ₃ CHO		
CN	SiN	HCO ⁺	H ₃ ⁺	H ₂ CO	CH ₃	HCOOH	CNCHO	CH ₃ CN	CH ₃ CCH		
CH ⁺	SO ⁺	HCN	SiCN	HNCO	C ₃ N ⁻	CH ₂ NH	HNCNH	NH ₂ CHO	CH ₃ NH ₂		
OH	CO ⁺	OCS	AINC	H ₂ CS	PH ₃	NH ₂ CN	CH ₃ O	CH ₃ SH	CH ₂ CHCN		
CO	HF	HNC	SiNC	C ₂ H ₂	HCNO	H ₂ CCO	NH ₃ D ⁺	C ₂ H ₄	HC ₅ N		
H ₂	N ₂	H ₂ S	HCP	C ₃ N	HOCN	C ₄ H	H ₂ NCO ⁺	C ₅ H	C ₆ H		
SiO	CF ⁺	N ₂ H ⁺	CCP	HNCS	HSCN	SiH ₄	NCCNH ⁺	CH ₃ NC	c-C ₂ H ₄ O		
CS	PO	C ₂ H	AlOH	HOCO ⁺	HOOH	c-C ₃ H ₂	CH ₃ Cl	HC ₂ CHO	CH ₂ CHOH		
SO	O ₂	SO ₂	H ₂ O ⁺	C ₃ O	I-C ₃ H ⁺	CH ₂ CN	MgC ₃ N	H ₂ C ₄	C ₆ H ⁻		
SiS	AlO	HCO	H ₂ Cl ⁺	I-C ₃ H	HMgNC	C ₅	HC ₃ O ⁺	C ₅ S	CH ₃ NCO		
NS	CN ⁻	HNO	KCN	HCN ⁺	HCCO	SiC ₄	NH ₂ OH	HC ₃ NH ⁺	HC ₅ O		
C ₂	OH ⁺	HCS ⁺	FeCN	H ₃ O ⁺	CNCN	H ₂ CCC	HC ₃ S ⁺	C ₅ N	HOCH ₂ CN		
NO	SH ⁺	HOC ⁺	HO ₂	C ₃ S	HONO	CH ₄	H ₂ CCS	HC ₄ H	HC ₄ NC		
HCl	HCl ⁺	SiC ₂	TiO ₂	c-C ₃ H	MgCCH	HCCNC	C ₄ S	HC ₄ N	H ₃ HNH		
NaCl	SH	C ₂ S	CCN	HC ₂ N	HCCS	HNCCC	CHOSH	c-H ₂ C ₃ O	c-C ₃ HCC ₃		
AlCl	TiO	C ₃	SiCSi	H ₂ CN		H ₂ COH ⁺		CH ₂ CNH			
KCl	ArH ⁺	CO ₂	S ₂ H					C ₅ N ⁻			
AIF	NS ⁺	CH ₂	HCS					HNCHCN			
PN	HeH ⁺	C ₂ O	HSC					SiH ₃ CN			
SiC	VO	MgNC	NCO					MgC ₄ H			
CP		NH ₂	CaNC					CH ₃ CO ⁺			
		NaCN	NCS					H ₂ CCCS			
		N ₂ O						CH ₂ CCH			

8 Atoms	9 Atoms	10 Atoms	11 Atoms	12 Atoms	13 Atoms	PAHs	Fullerenes
HCOOCH ₃	CH ₃ OCH ₃	CH ₃ COCH ₃	HC ₉ N	C ₆ H ₆	C ₆ H ₅ CN	1-C ₁₀ H ₇ CN	C ₆₀
CH ₃ C ₃ N	CH ₃ CH ₂ OH	HOCH ₂ CH ₂ OH	CH ₃ C ₆ H	n-C ₃ H ₇ CN	HC ₁₁ N	2-C ₁₀ H ₇ CN	C ₆₀ ⁺
C ₇ H	CH ₃ CH ₂ CN	CH ₃ CH ₂ CHO	C ₂ H ₅ OCHO	i-C ₃ H ₇ CN		C ₉ H ₈	C ₇₀
CH ₃ COOH	HC ₇ N	CH ₃ C ₅ N	CH ₃ COOCH ₃	1-C ₅ H ₅ CN			
H ₂ C ₆	CH ₃ C ₄ H	CH ₃ CHCH ₂ O	CH ₃ COCH ₂ OH	2-C ₅ H ₅ CN			
CH ₂ OHCHO	C ₈ H	CH ₃ CH ₂ OH	C ₅ H ₆				
HC ₆ H	CH ₃ CONH ₂						
CH ₂ CHCHO	C ₈ H ⁻						
CH ₂ CCHCN	CH ₂ CHCH ₃						
NH ₂ CH ₂ CN	CH ₃ CH ₂ SH						
CH ₃ CHNH	HC ₇ O						
CH ₃ SiH ₃	CH ₃ NHCHO						
NH ₂ CONH ₂	H ₂ CCCCCCH						
HCCCC ₂ CN	HCCCCCHCN						
CH ₂ CHCCH	H ₂ CCHC ₃ N						

241 species (as of 2021) detected in the radio, IR, optical, and UV bands



McGuire (2022)

Complex organic molecules in space

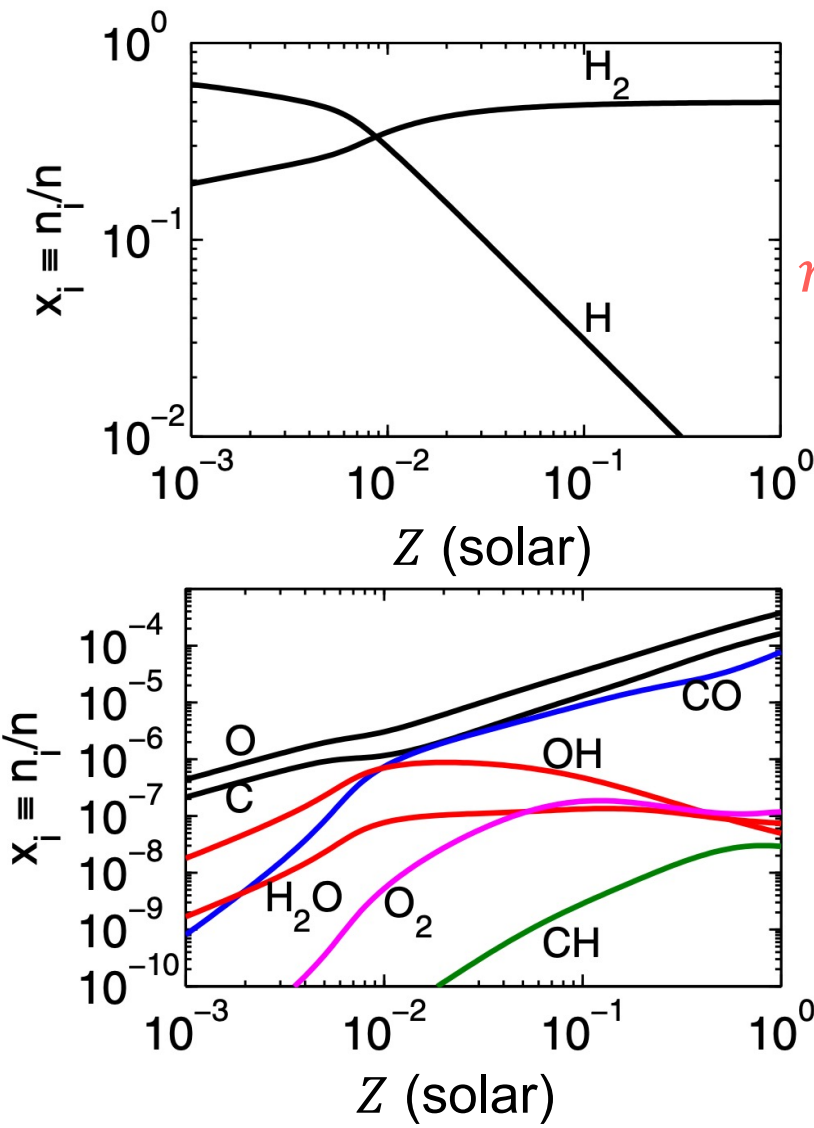
Species	Name
Hydrocarbons	
C ₂ H ₄	Ethene
HC ₄ H	Butadiyne
H ₂ C ₄	Butatrienylidene
C ₅ H	Pentadiynyl
CH ₃ C ₂ H	Propyne
C ₆ H	Hexatriynyl
C ₆ H ⁻	Hexatriynyl ion
H ₂ C ₆	Hexapentaenylidene
HC ₆ H	Triacetylene
C ₇ H	Heptatriynyl
CH ₃ C ₄ H	Methyldiacetylene
CH ₃ CHCH ₂	Propylene
C ₈ H	Octatetraynyl
C ₈ H ⁻	Octatetraynyl ion
CH ₃ C ₆ H	Methyltriacetylene
C ₆ H ₆	Benzene

Species	Name
O-Containing	
CH ₃ OH	Methanol
HC ₂ CHO	Propynal
c-C ₃ H ₂ O	Cyclopropenone
CH ₃ CHO	Acetaldehyde
C ₂ H ₃ OH	Vinyl alcohol
c-CH ₂ OCH ₂	Ethylene oxide
HCOOCH ₃	Methyl formate
CH ₃ COOH	Acetic acid
HOCH ₂ CHO	Glycolaldehyde
C ₂ H ₃ CHO	Propenal
C ₂ H ₅ OH	Ethanol
CH ₃ OCH ₃	Methyl ether
CH ₃ COCH ₃	Acetone
HOCH ₂ CH ₂ OH	Ethylene glycol
C ₂ H ₅ CHO	Propanal
HCOOC ₂ H ₅	Ethyl formate

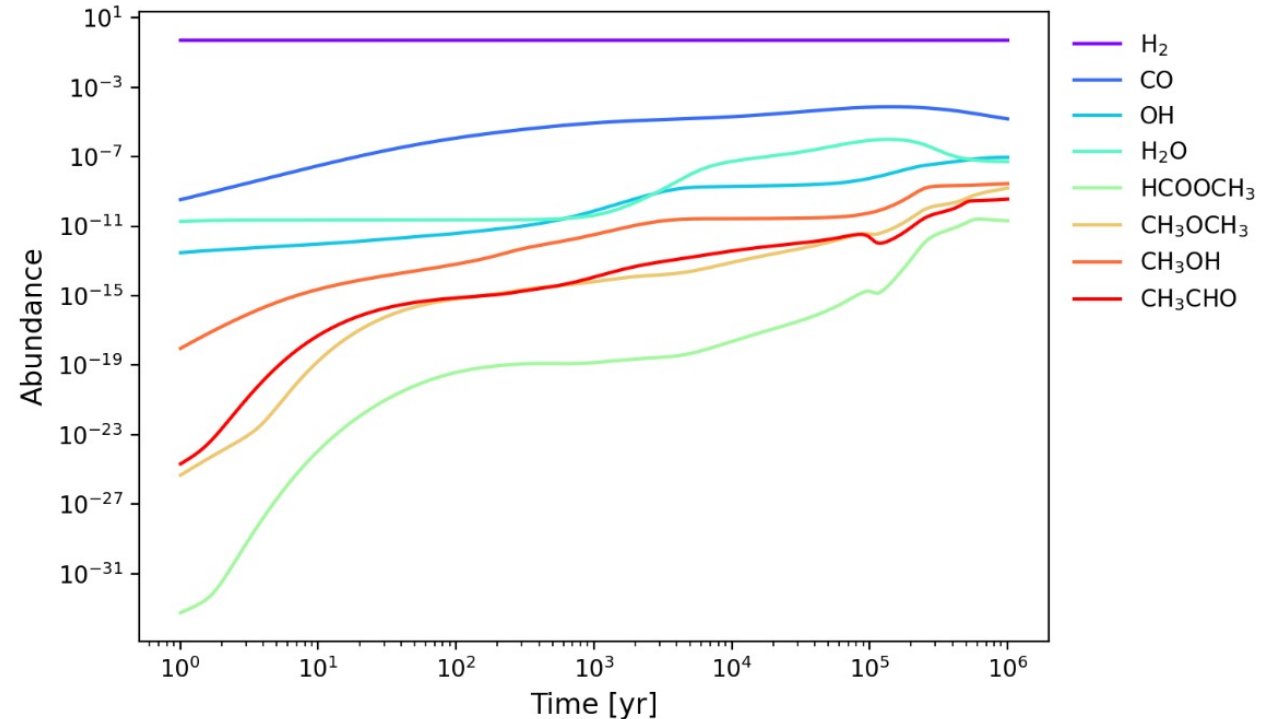
Species	Name
N-Containing	
CH ₃ CN	Acetonitrile
CH ₃ NC	Methylisocyanide
CH ₂ CNH	Keteneimine
HC ₃ NH ⁺	Prot. cyanoacetylene
C ₅ N	Cyanobutadiynyl
HC ₄ N	Cyanopropynylidene
CH ₃ NH ₂	Methylamine
C ₂ H ₃ CN	Vinylcyanide
HC ₅ N	Cyanodiacylene
CH ₃ C ₃ N	Methylcyanoacetylene
CH ₂ CCHCN	Cyanoallene
NH ₂ CH ₂ CN	Aminoacetonitrile
HC ₇ N	Cyanotriacylene
C ₂ H ₅ CN	Propionitrile
CH ₃ C ₅ N	Methylcyanodiacetylene
HC ₉ N	Cyanotetraacylene
C ₃ H ₇ CN	N-propyl cyanide
HC ₁₁ N	Cyanopentaacylene
S-Containing	
CH ₃ SH	Methyl mercaptan
N,O-Containing	
NH ₂ CHO	Formamide
CH ₃ CONH ₂	Acetamide

Herbst & van Dishoeck (2009)

Molecular abundance (rule of thumb)



$$x_i = \frac{n_i}{n}$$
$$n = n_H + 2 n_{H_2}$$



Molecular abundances as a function of metallicity ([Bialy & Sternberg \(2015\)](#)) and a function of time ([Westlake model](#))

Chemical reactions

Formation of bonds

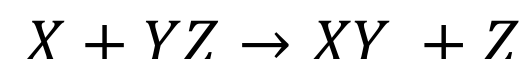
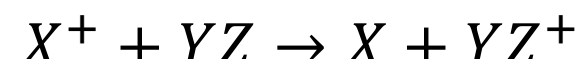
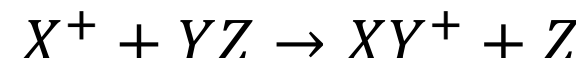
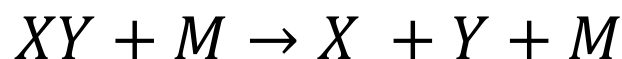
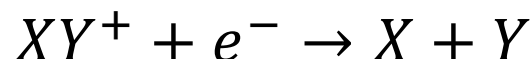
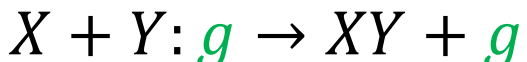
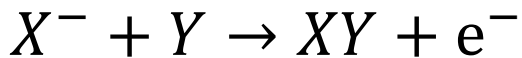
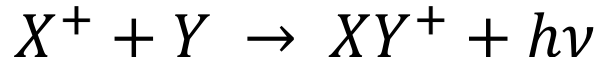
- Radiative association
- Associative detachment
- Grain surface

Destruction of bonds

- Photo-dissociation
- Dissociative recombination
- Collisional dissociation

Rearrangement of bonds

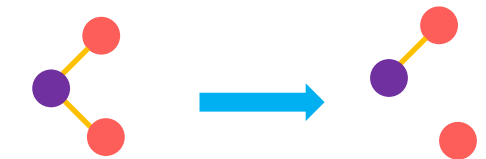
- Ion-molecule reactions
- Charge-transfer reactions
- Neutral-neutral reactions



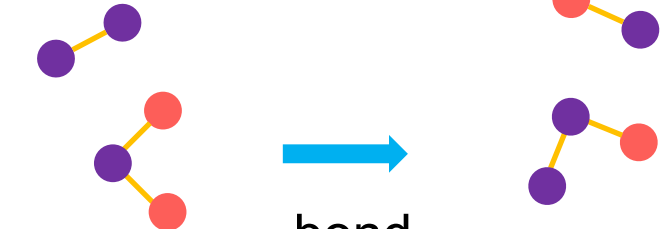
bond form



dust grain



bond destroyed

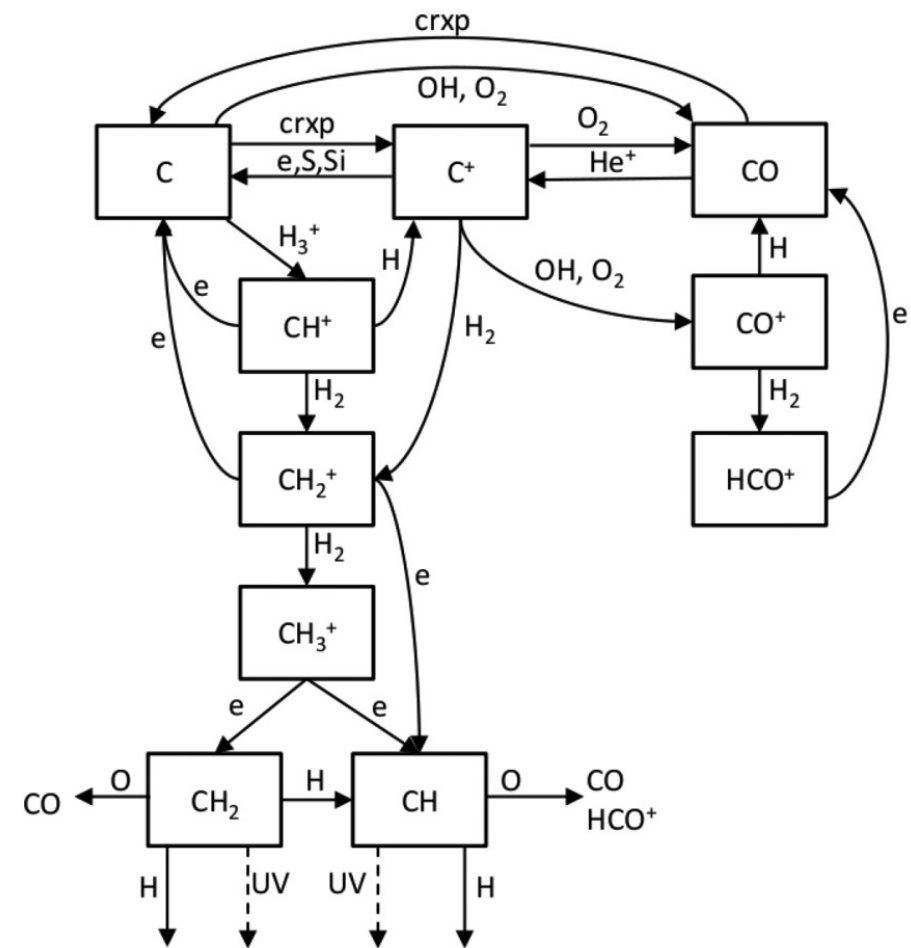
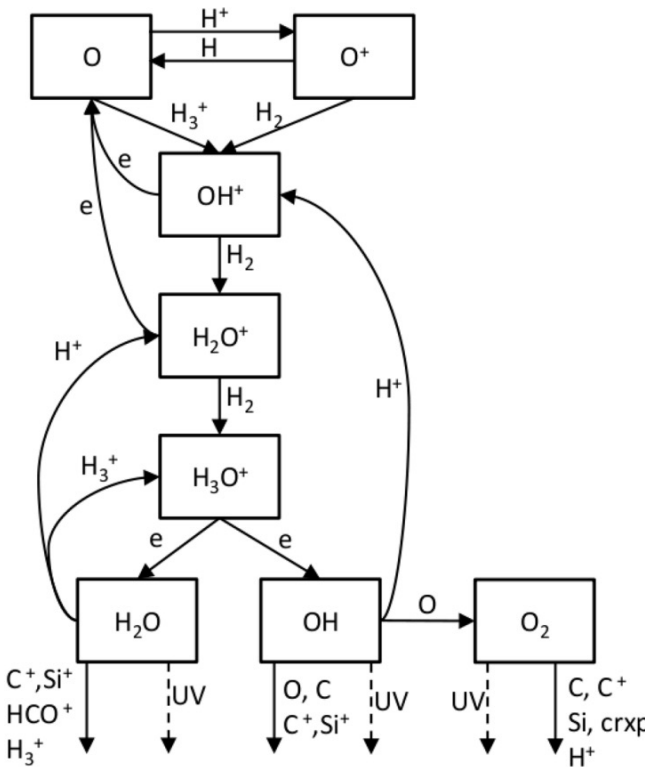
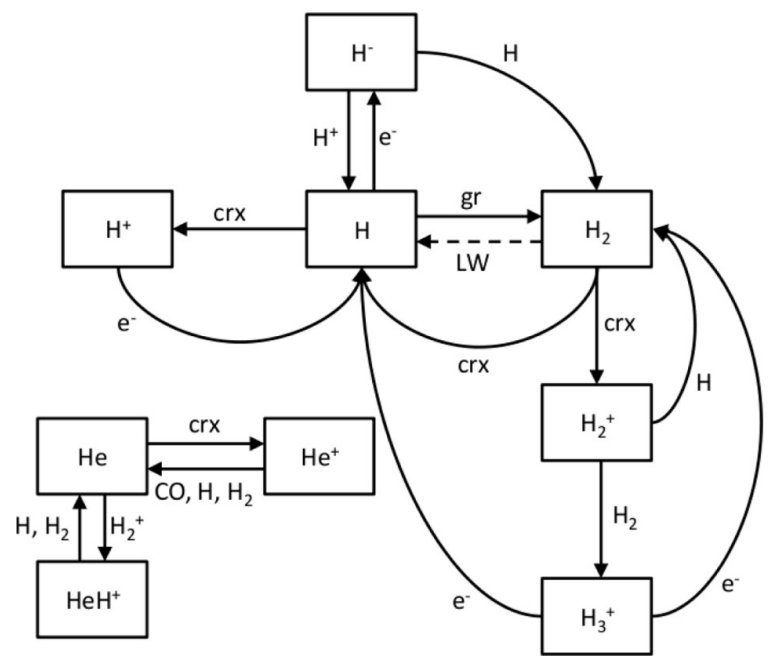


bond rearranged

Exemplary Chemical network

- crx: Cosmic ray and X-ray ionization
 - gr: grain
 - crxp: Cosmic ray and X-ray photodissociation
 - LW: 912 – 1108 Å Lyman-Werner band

Bialy & Sternberg (2015)



Sublimation temperatures

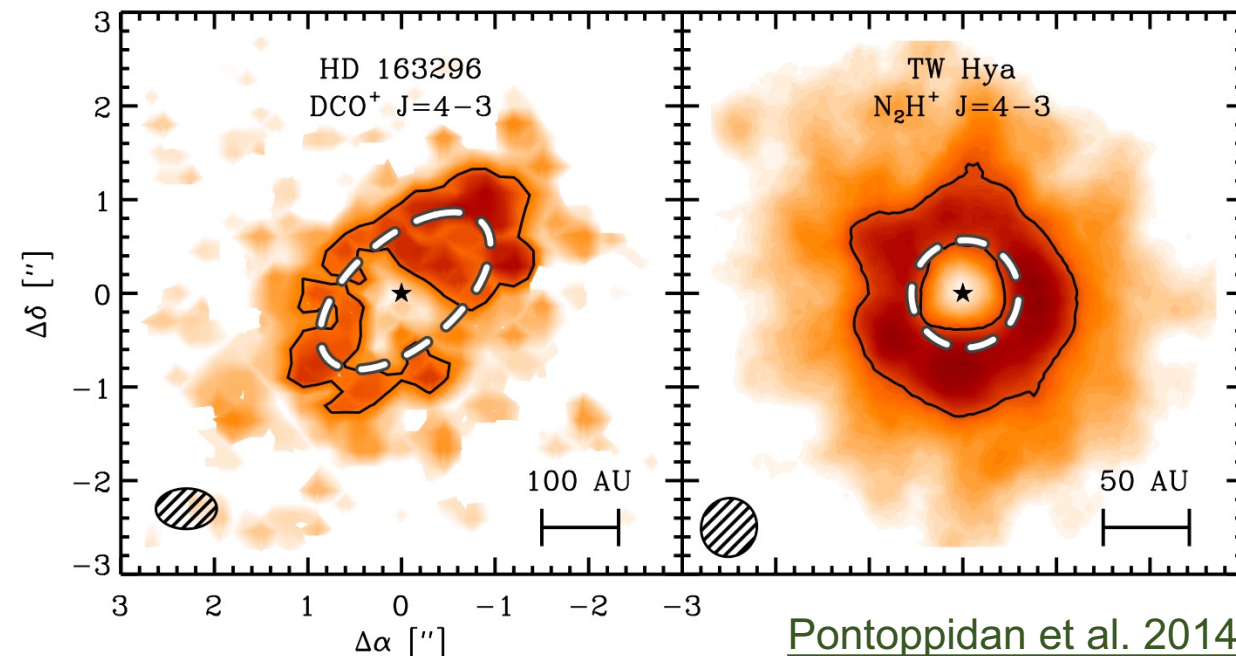
Species	$T_{\text{sub}}^{\text{lab}}$ (K)
H ₂ O	150
CH ₃ OH	99
HCN	95
SO ₂	83
NH ₃	78
CO ₂	72
H ₂ CO	64
H ₂ S	57
CH ₄	31
CO	25
N ₂	22

Mumma et al. 1993 & Collings et al. 2004

Sublimate: conversion from solid state to gaseous state (skipping the liquid state)

Sublimation temperatures for pure ices as measured in lab are **higher** than species in space due to lower densities of the latter.

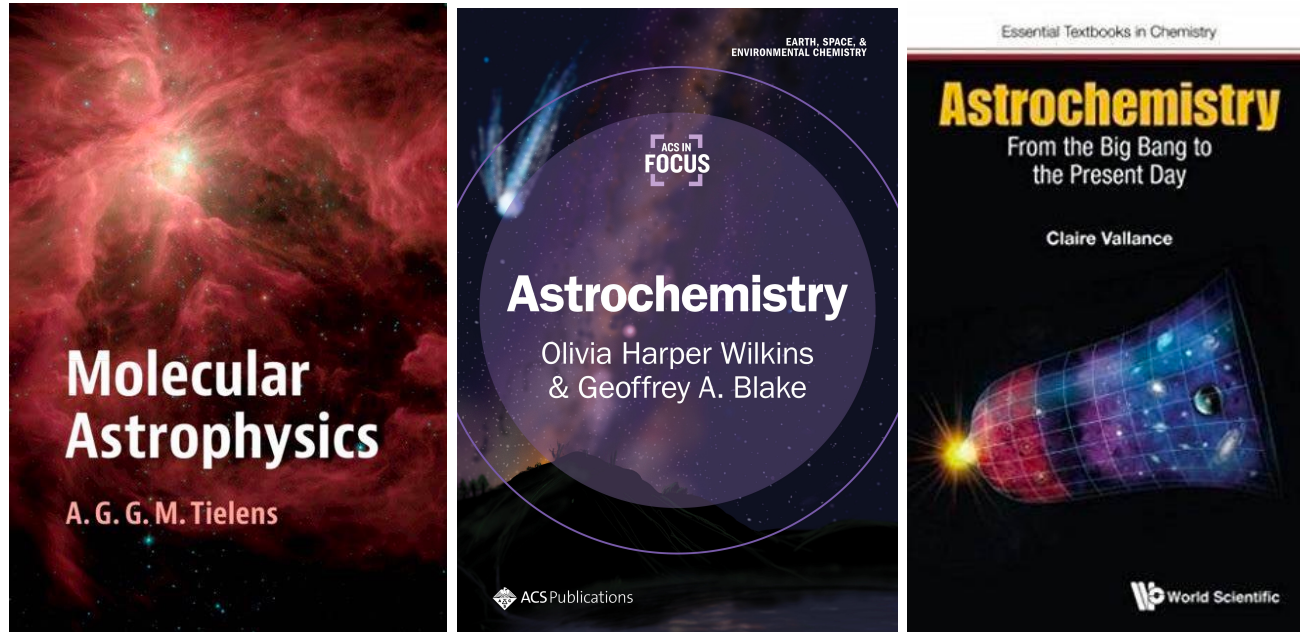
Snowline: distance at which molecular species are frozen (17 K isotherms, CO frozen out)



Pontoppidan et al. 2014

More about astrochemistry/astrobiology

- Molecular abundances evolution
→ **astrochemistry**
- Molecules as physical diagnostics
→ **astrophysics**
- Molecules in comet & exoplanet atmosphere
→ **astrobiology**
- Observing & lab facilities
→ **engineering+**



<https://home.strw.leidenuniv.nl/~leemker/astrochemistry/>

Astrochemistry

HOME SCHEDULE LECTURE SLIDES PROBLEM SETS TALKS LITERATURE LINKS

Astrochemistry Lectures

6.1.4 More about astrochemistry/astrobiology

26

Chpt.6 Molecular and dust processes

Nittler & Ciesla (2016)

6.1 Molecular processes

6.2 Dust processes

6.2.1 Dust and molecules

6.2.2 Dust properties

6.2.3 Extinction curve

6.2.4 X-ray dust scattered ring

6.2.5 X-ray dust extinction feature

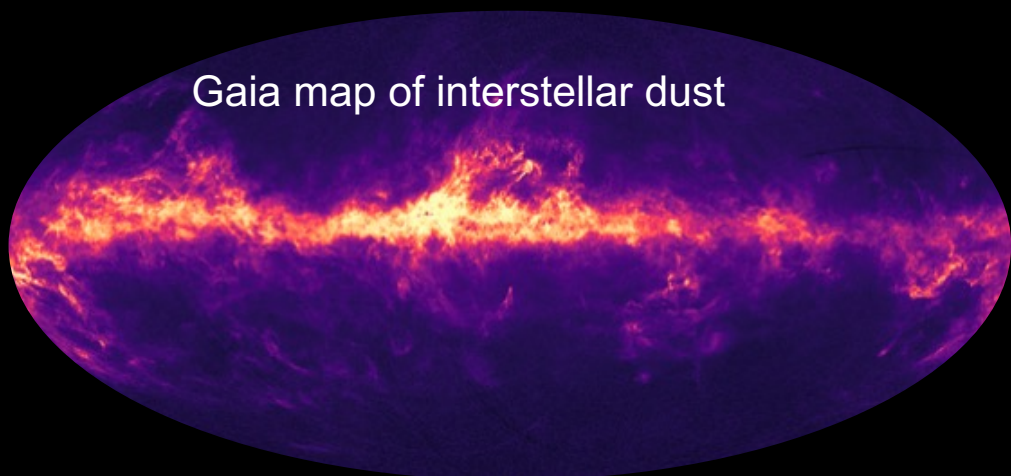
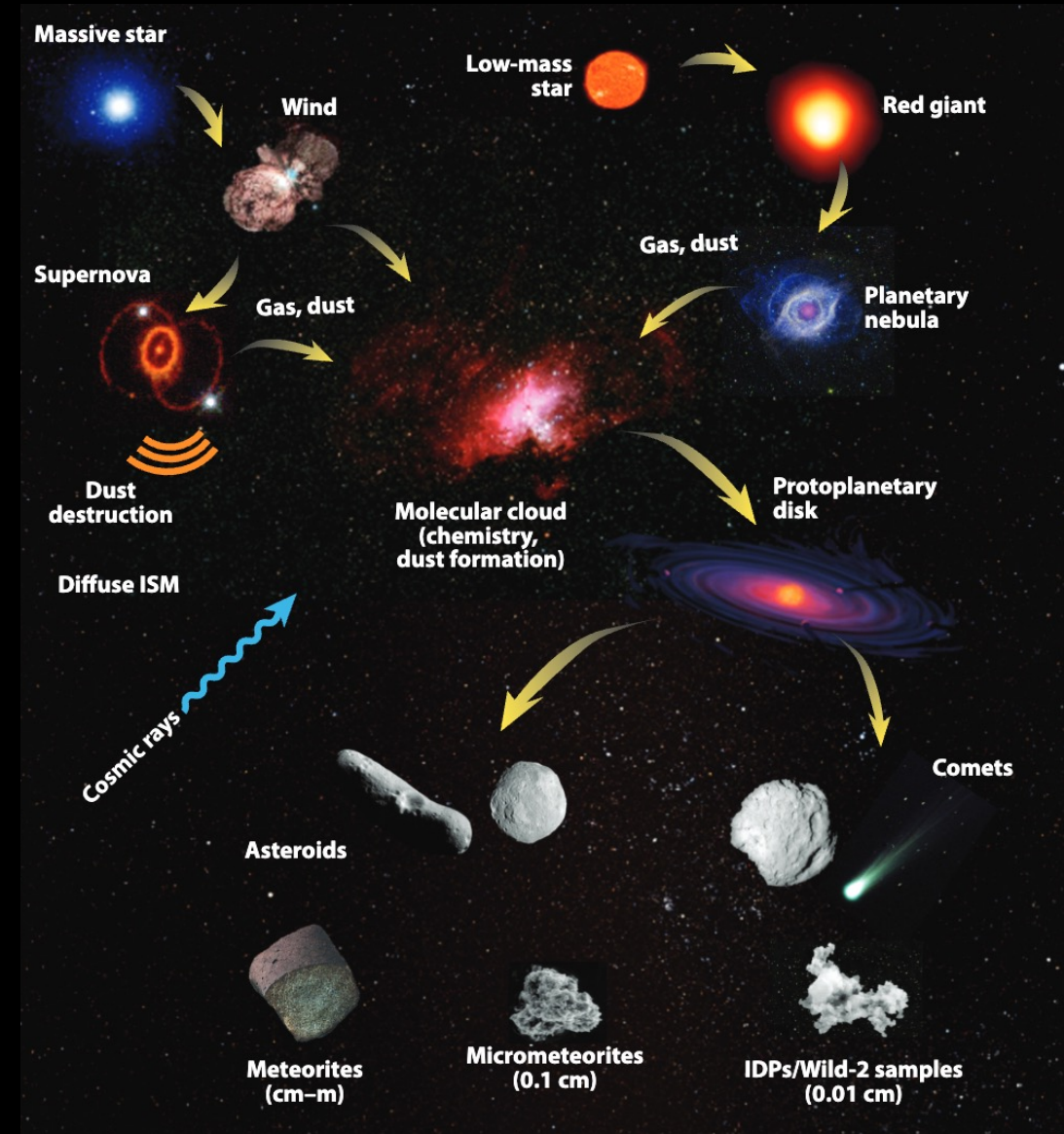


Image credit: DPAC; Gaia Coordination Unit 8; M. Fouesneau / R. Andrae / C.A.L Bailer-Jones, MPA



Dust and molecules

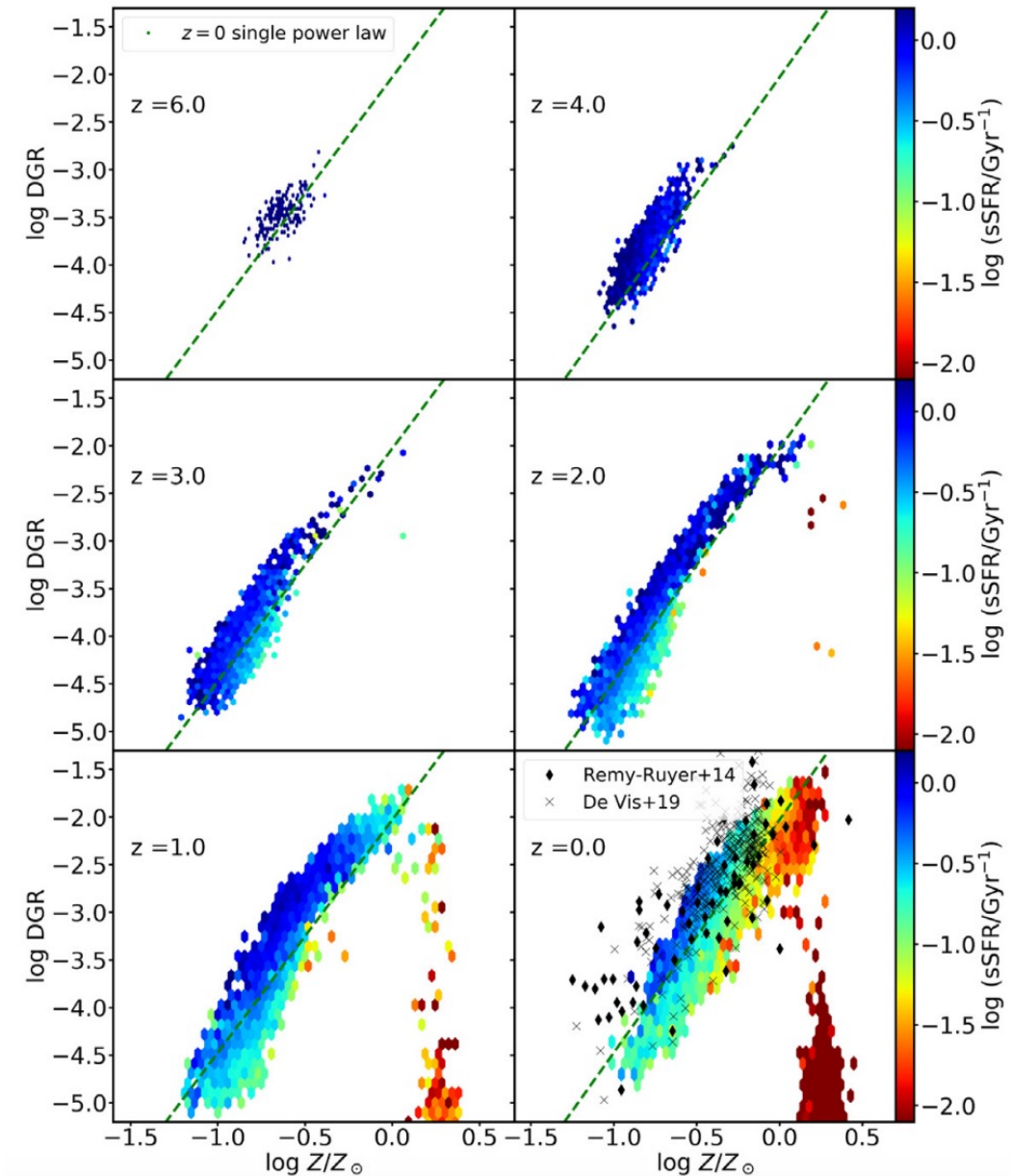
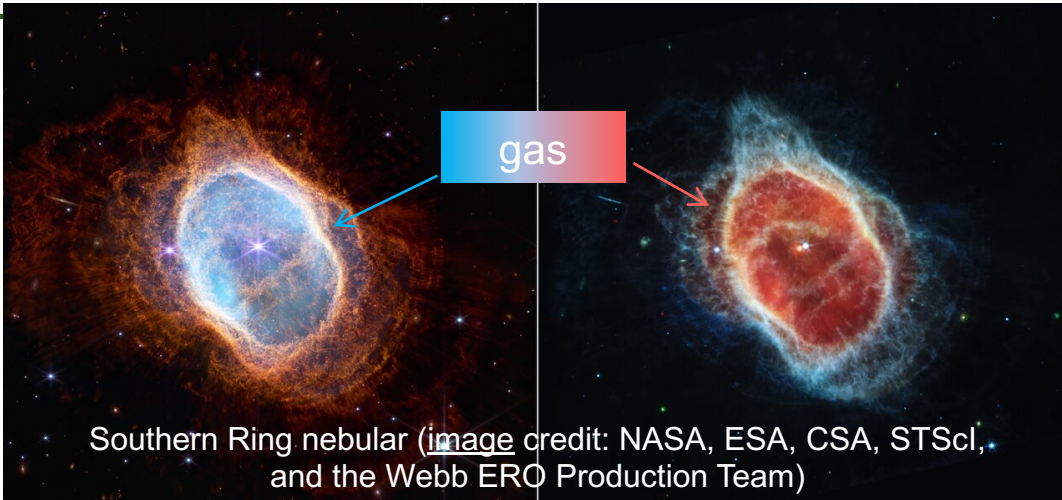
Interstellar medium consists of gas and **dust grains** (solid-phase of material composed of metals).

dust to gas (DTG) ratio

gas metallicity of star-forming main sequence

$$\log \text{DTG} = (2.445 \pm 0.006) \log \frac{Z_{\text{gas}}}{Z_{\odot}} - (2.029 \pm 0.003)$$

Li et al. 2019



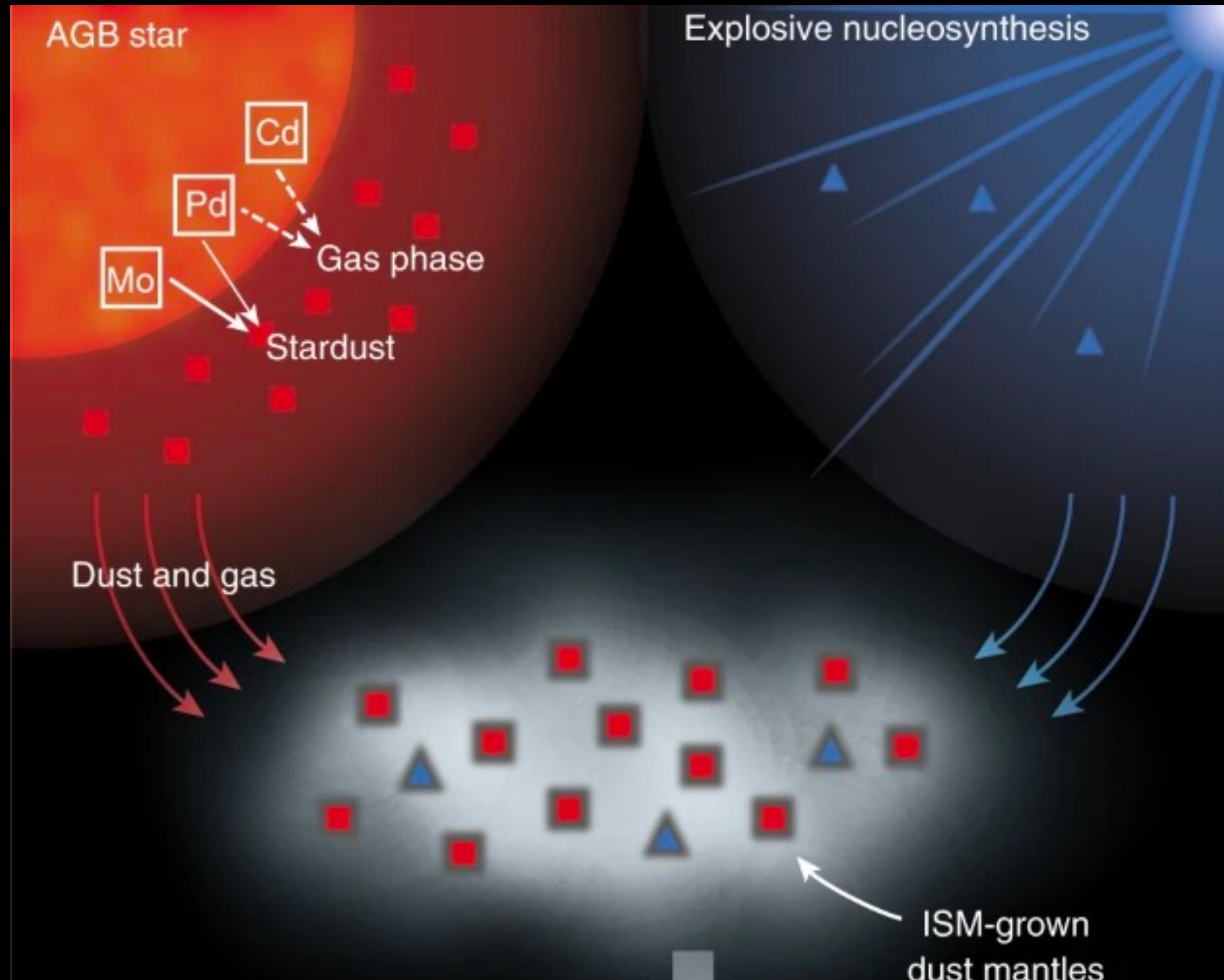
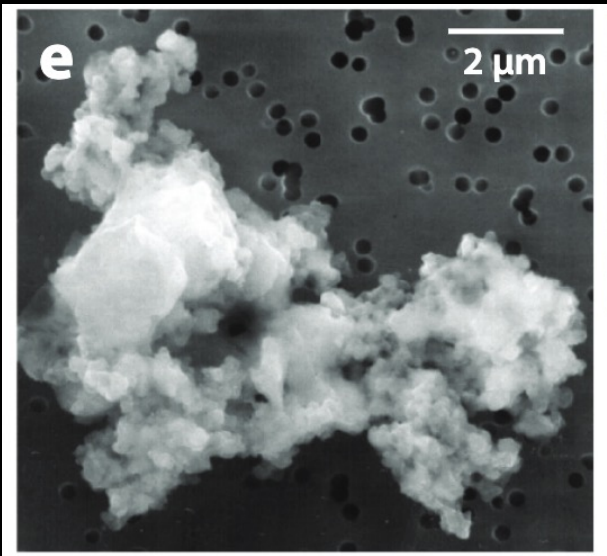
Formation of interstellar dust

Ek et al. 2020

Dust grains can be sourced from supernovae (SNe), Red Super Giant (RSG) stars, Wolf-Rayet (WR) stars, Asymptotic Giant Branch (AGB) stars, Young Stellar Objects (YSO), etc.

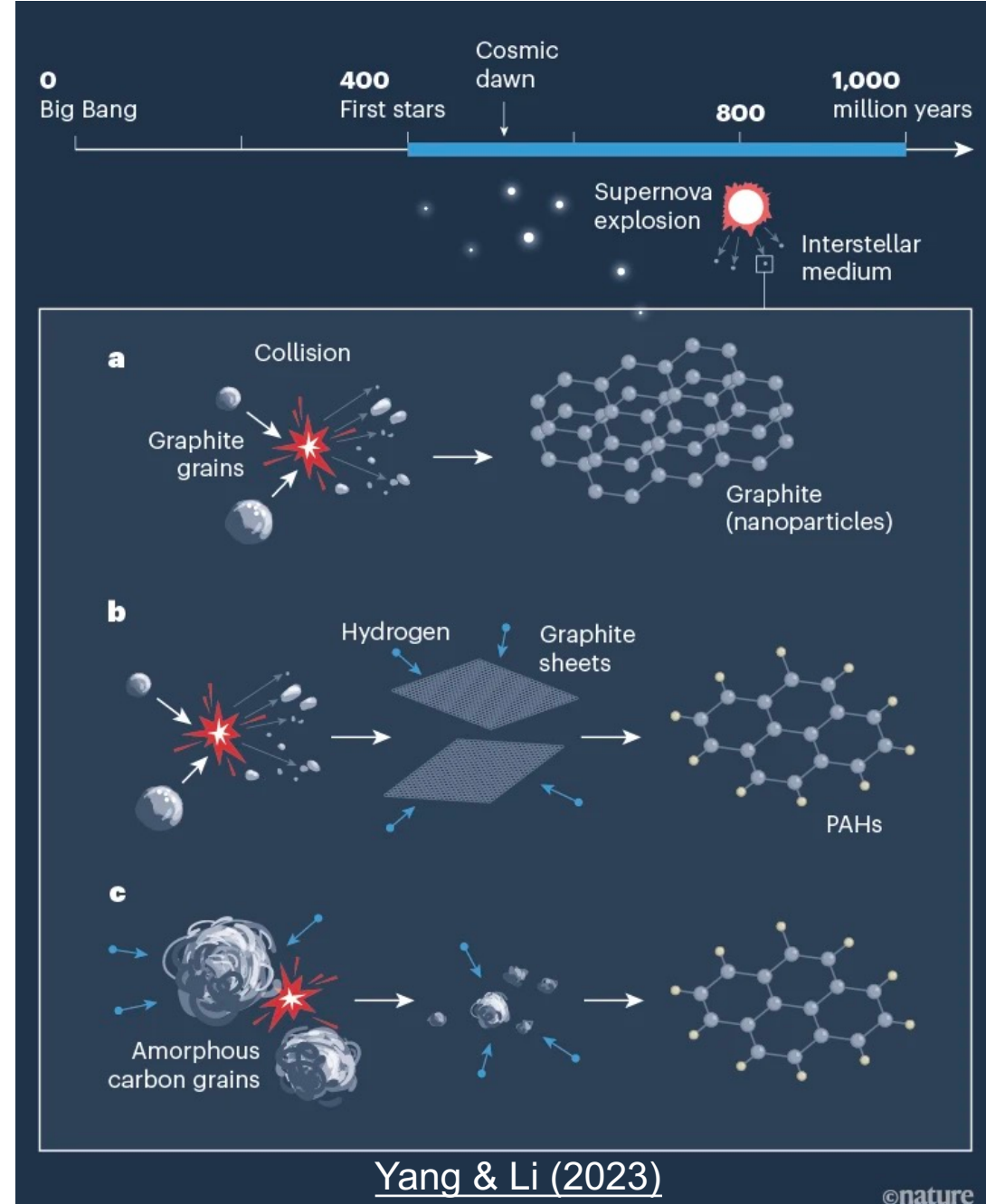
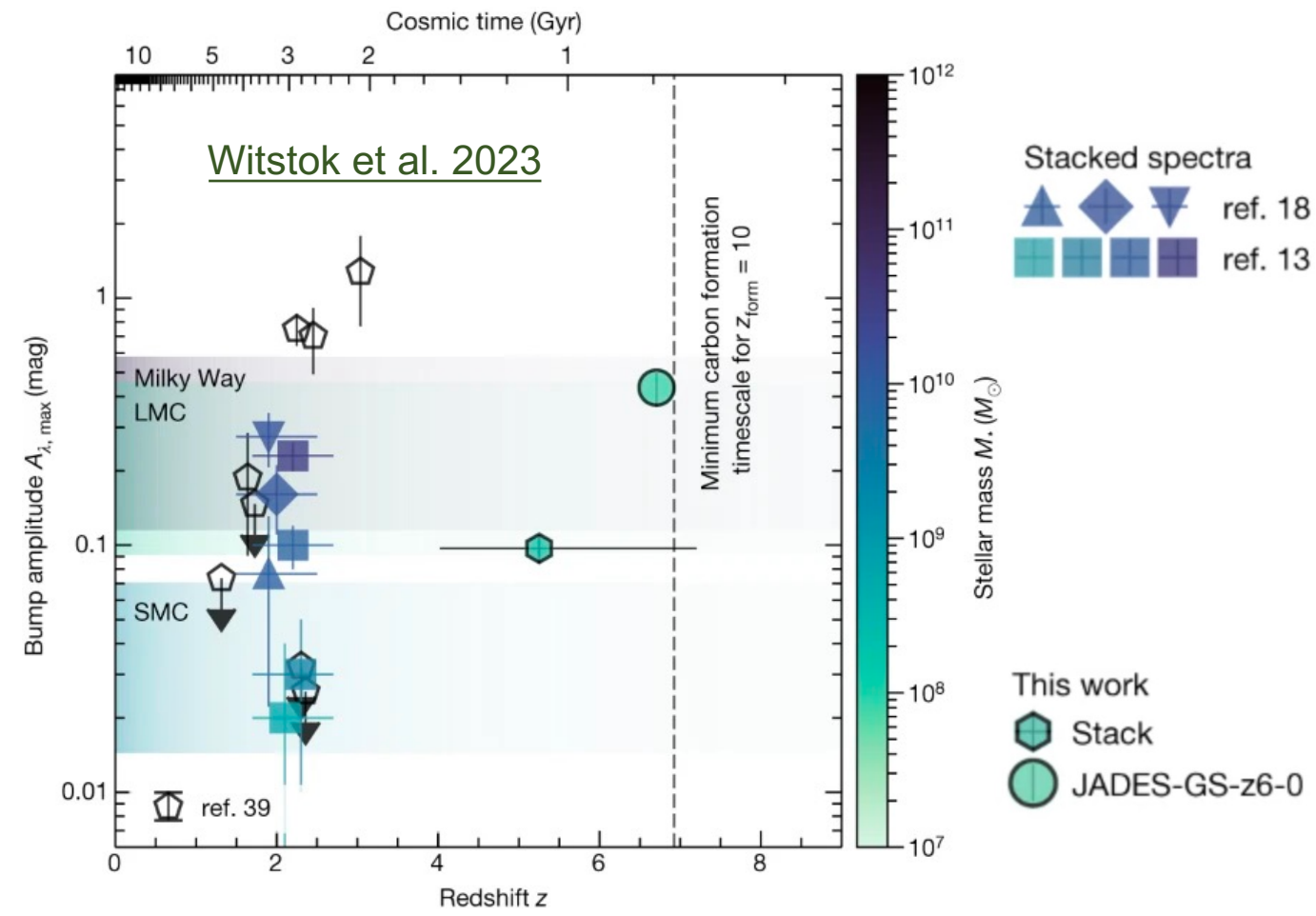
Tielens (2001)

Nittler & Ciesla (2016)
extraterrestrial dust



Fast formation of dust formation

Dust observed in galaxies at $z \sim 7$ (i.e., the age of the Universe is $\lesssim 1$ Gyr), requiring a rapid dust formation channel (Wolf-Rayet stars or supernova)



Dust chemical composition

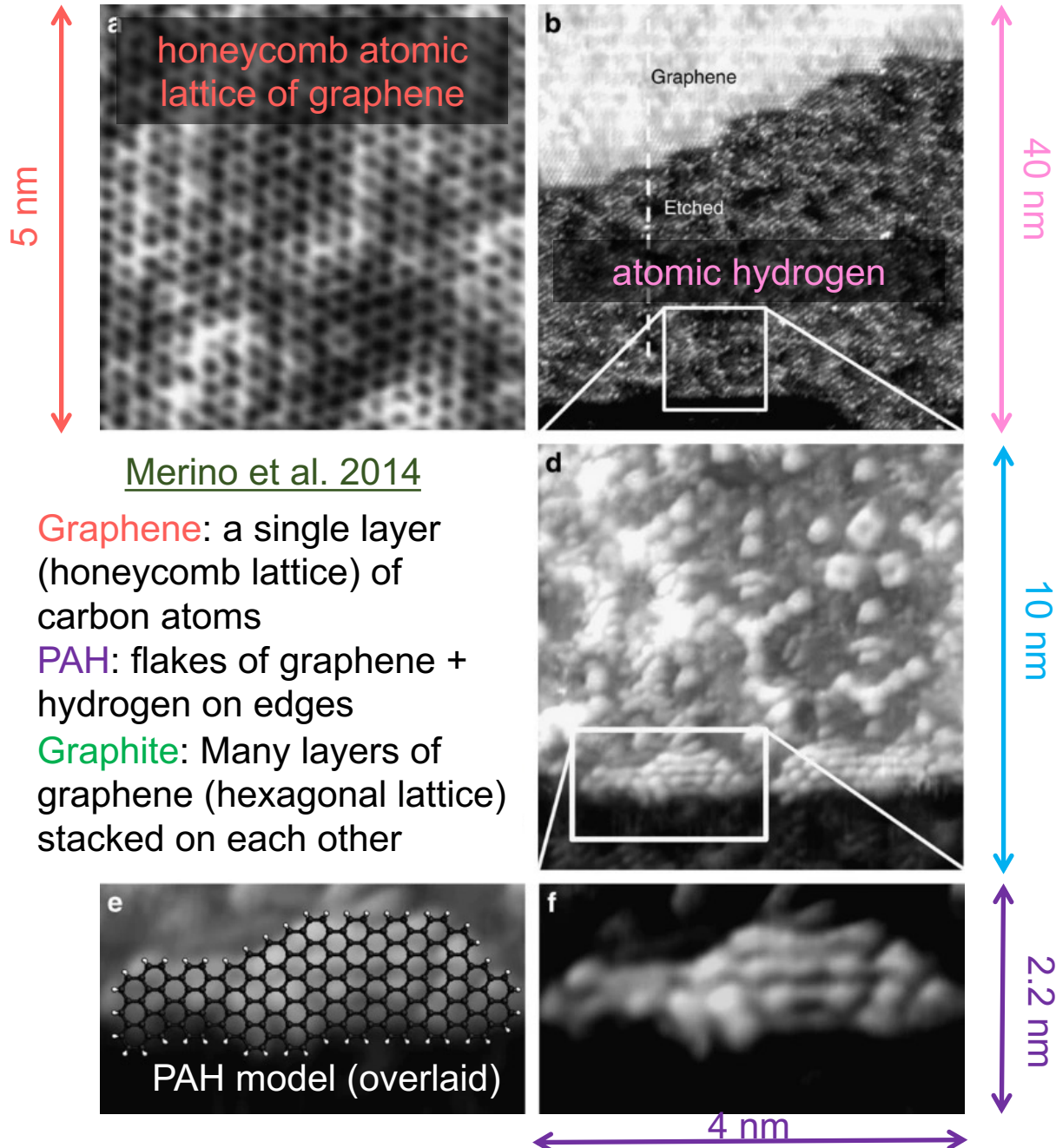
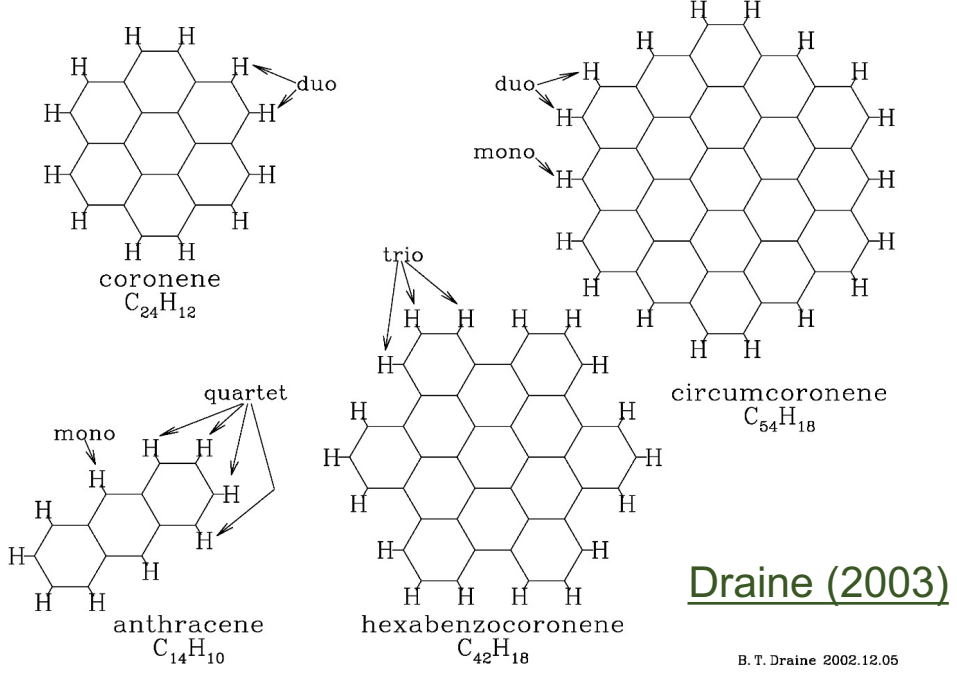
□ Major

- Carbonaceous
 - Graphite
 - PAH (polycyclic aromatic hydrocarbons)

○ Silicate

□ Minor

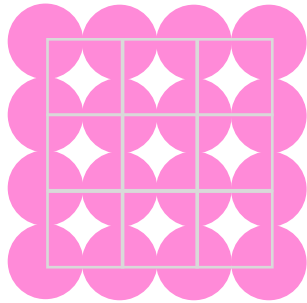
- Other metals



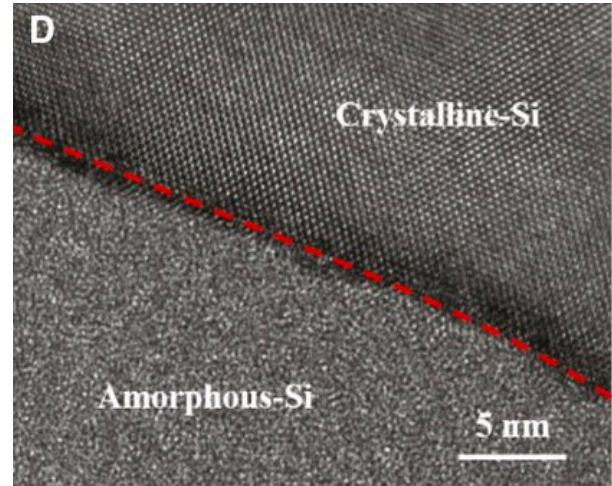
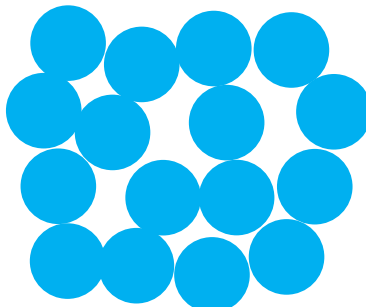
Dust composition and form

Jiang et al. 2019

□ Crystalline



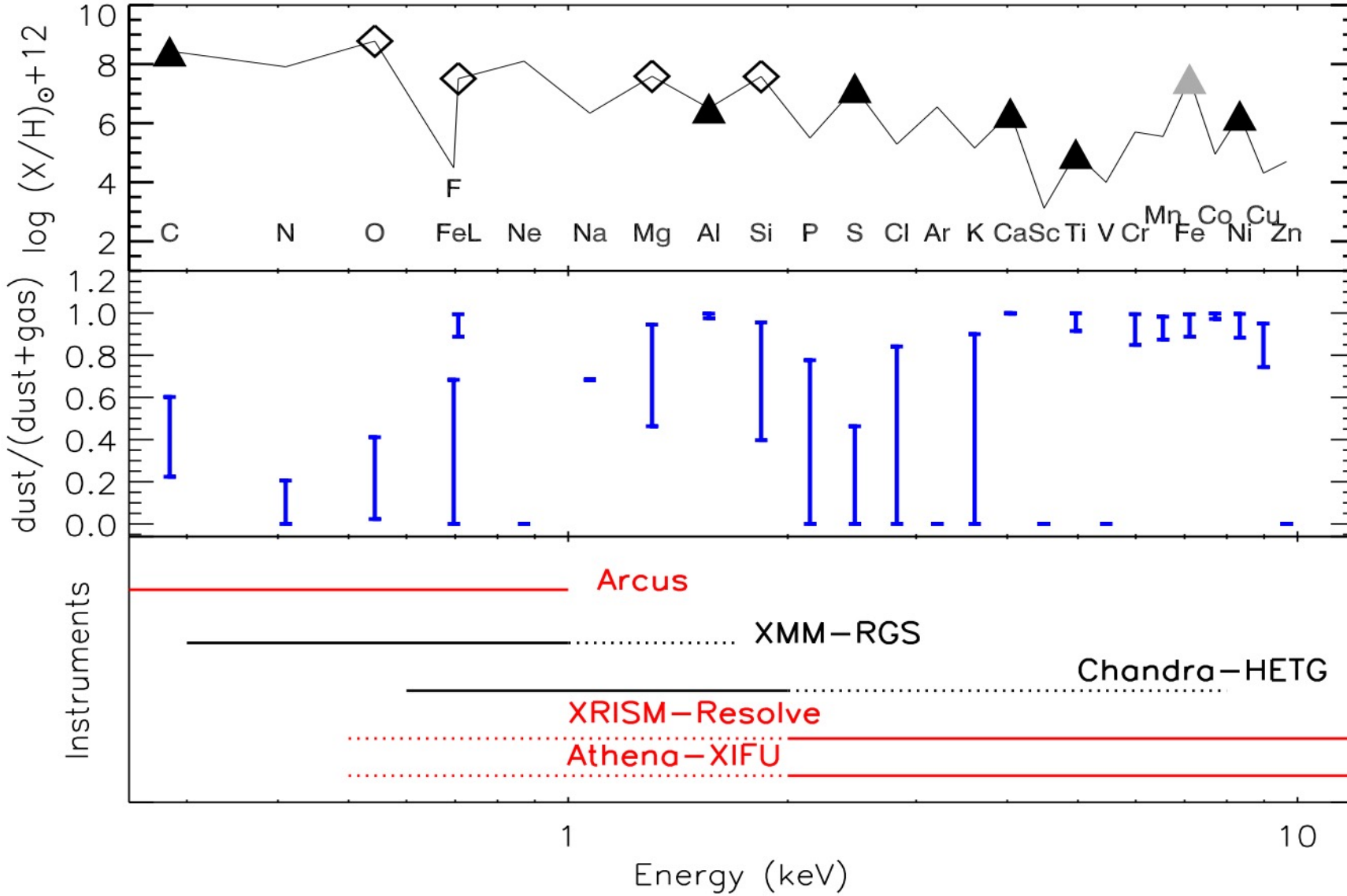
□ Amorphous



C	Si	Fe	Ni
SiC	FeS	Fe ₇ S ₈	SiO ₂
Si ₃ N ₄	MgO	Al ₂ O ₃	MnS
FeS ₂	TiO ₂	CH	Mg ₂ SiO ₄
MgSiO ₃	MgAl ₂ O ₄	CaAl ₂ O ₄	Ca ₃ Al ₂ O ₆
Fe ₂ SiO ₄	MgFeSiO ₄	Mg _{1.56} Fe _{0.4} Si _{0.91} O ₄	Mg _{0.6} Fe _{0.4} SiO ₃
Mg _{0.75} Fe _{0.25} SiO ₃	Mg _{0.9} Fe _{0.1} SiO ₃	Mg _{1.502} Fe _{0.498} Si ₂ O ₆	MgCaSi ₂ O ₆
CaAl ₂ Si ₂ O ₈	crystalline	amorphous	both

Metal depletion fraction

Costantini et al. 2019



With metals locked into dust, metals are under-abundant in the ISM of Milky Way ([Jenkins 2009](#)), SMC ([Jenkins & Wallerstein 2017](#)), LMC and damped ([De Cia 2018](#)), and beyond ([Péroux & Howk 2020](#)).

Dust size distribution

classical MRN dust size distribution ([Mathis, Rumpl, Nordsieck 1977](#)):

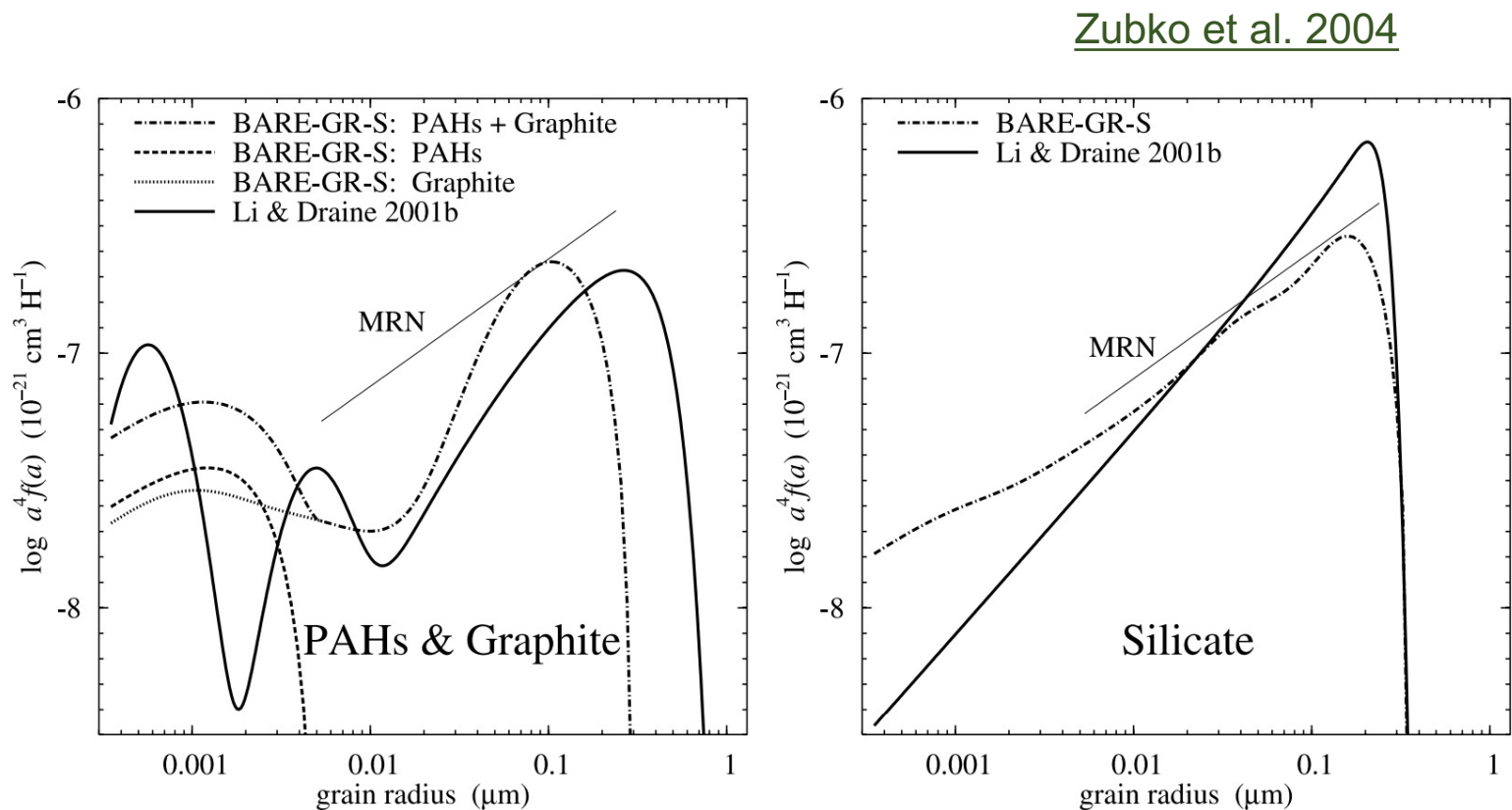
$$n(a) \propto a^{-3.5} \text{ for } 0.005 \mu\text{m} \leq a \leq 0.25 \mu\text{m}$$

the min. and max. size might vary from paper to paper

original MRN paper:

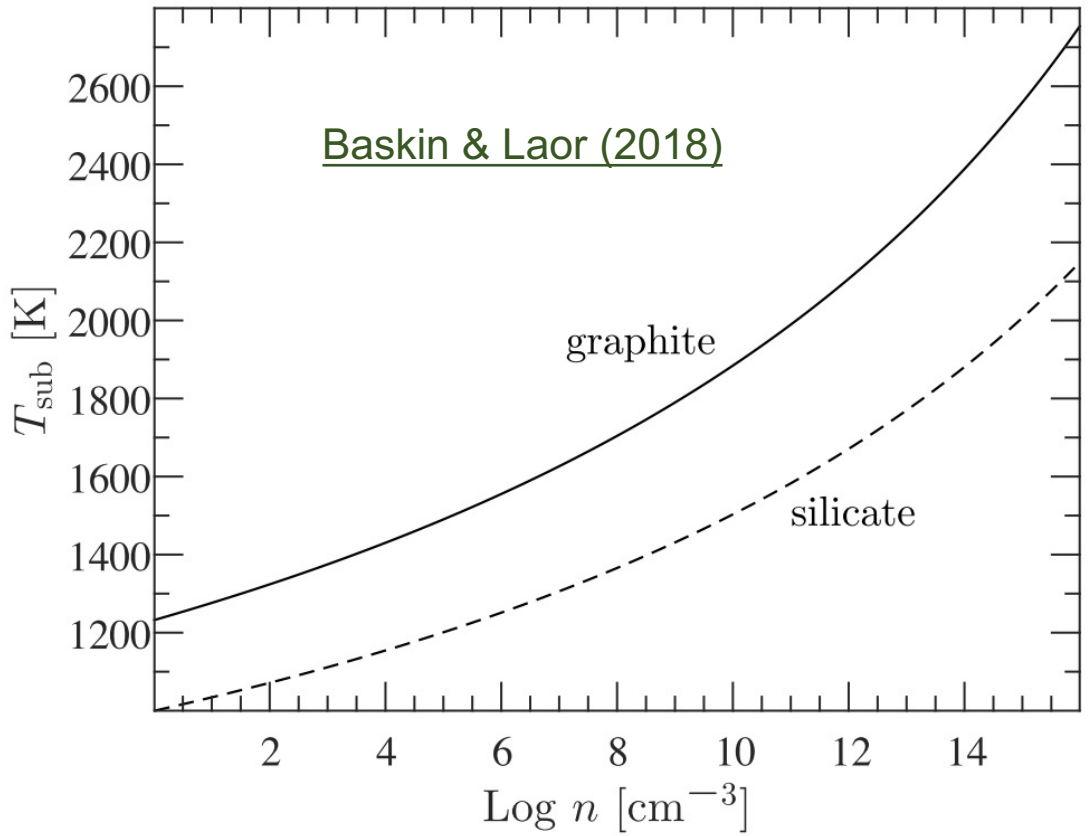
- power-law index -3.3 to -3.6
- $a \in (0.005, 0.1) \mu\text{m}$

other size distributions have also been proposed

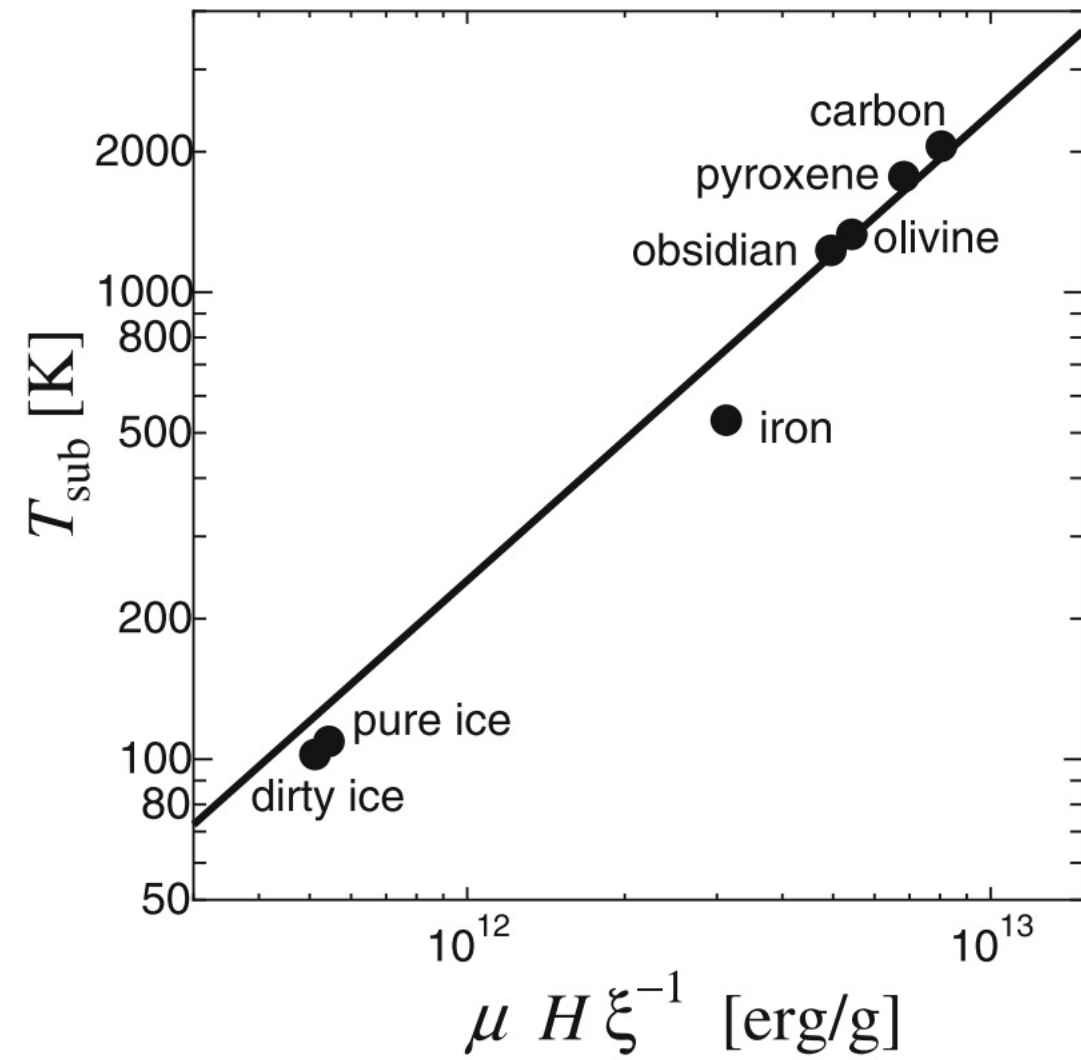


Dust sublimation temperature

Generally speaking, dust will sublimate at the temperature of 1000 – 2000 K. Exact values depend on the composition, size, density, etc.



Kobayashi et al. 2011



Dust extinction curve

Dust extinction optical depth

$$\tau_\lambda = \int n_{\text{dust}} \sigma_{\text{ext}}(\lambda) dl$$

dimensionless

extinction cross section

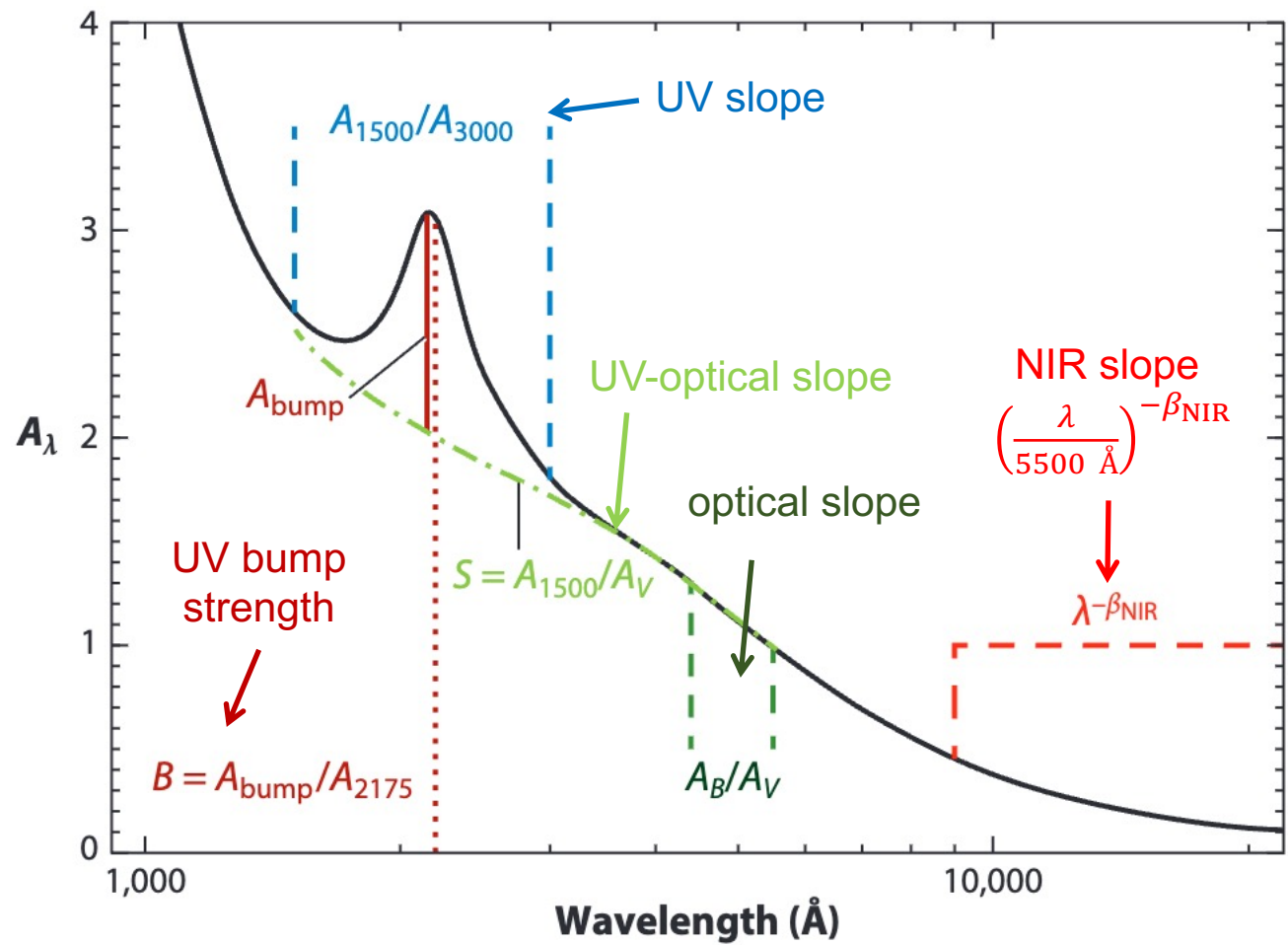
dust number density

$$\frac{A_\lambda}{\text{mag}} = 2.5 \log_{10} \frac{F_\lambda^0}{F_\lambda}$$

intrinsic flux

$$= 2.5 \log_{10} e^{\tau_\lambda} = 1.086 \tau_\lambda$$

Salim & Narayanan (2020)
values of the y-axis are arbitrary



UV (2175 Å) bump

The UV (2175 Å) bump was discovered in 1965 ([Stecher 1965](#)). It is likely related to dust grains mainly made of carbon, but the exact origin is still an open question.

[Ma et al. 2020](#)
a recent interpretation (as an example)

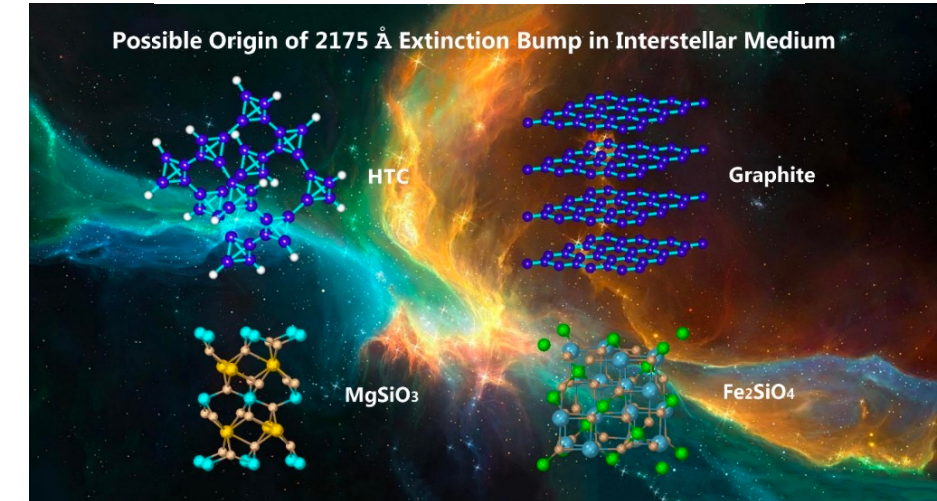
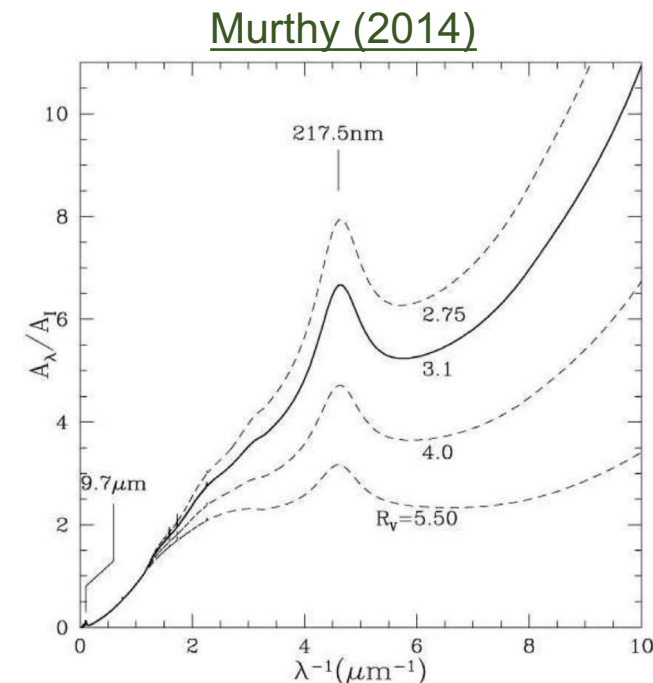
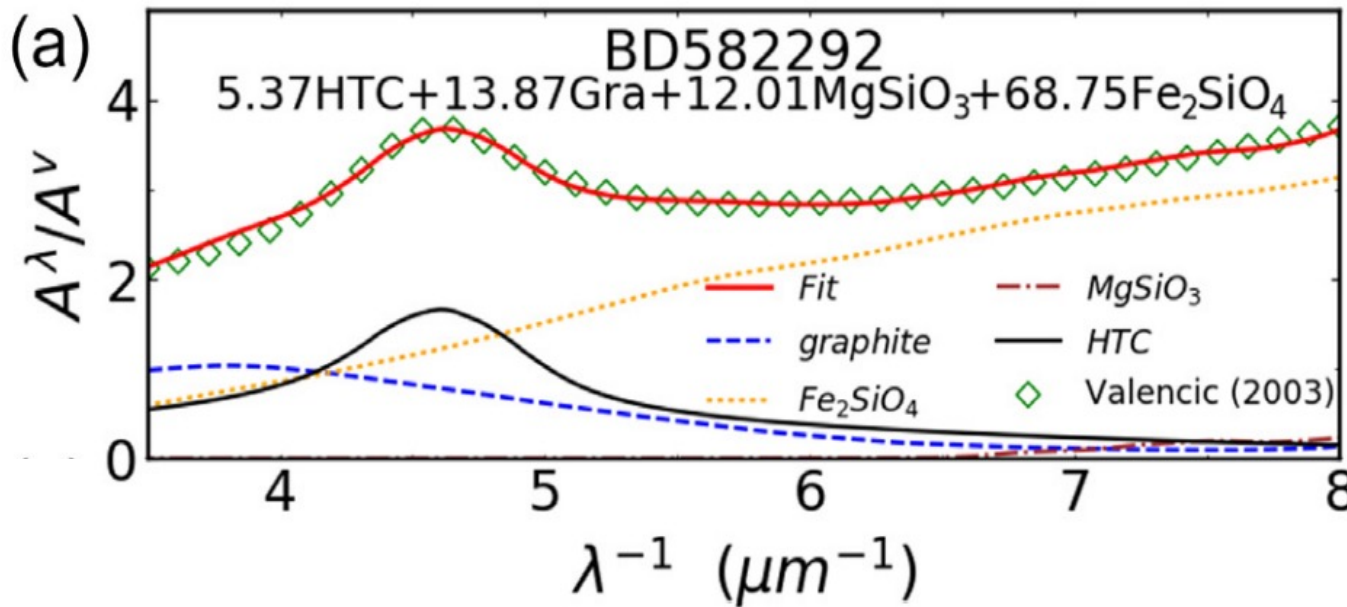
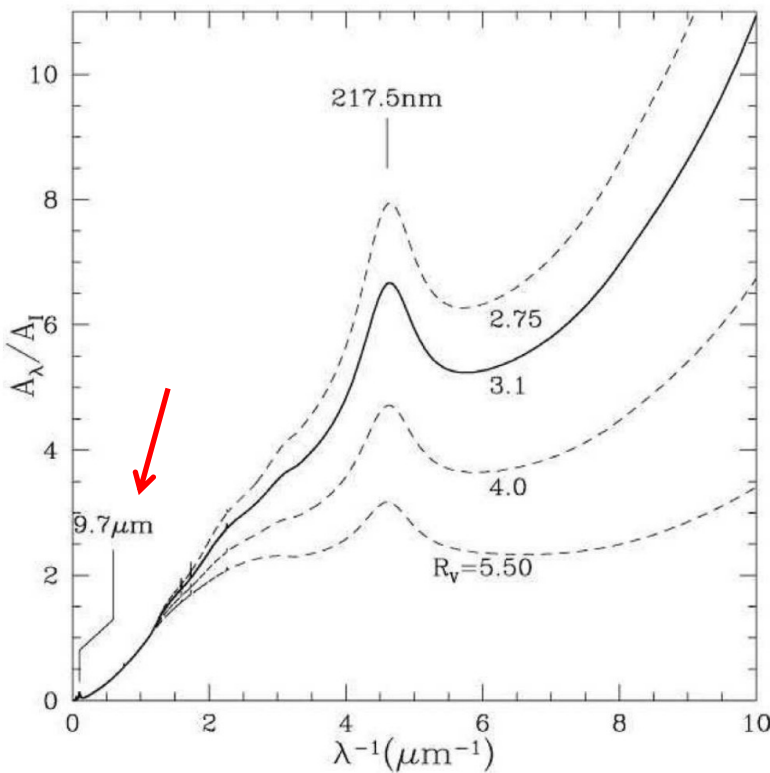


[Image credit: KITS, NASA, ESA, HST](#)

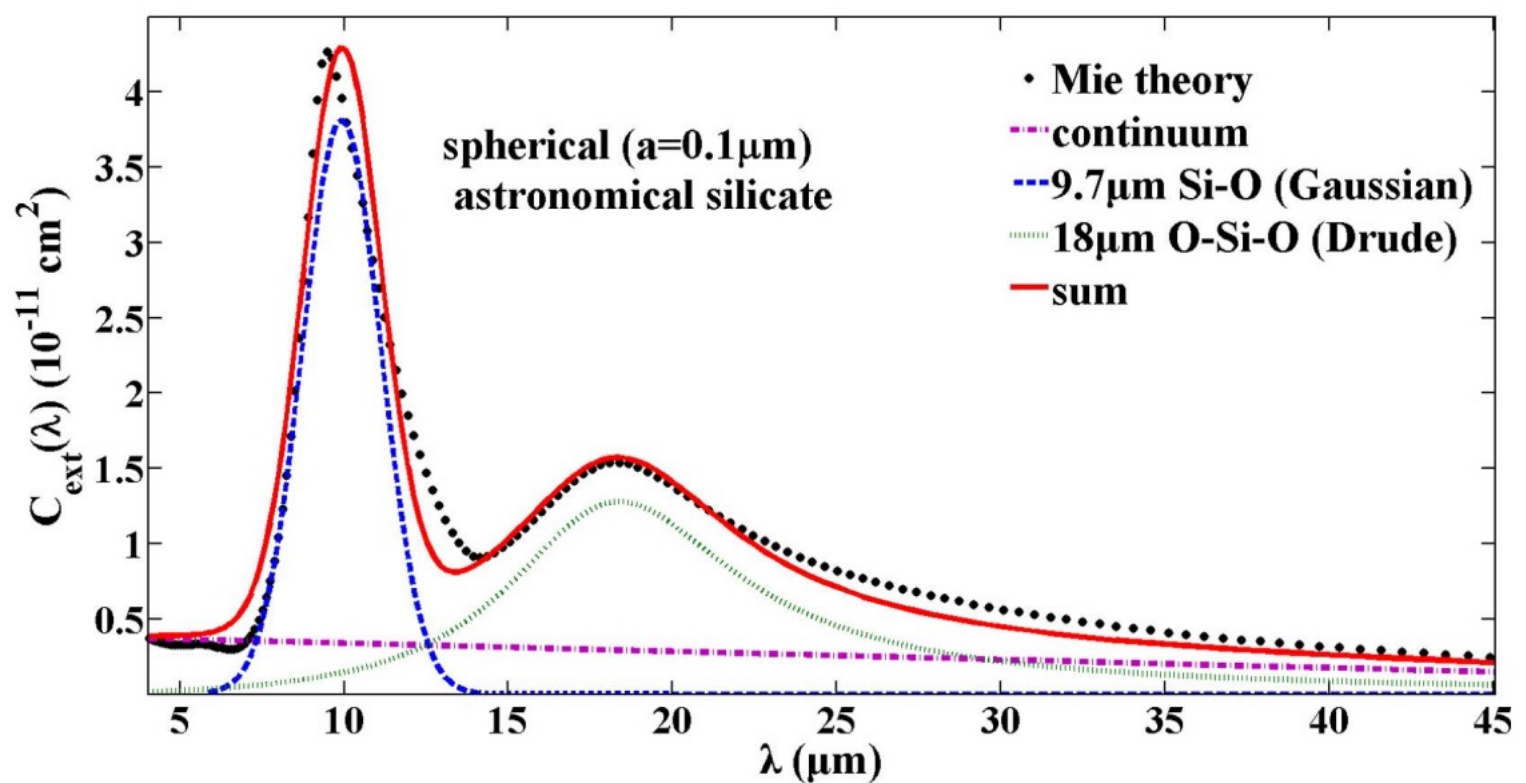
IR silicate feature

- 9.7 μm : Si-O stretch (amorphous silicate)
- 18 μm : O-Si-O stretch (amorphous silicate)

Murthy (2014)



Shao et al. 2017



Dust extinction law

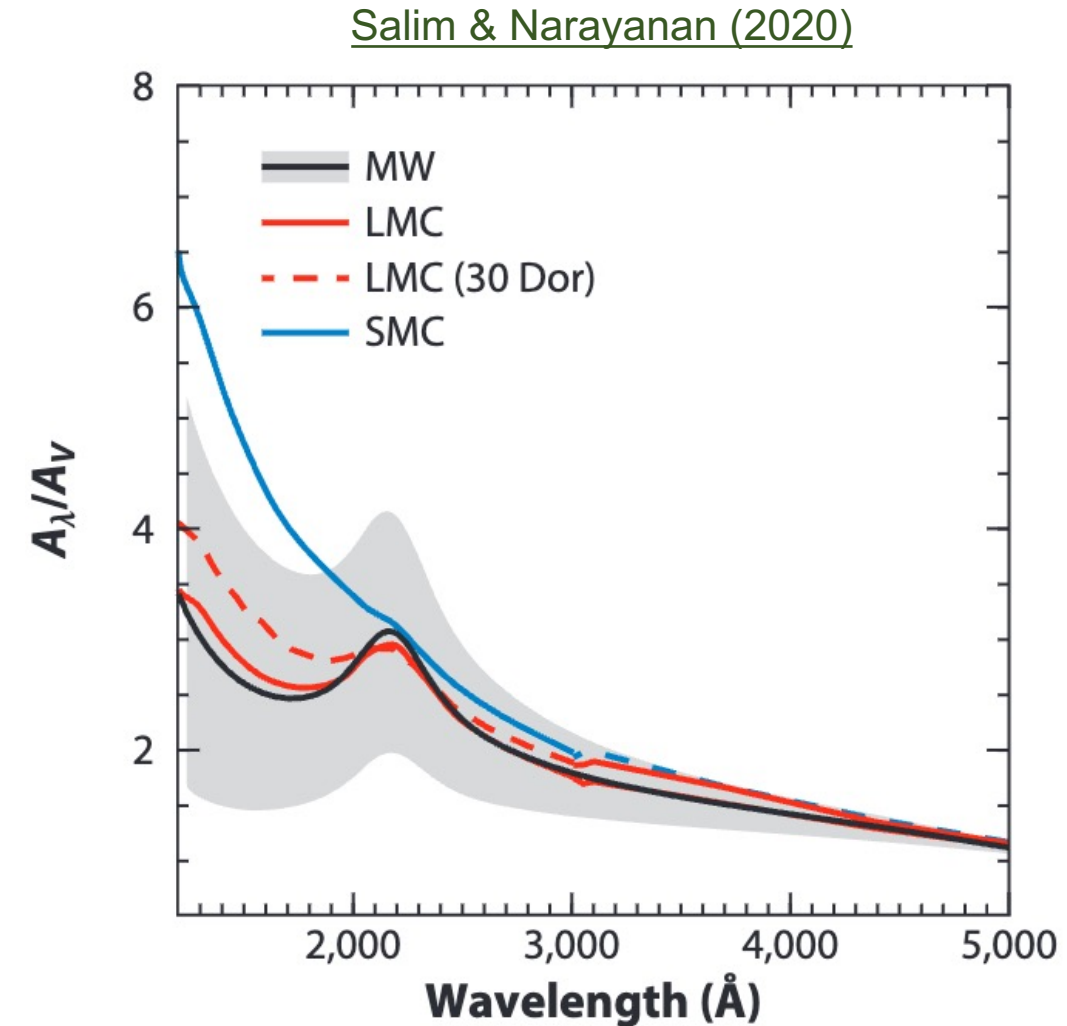
extinction
 $\frac{A_\lambda}{A_V} = a_\lambda + \frac{b_\lambda}{R_V}$
V band magnitude

parameters in e.g., [Cardelli et al. 1989](#),
[O'Donnell 1994](#), [Gordon et al. 2003](#)

$R_V = \frac{A_V}{A_B - A_V} = \frac{A_V}{E(B - V)}$

$R_V = 3.1$ for Milky Way
 $R_V = 4.0$ for SMC

color excess
reddening



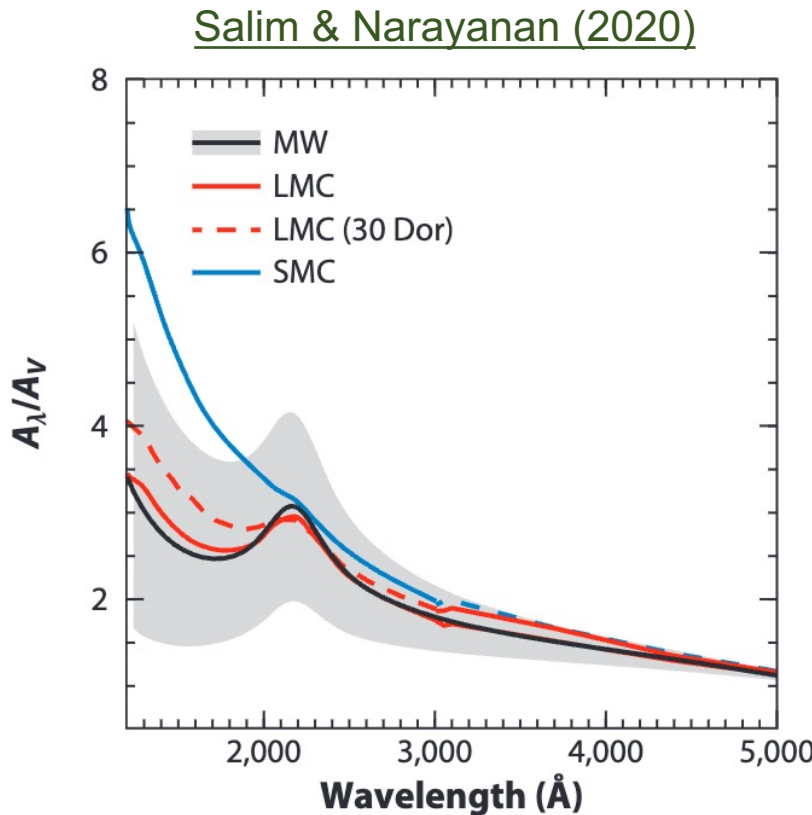
Interstellar reddening

prev. sl.

$$\frac{A_\lambda}{\text{mag}} = 2.5 \log_{10} \frac{F_\lambda^0}{F_\lambda}$$

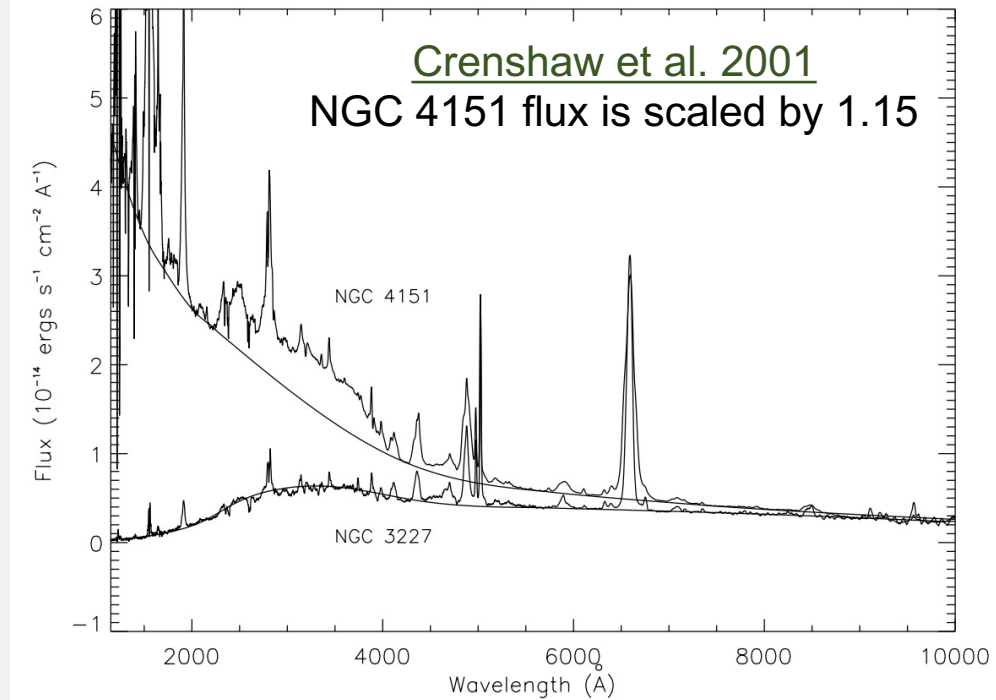
intrinsic flux

$$F_\lambda^0 = F_\lambda 10^{0.4 A_\lambda}$$



Slide 5.4.7.3

Crenshaw et al. 2001
NGC 4151 flux is scaled by 1.15

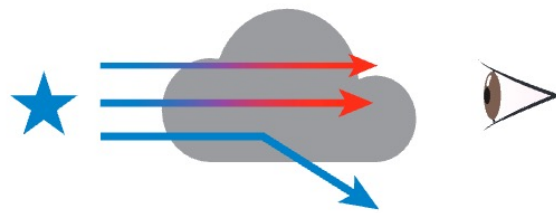


In practice, the observed H α /H β ratio might be higher than expected value while the H γ /H β ratio might be lower than expected value. This is due to (line-of-sight) interstellar reddening.

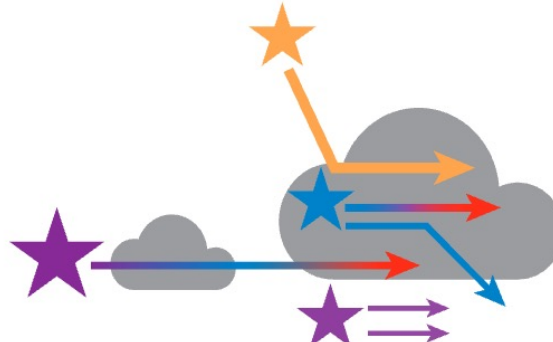
The more the interstellar dust, the larger the discrepancy between theory and observation.

Extinction and attenuation curves

a Extinction



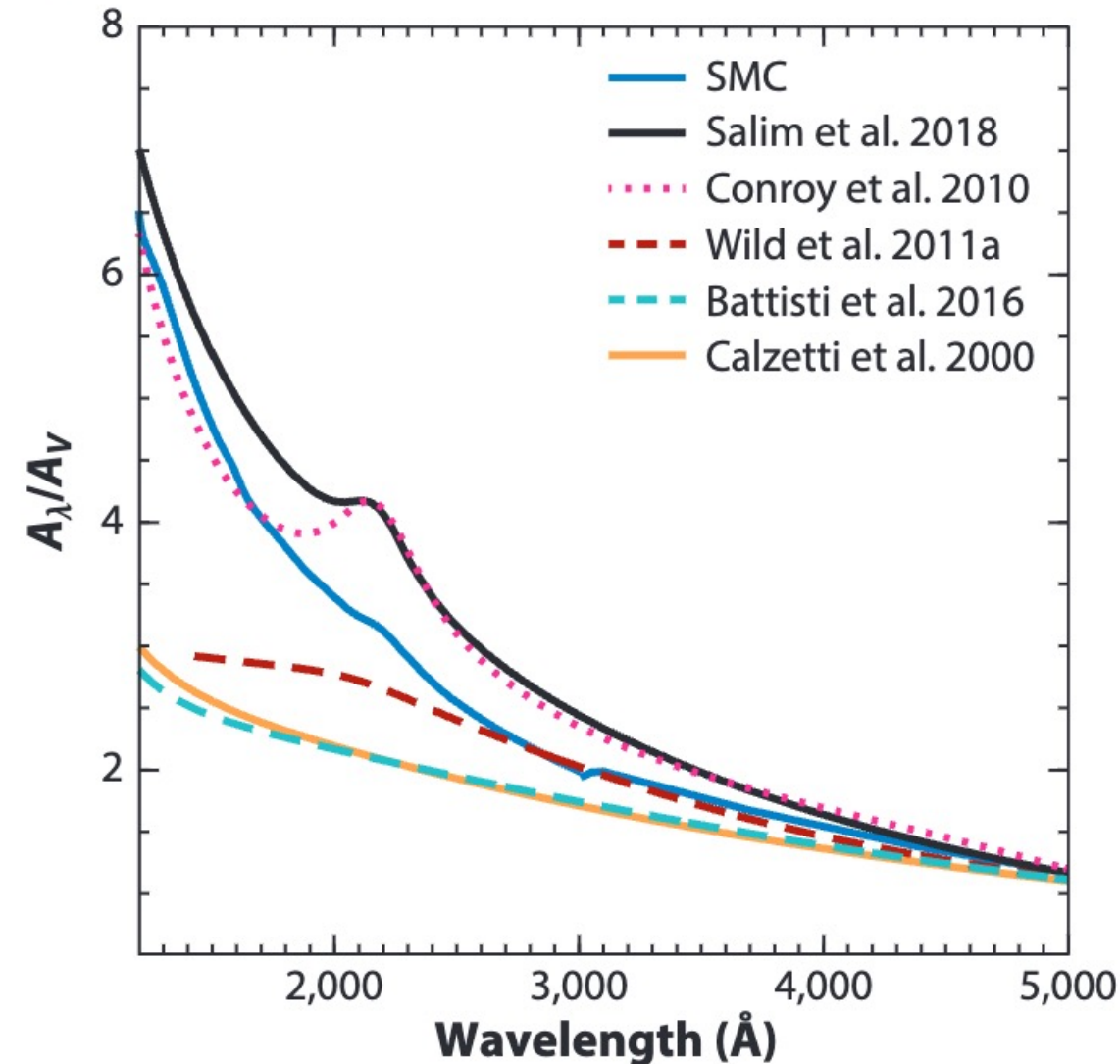
b Attenuation



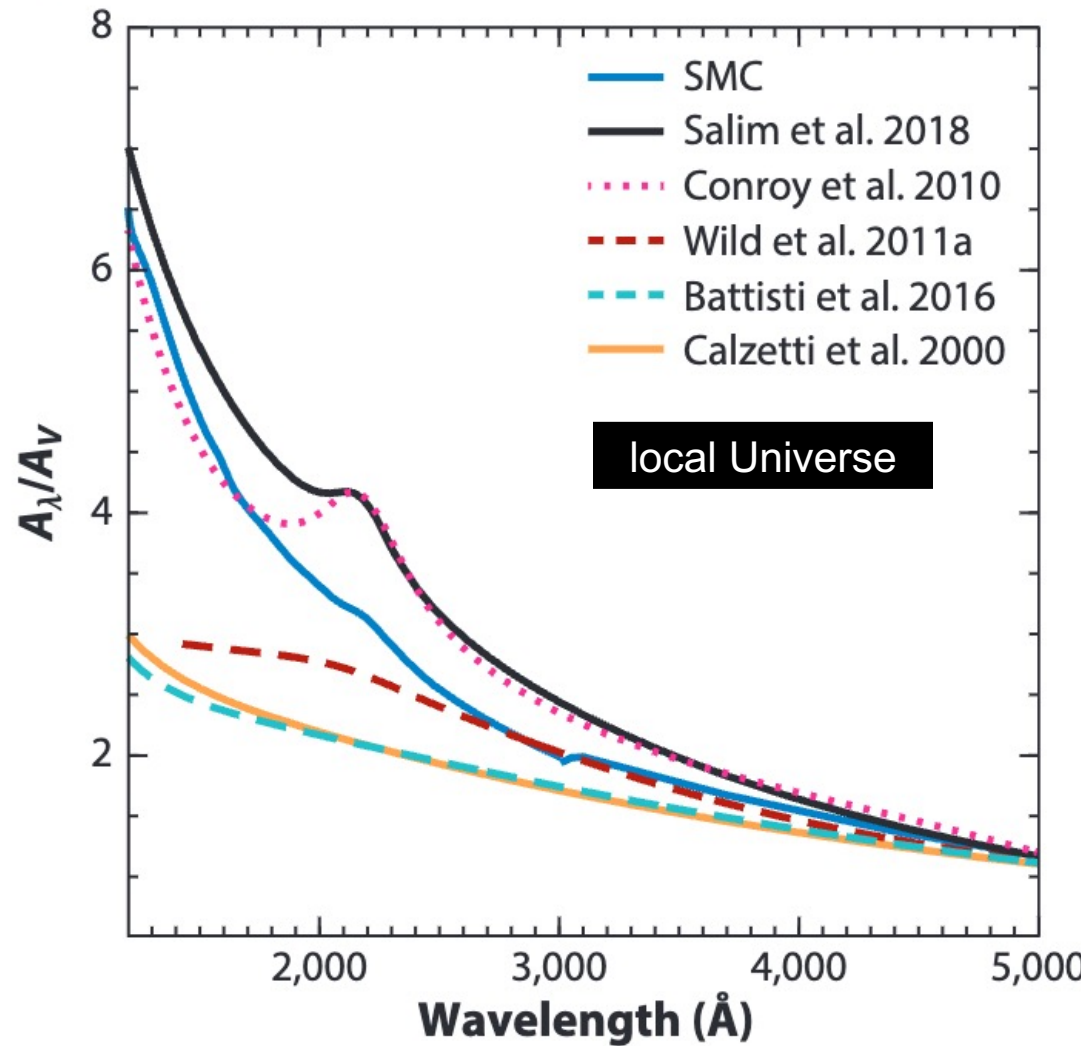
Salim & Narayanan (2020)

- Extinction: absorption and scattering out of the line of sight
- Attenuation: extinction plus scattering back into the line of sight

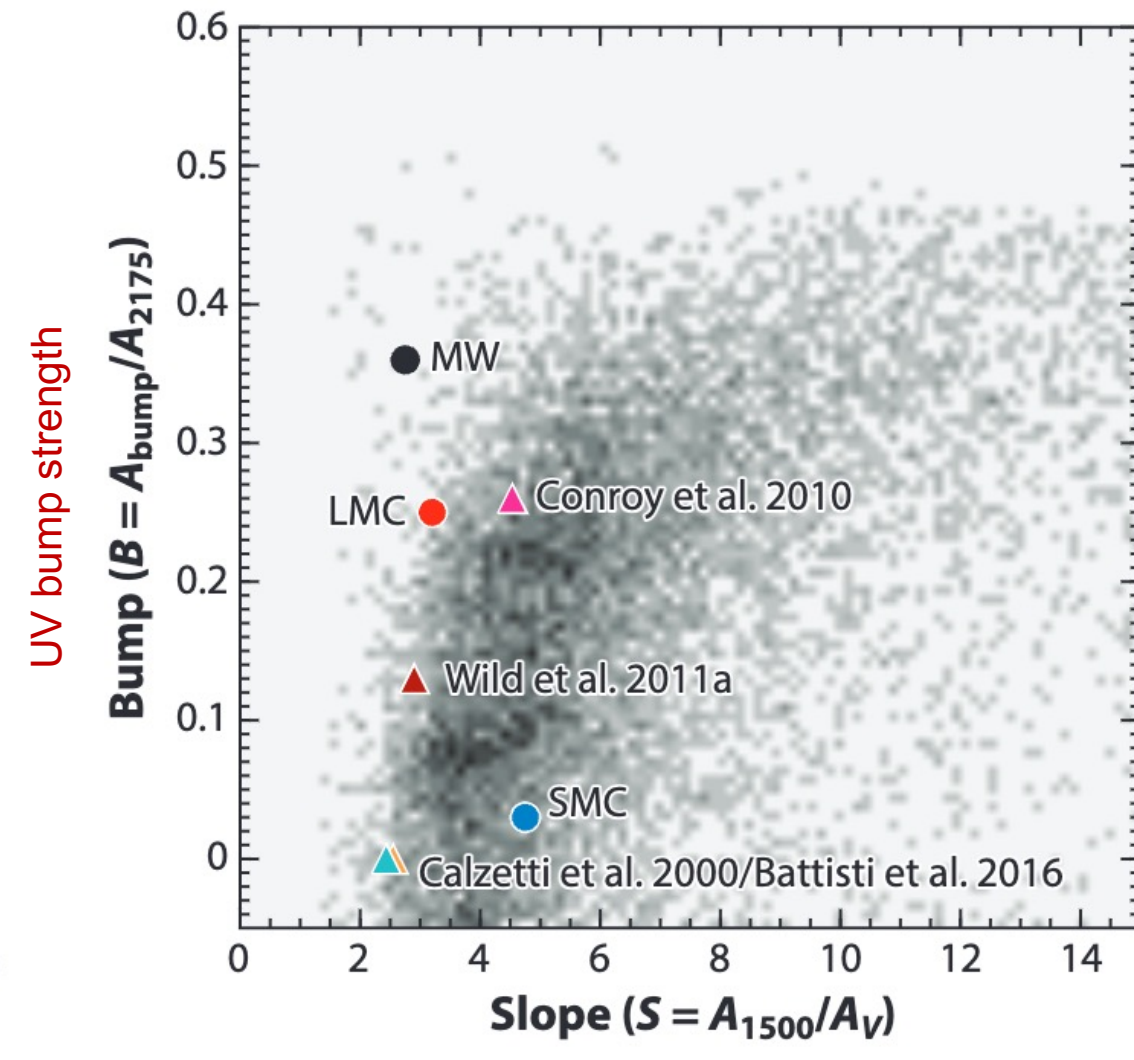
Reference attenuation curves vs.
the SMC extinction curve



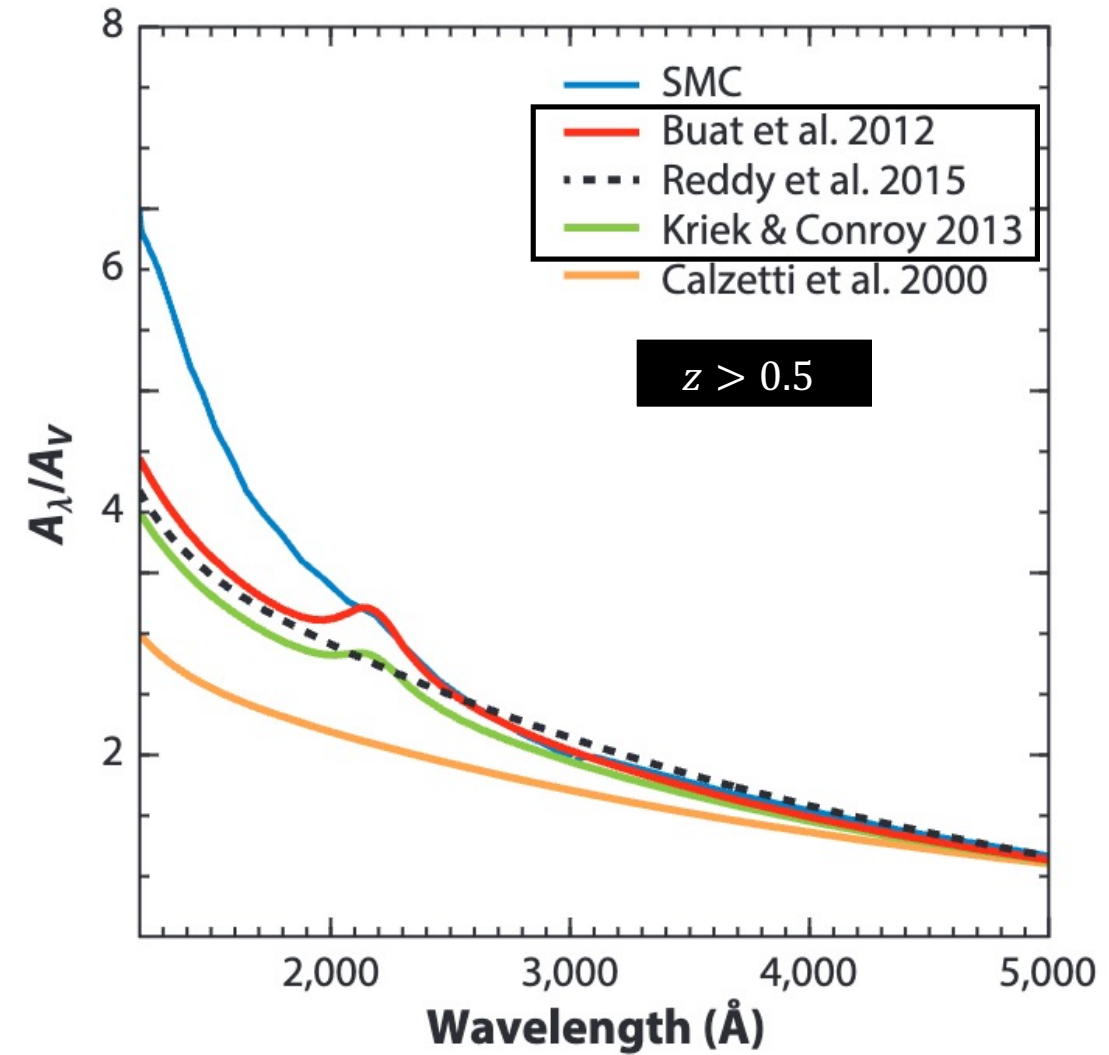
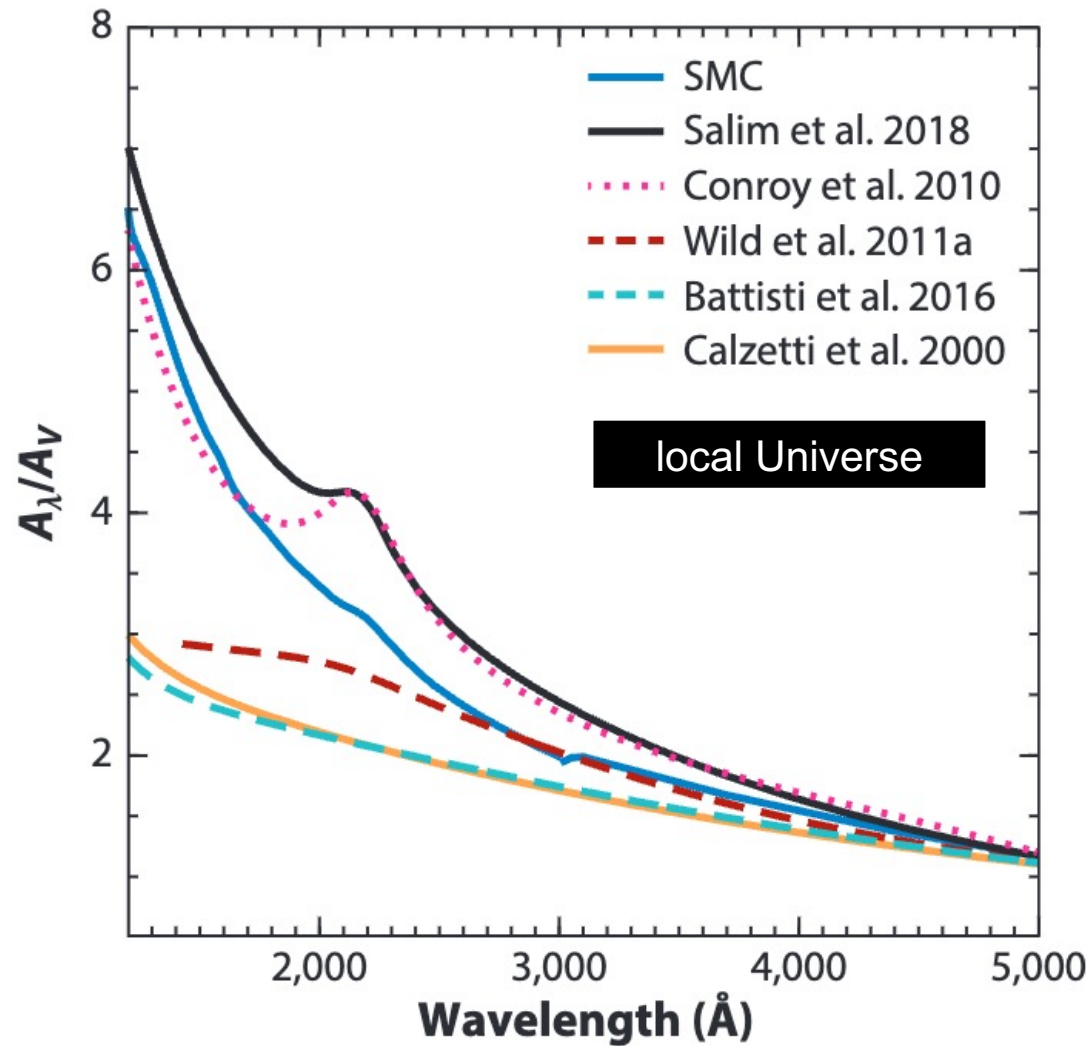
Attenuation curve variety



Salim & Narayanan (2020)

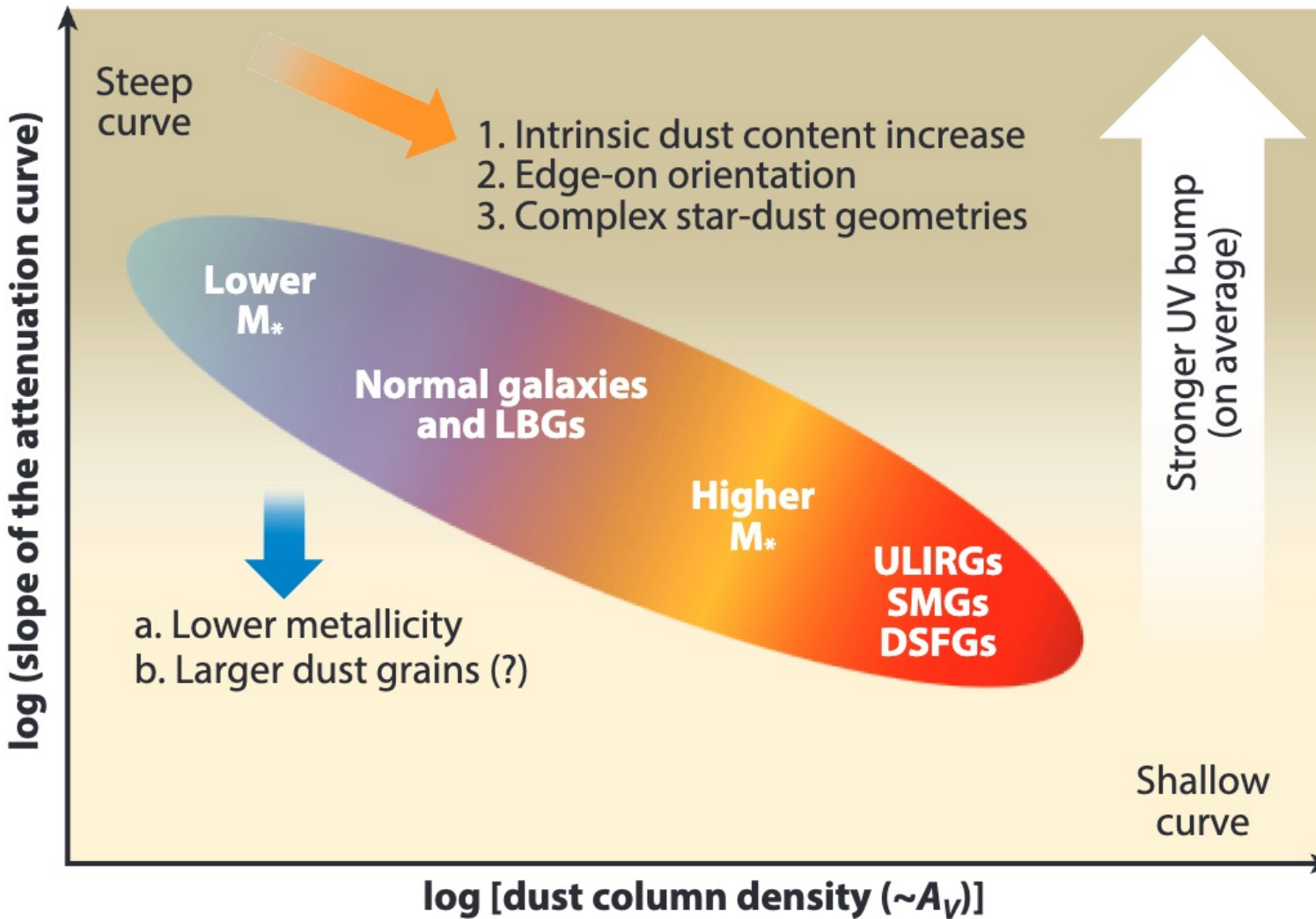


Attenuation curve variety (cont.)



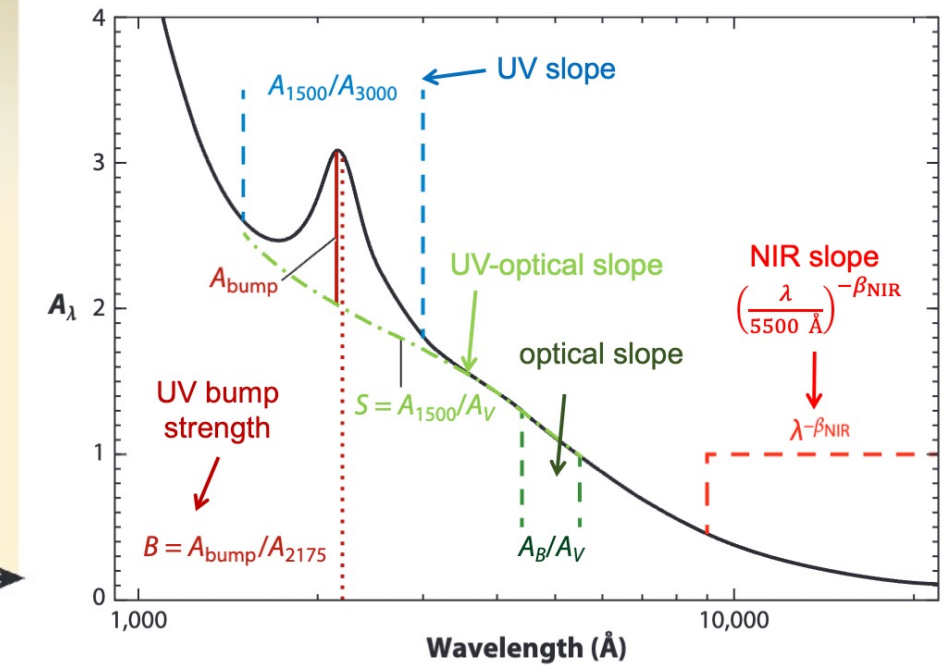
Salim & Narayanan (2020)

Behind various attenuation curves



Salim & Narayanan (2020)

LBGs: Lyman-break galaxies
ULIRGs: ultra-luminous infrared galaxies
SMGs: Submillimeter galaxies
DSFGs: dusty star-forming galaxies



Extinction and hydrogen column density

HI4PI collaboration (2016)

prev. sl.

$$\frac{A_\lambda}{A_V} = a_\lambda + \frac{b_\lambda}{R_V}$$

$$R_V = \frac{A_V}{E(B - V)}$$

Draine (2011)

$$\frac{N_H}{E(B - V)} = 5.8 \times 10^{21} \text{ cm}^{-2} \text{ mag}^{-1}$$

Güver & Özel (2009)

$$\frac{N_H / \text{cm}^{-2}}{A_V / \text{mag}} = (2.21 \pm 0.09) \times 10^{21}$$

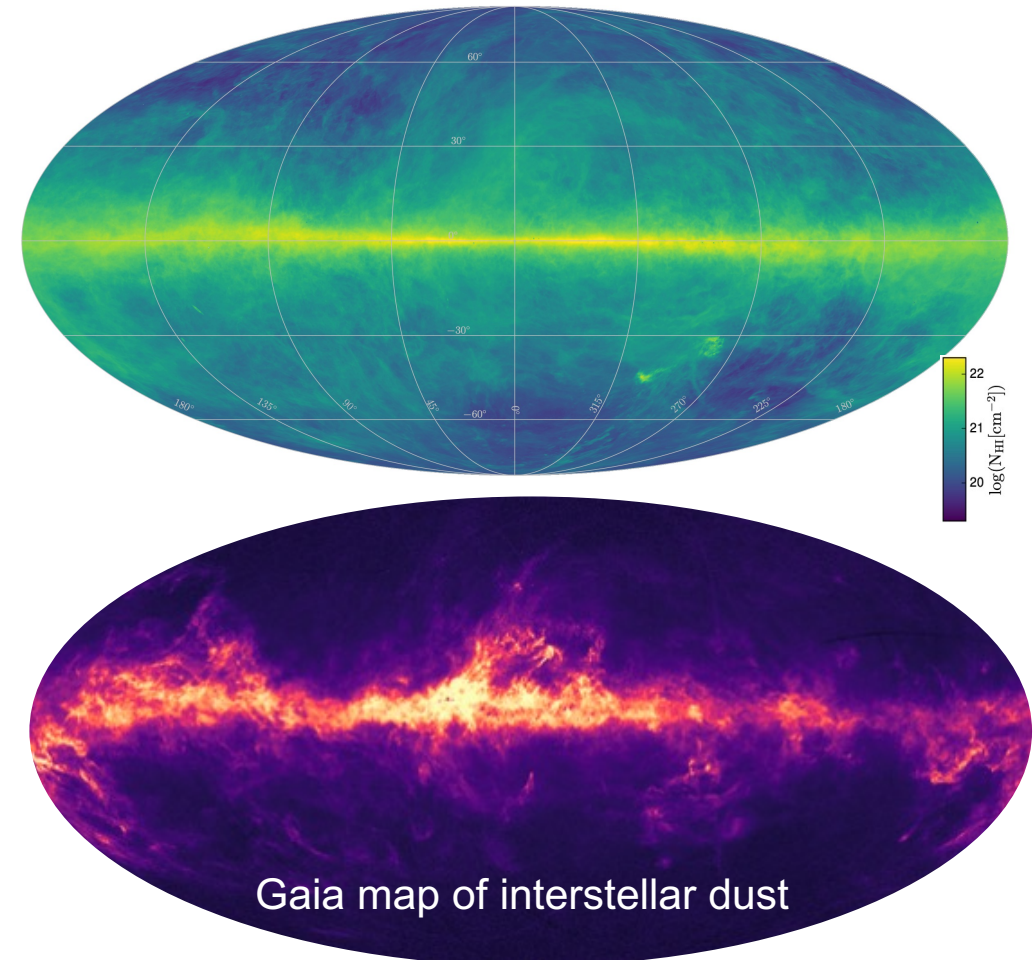


Image credit: DPAC; Gaia Coordination Unit 8; M. Fouesneau / R. Andrae / C.A.L Bailer-Jones, MPA

Getting hydrogen column density



- ## NASA's HEASARC: Tools
- NH column density

HI4PI collaboration (2016)

```
Input Equatorial coordinates:  
V404 Cyg, resolved by SIMBAD (local cache) to  
[ 306.015939°, 33.867212° ], equinox J2000  
Cone Radius: 0.1°  
  
>>>>> NH version 3  
  
>> Using map h1_nh_HI4PI.fits  
  
LII , BII 73.118972 -2.091707  
Requested position at X and Y pixel 1083.83 947.57  
Search nh in 12 X 12 box  
Each pixel is 0.083 deg 0.083 deg  
  
RA DEC Dist nh  
306.1115 33.9025 0.0868 6.32E+21  
306.0510 33.8305 0.0469 6.24E+21  
306.0314 33.9455 0.0793 6.44E+21  
305.9710 33.8735 0.0379 6.44E+21  
  
nh calculated using all points within 0.1000 deg from input position  
h1_nh_HI4PI.fits >> Average nh (cm**-2) 6.36E+21  
h1_nh_HI4PI.fits >> Weighted average nh (cm**-2) 6.36E+21
```

<https://heasarc.gsfc.nasa.gov/cgi-bin/Tools/w3nh/w3nh.pl>

nH 

Calculate the H I Column Density for a Sky Position
(Powered by [HEASoft](#))

target name(s) or coordinate(s)

Object Name or Coordinates: Use semicolons to separate multiple object names or coordinate pairs (e.g., [Cyg X-1](#) ; [101.295, -16.699](#) ; [6 45 10.8, -16 41 58](#))

Name Resolver: GRB, then SIMBAD else VizieR (Sesame), then NED

Coordinate System: Equatorial FK5

Equinox: 2000 (Only applies to Equatorial coordinates.)

Cone Radius: 0.1 degrees

Map: HI 4 Pi Survey (HI4PI, Combined 1st EBHIS and 3rd GASS Surveys)

Calculate nH **Reset**

R.A. and Dec. can be entered in ddd.ddd/[s]dd.ddd or hh mm ss.s/[s]dd mm ss.s .

References: HI4PI Collaboration, N. Ben Bekhti, L. Floer, et al., 2016, *Astronomy & Astrophysics*, 594, A116 (HI4PI Map). Kalberla et al. 2005, *Astronomy & Astrophysics*, 440, 775 (LAB Map). Dickey & Lockman, 1990, *ARA&A*, 28, 215 (DL Map).

nH is a web version of the nh [FTOOL](#), which was developed by [Lorella Angelini](#) at the HEASARC. The web interface is maintained by [Edward J. Sabol](#) of the HEASARC.

Note: An alternative tool is available at the [Argelander-Institut für Astronomie \(Alfa\)](#). Another tool to calculate the H I and H₂ column density in a given direction is available at the [UK Swift Science Data Centre](#). (See [Willingale et al. 2013, MNRAS, 431, 394](#) for more details.)

[HEASARC Home](#) | [Observatories](#) | [Archive](#) | [Calibration](#) | [Software](#) | [Tools](#) | [Students/Teachers/Public](#)

Getting E(B-V) reddening

<https://irsa.ipac.caltech.edu/applications/DUST/>

NASA/IPAC INFRARED SCIENCE ARCHIVE

IRSA | DATA SETS | SEARCH | **TOOLS** | HELP

Tools

General

Mission Specific Tools

Montage Mosaics

Table Validation

Program Interface Instructions

Time Series Tool

Dust Extinction

Moving Object Search Tool

Sky Background Model (ENSCI)

IDL Tools

How to Contribute Data

Image Validation

Object lookup

A red arrow points to the "Dust Extinction" link.

NEW (July 2013): Newer estimates of Galactic dust extinction from Schlafly and Finkbeiner (2011) are now provided alongside those of Schlegel, Finkbeiner & Davis.

Single Location ○ **Upload Table** ○

Coordinate/Object:

Image Size: (2.0 to 10.0 deg)

Coordinate Examples: [?](#) 19h17m32s 11d58m02s Equ J2000 | 46.5377 -0.2518 gal | M 31
Default Coordinate System: Equatorial J2000

Submit

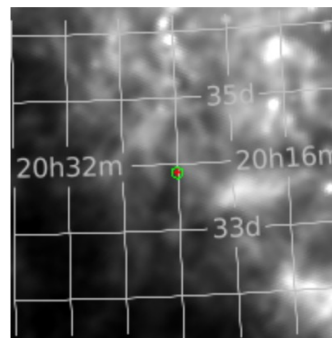
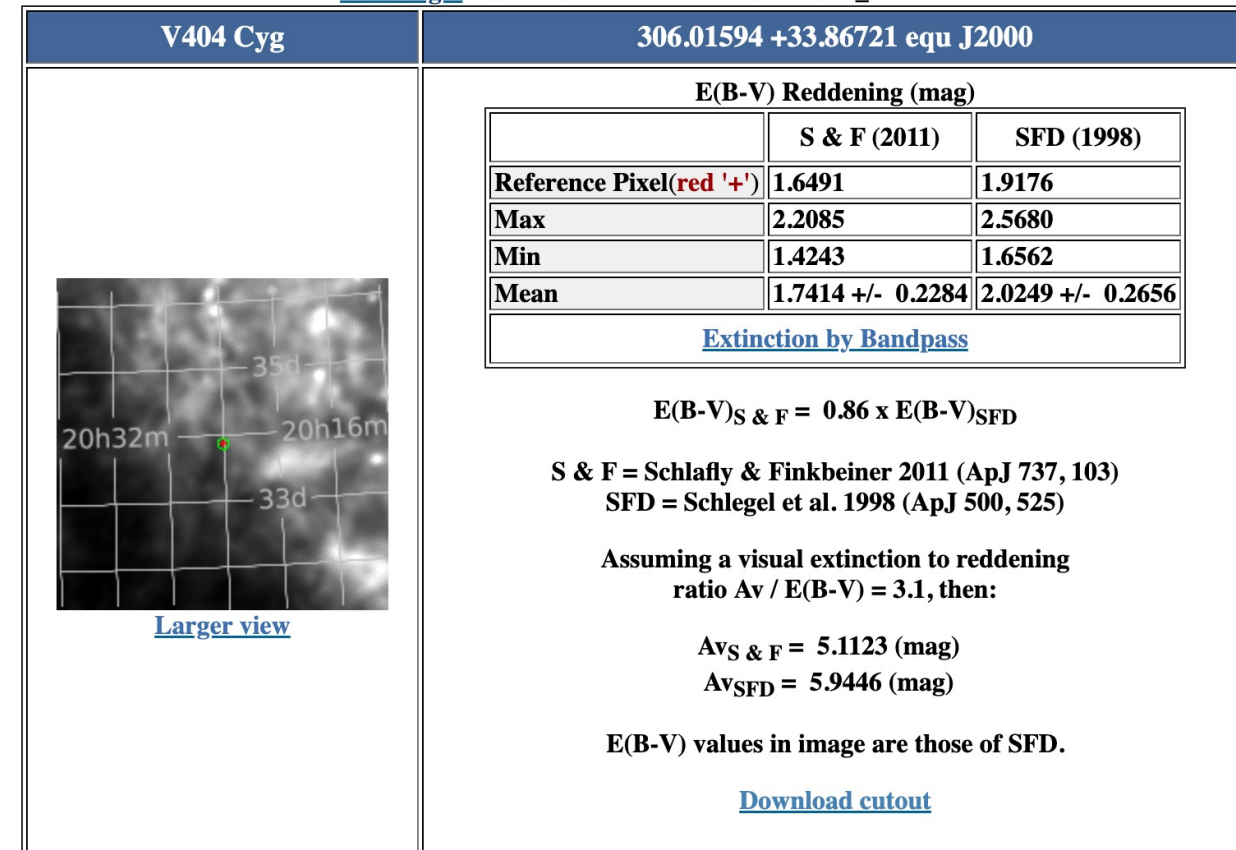
Reset

[Service Help](#)

target name(s) or coordinate(s)

Area statistics are for the 5 arcmin radius **circle** shown in green.
You may select a new location by clicking any image. [Back to Main page](#)

Data Tag: ADS/IRSA.Dust#2023/1223/231207_31984



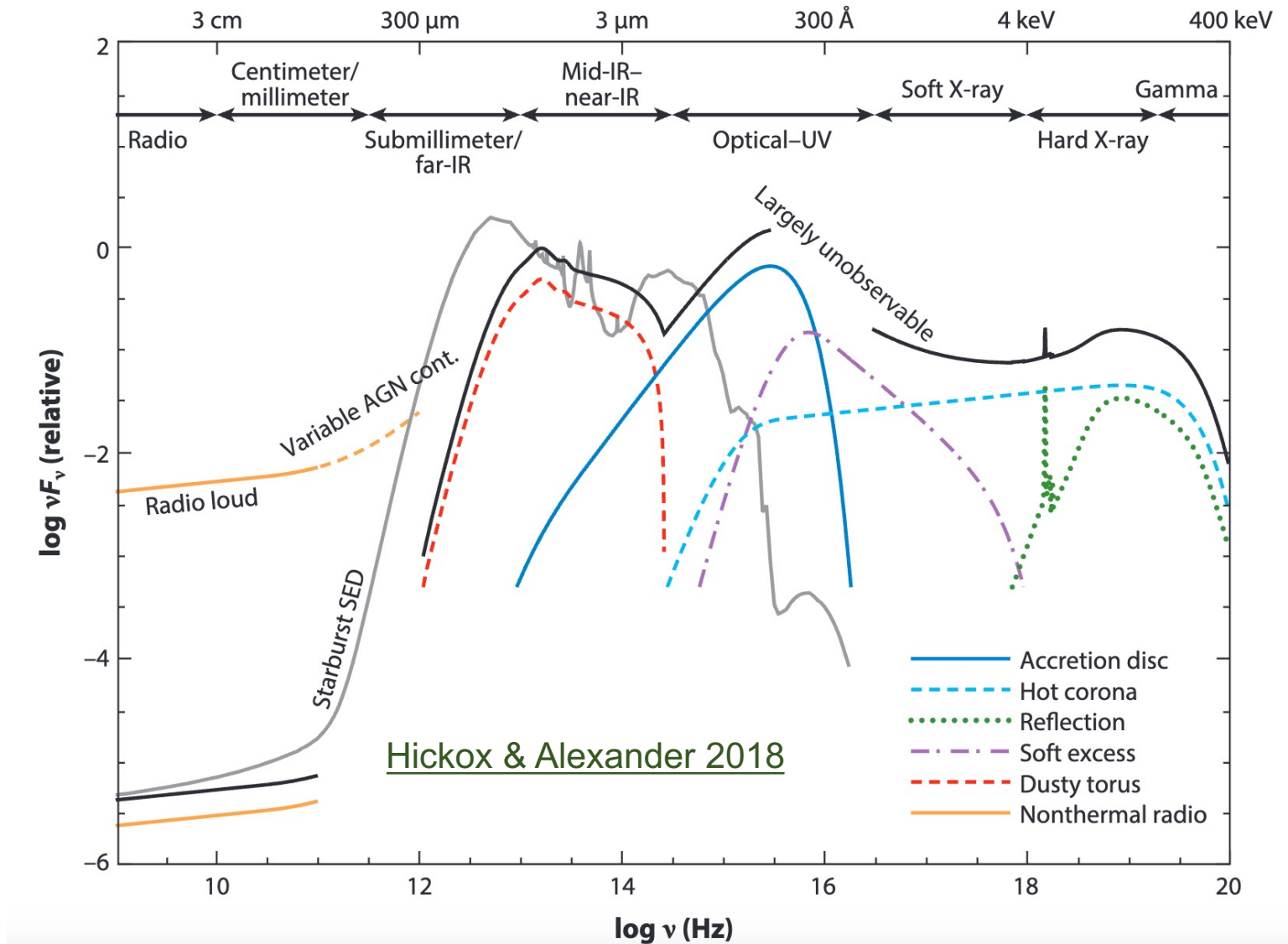
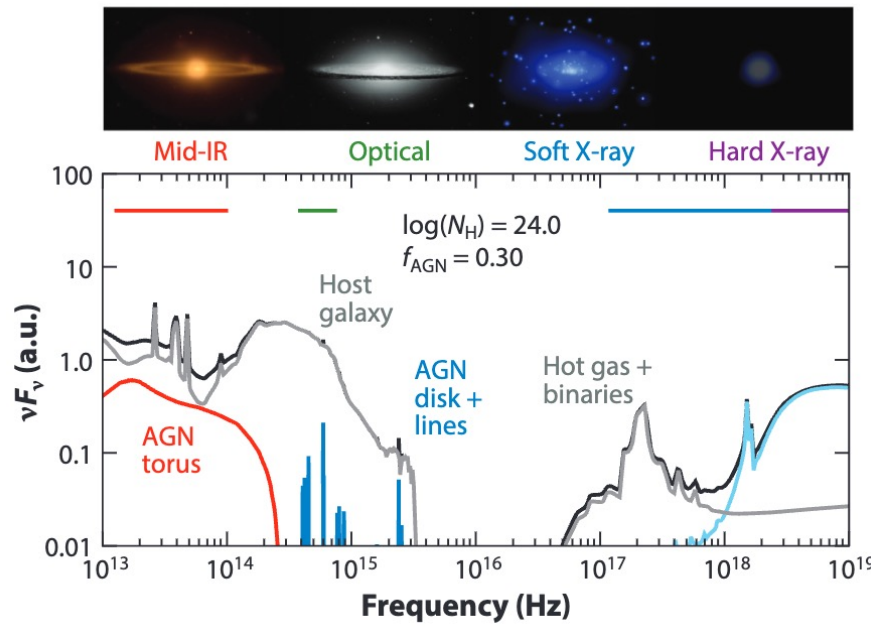
[Larger view](#)

- [Schlafly & Finkbeiner \(2011\)](#)
- [Schlegel et al. 1998](#)

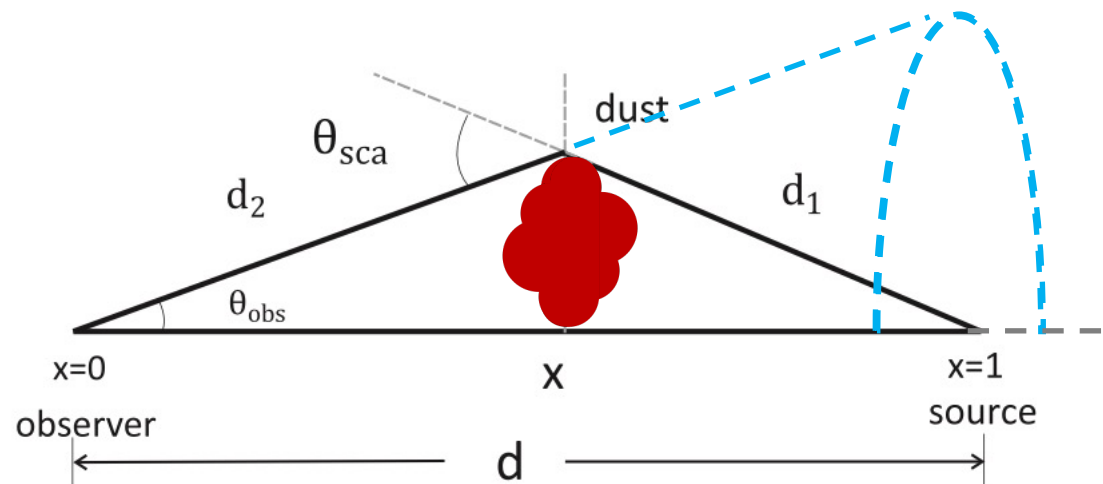
Dust IR feature (broadband)

The presence of (a large amount of) dust will greatly diminish the UV luminosity will enhance the IR luminosity.

Hickox & Alexander 2018



X-ray dust scattered ring



Background source	References (e.g.)
Gamma-Ray Burst	Vaughan et al. 2004, 2006
Anomalous X-ray Pulsar	Tiengo et al. 2010
Normal X-ray binary	Predehl et al. 2000, Smith et al. 2002
Super-Fast X-ray Transient	Mao et al. 2014

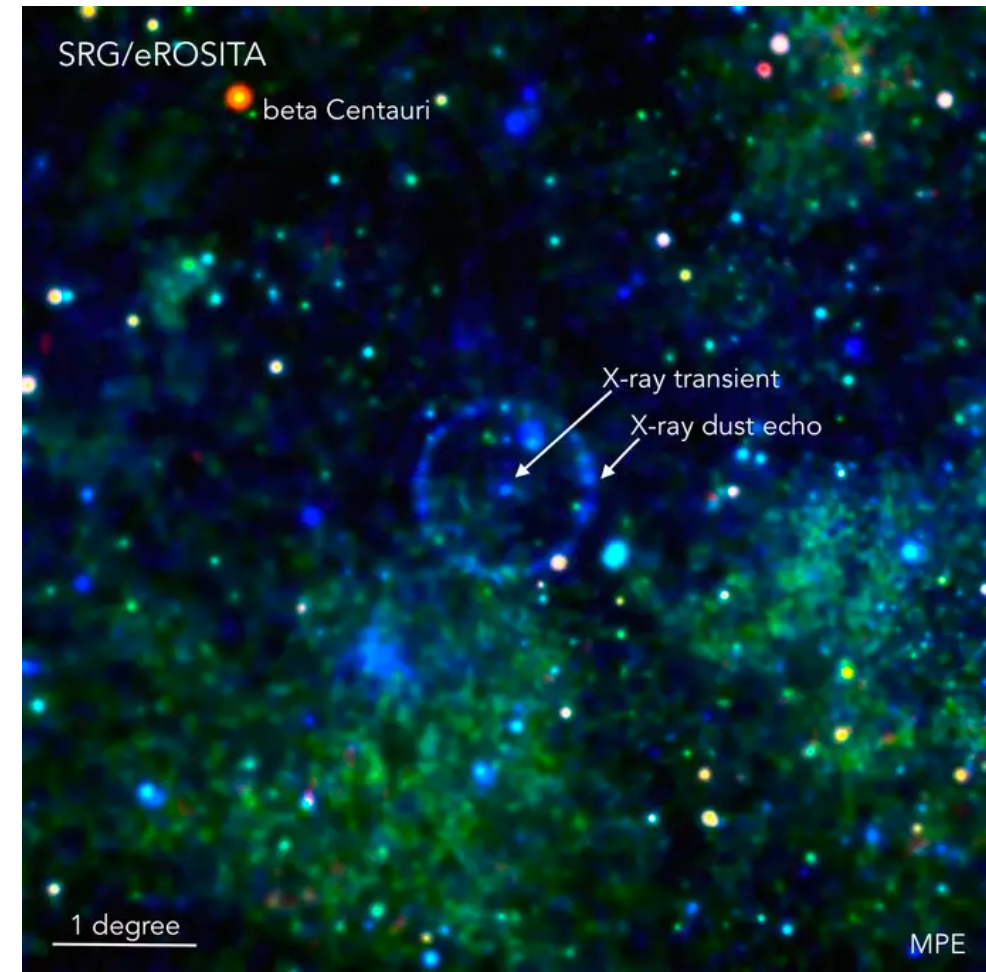


Image credit: Georg Lamer (Leibniz-Institut für Astrophysik Potsdam), Davide Mella

X-ray dust scattered (multi-)rings

Costantini & Corrales (2022)

Dust scattered rings around GRB 221009A

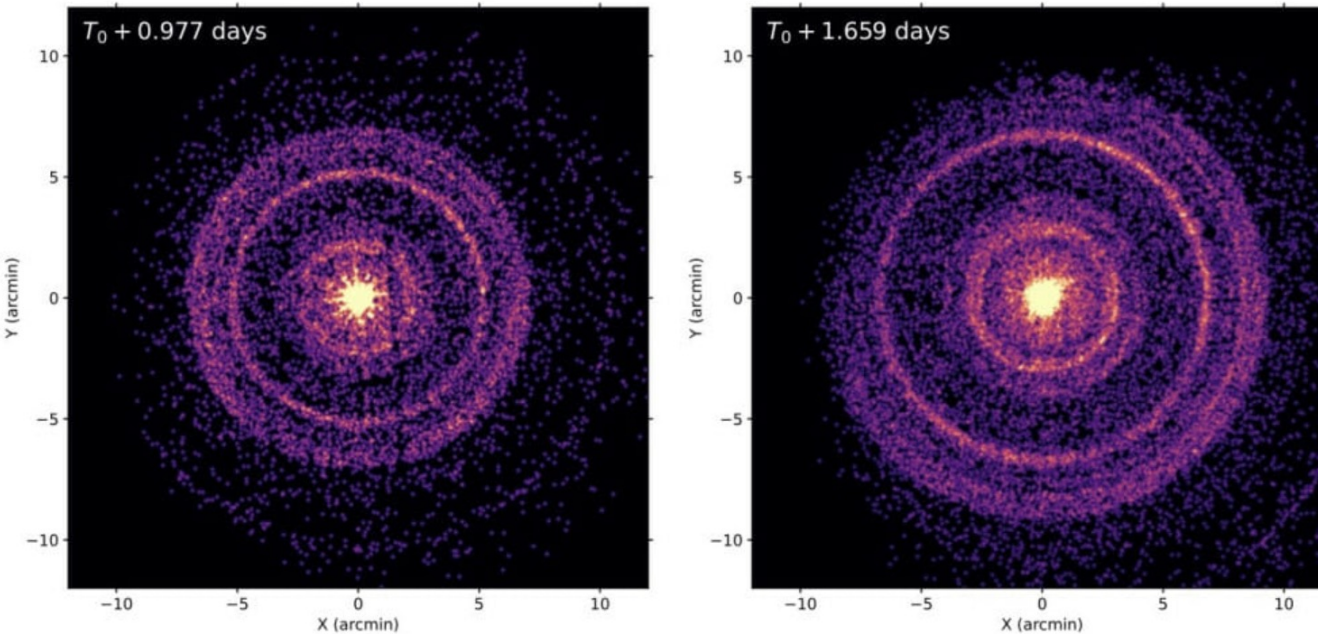
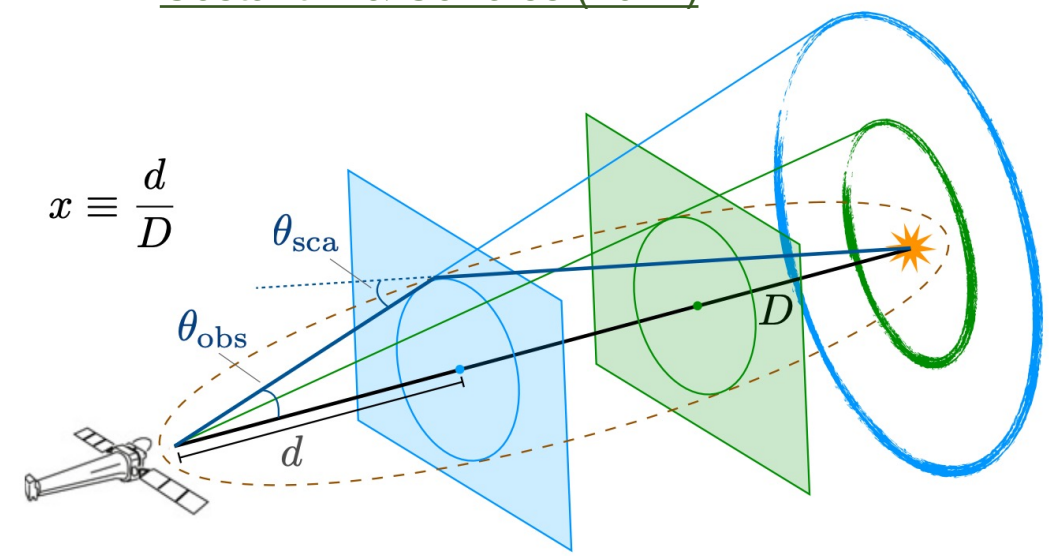
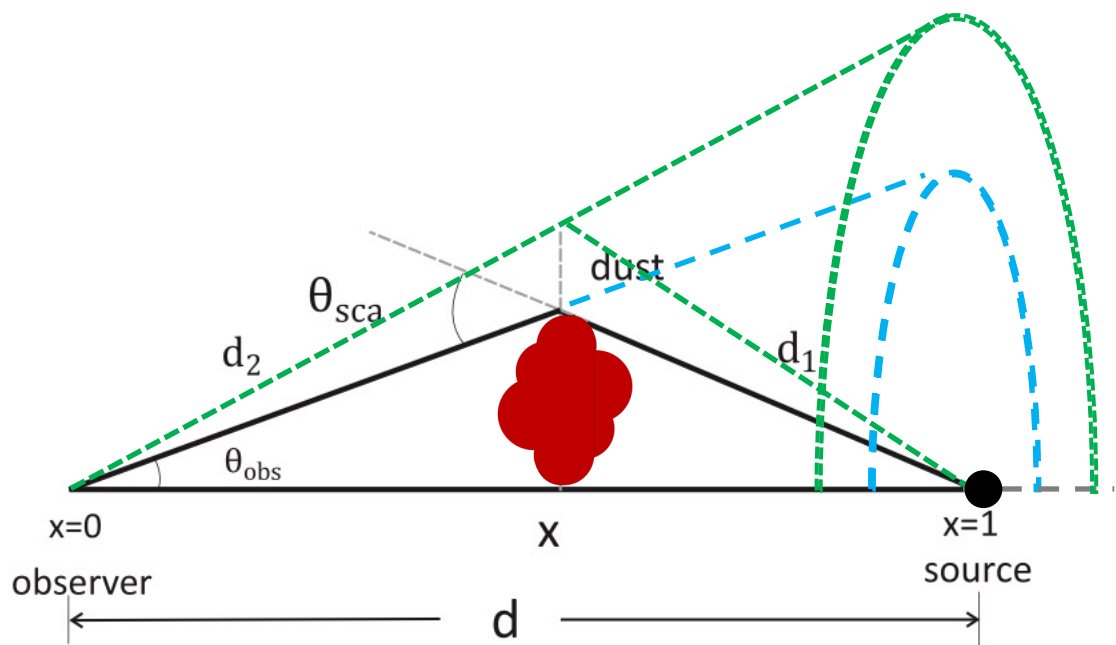


Image credit: NASA/Swift/A. Beardmore
(University of Leicester)



- near cloud: large ring
- distant cloud: small ring
- near or far with respect to the observer

X-ray dust scattered evolving ring

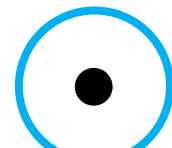


Mao et al. 2014

$$d_2 + d_1 > d$$

time delay: as time goes by, the ring increases the size

$t = t_1$



$t = t_2$

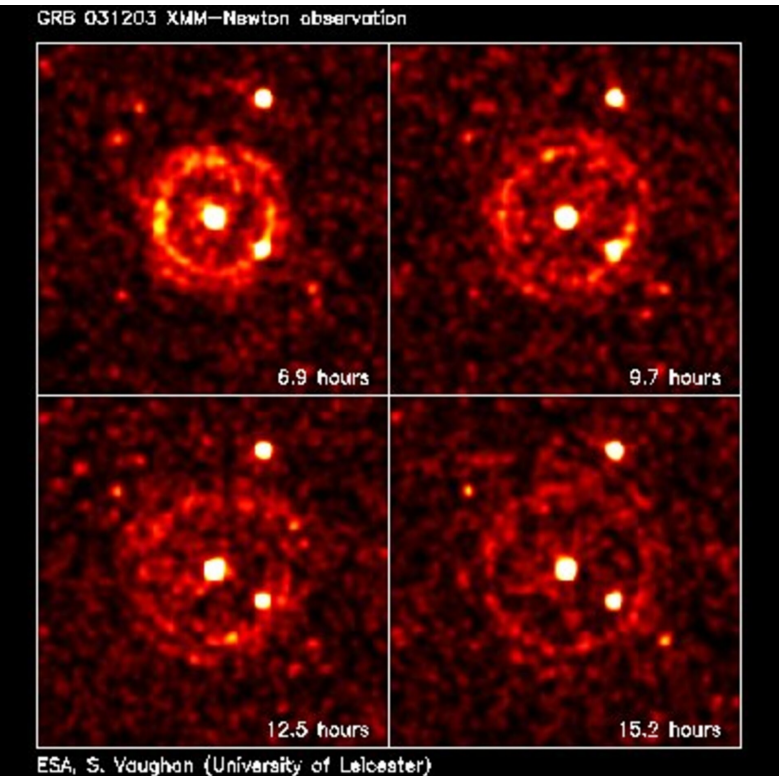
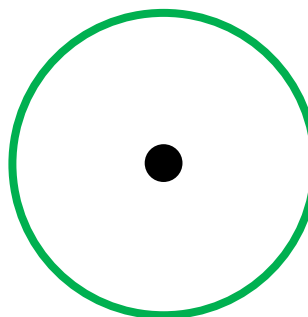
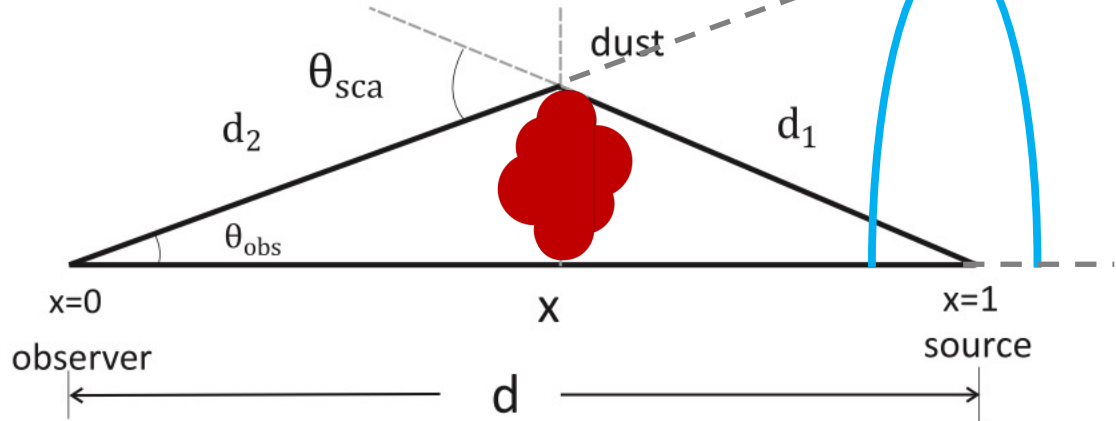


Image credit: ESA, S. Vaughan (Univ. of Leicester)

Time delay of dust scattered ring

[Heinz et al. 2016](#)

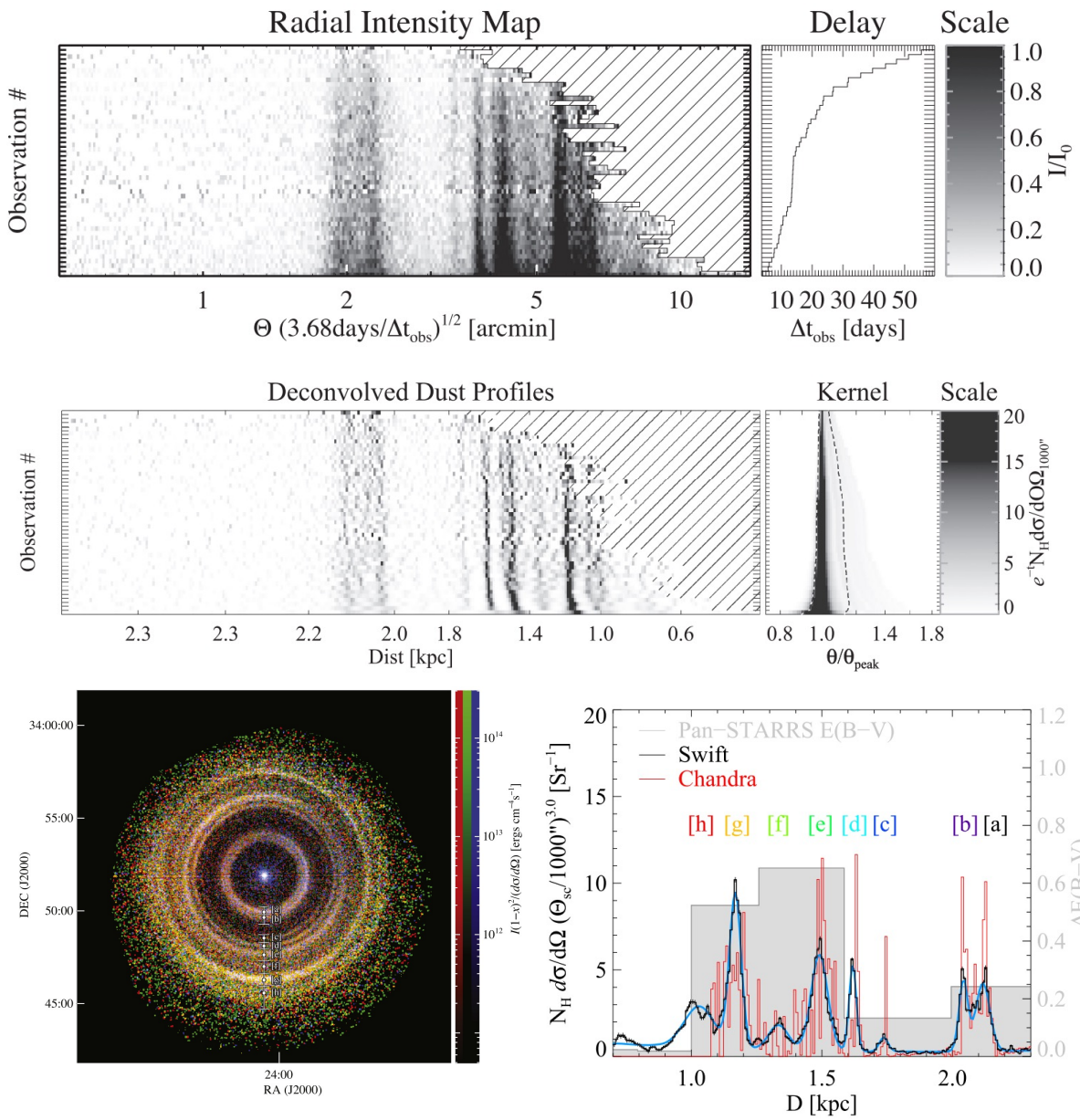
[Mao et al. 2014](#)



[Trümper & Schönfelder \(1973\)](#)

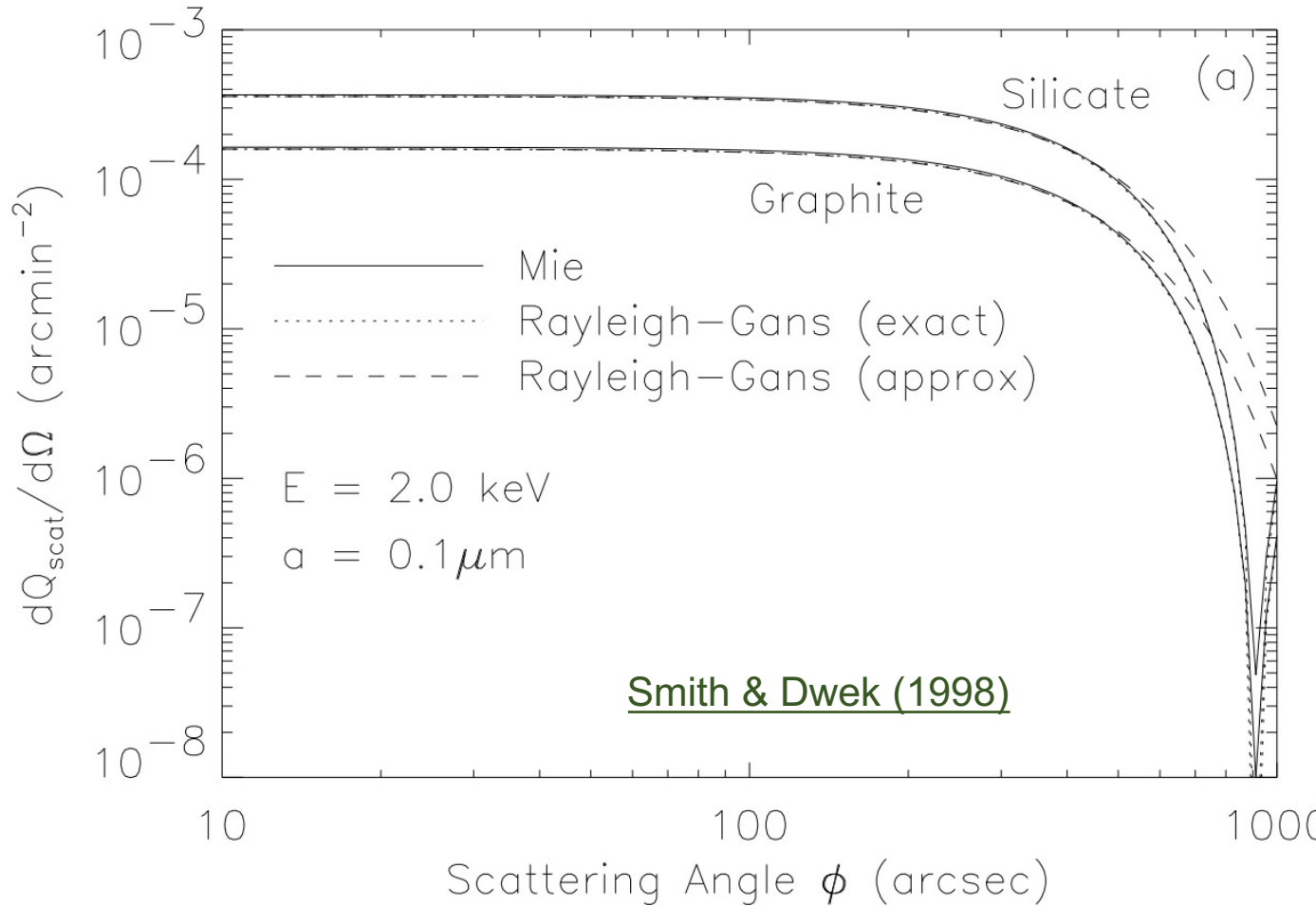
$$\frac{\Delta t}{\text{ks}} = 1.21 \times 10^{-3} \frac{x}{1-x} \left(\frac{d}{\text{kpc}} \right) \left(\frac{\theta_{\text{obs}}}{\text{arcsec}} \right)^2$$

Distance of the dusty cloud can be determined if the background source distance is known and vice versa



Small angle dust scattering

The scattering cross section depends on the scattering angle, incident photon energy, dust grain size, composition, etc.



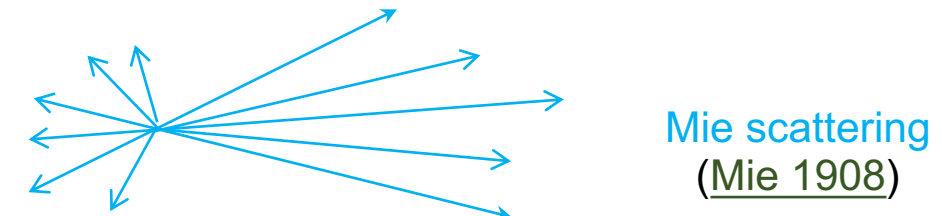
Rayleigh-Gans scattering (condition below)

dust grain size $\left(\frac{a}{\mu\text{m}}\right)$ (keV) $\left(\frac{\rho}{3 \text{ g cm}^{-3}}\right) \ll 0.316$

incident photon energy

Smith & Dwek (1998)

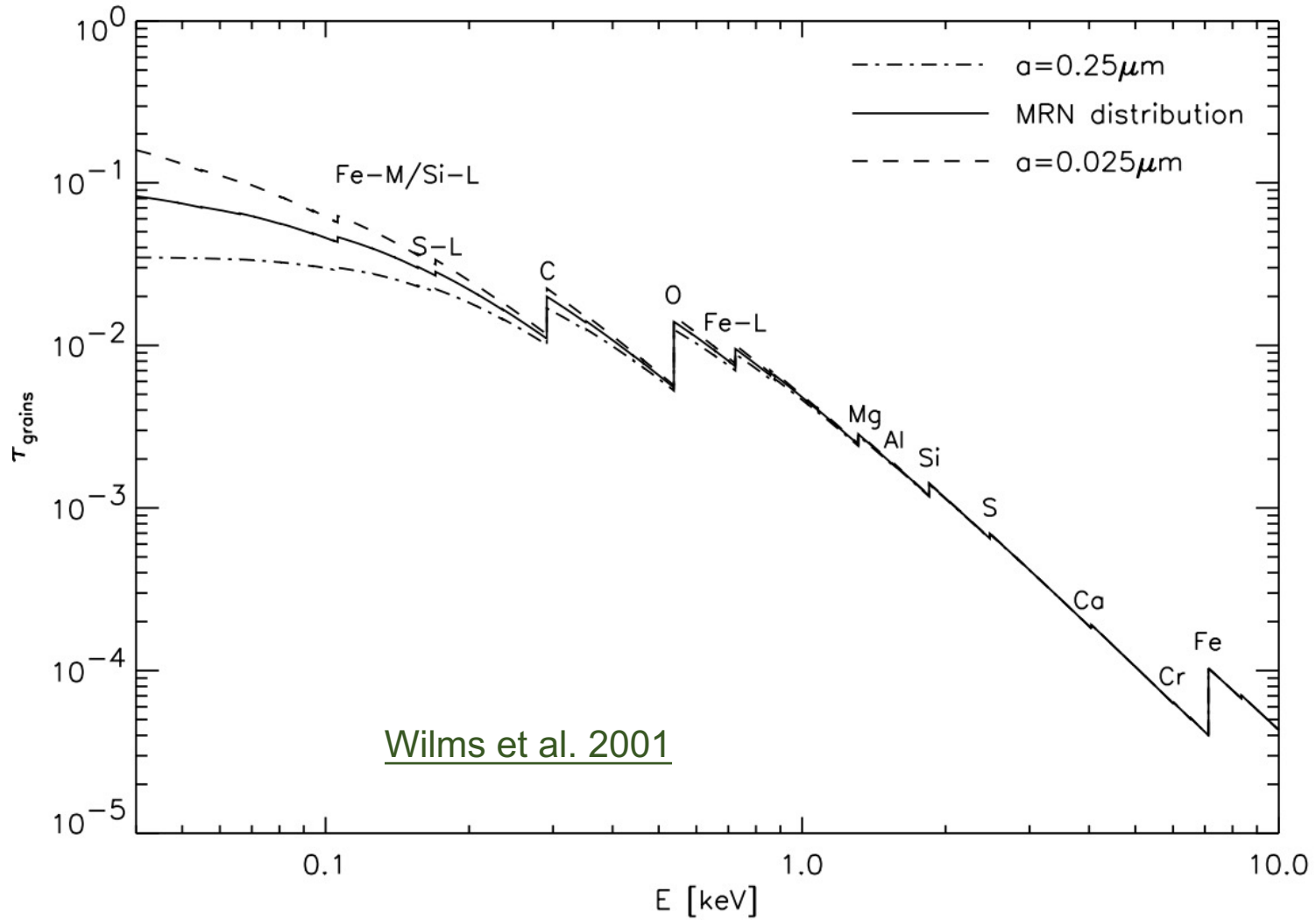
$$\left(\frac{a}{\mu\text{m}}\right) \left(\frac{\text{keV}}{E}\right) \left(\frac{\rho}{3 \text{ g cm}^{-3}}\right) \ll 0.316$$



Dust X-ray absorption edges

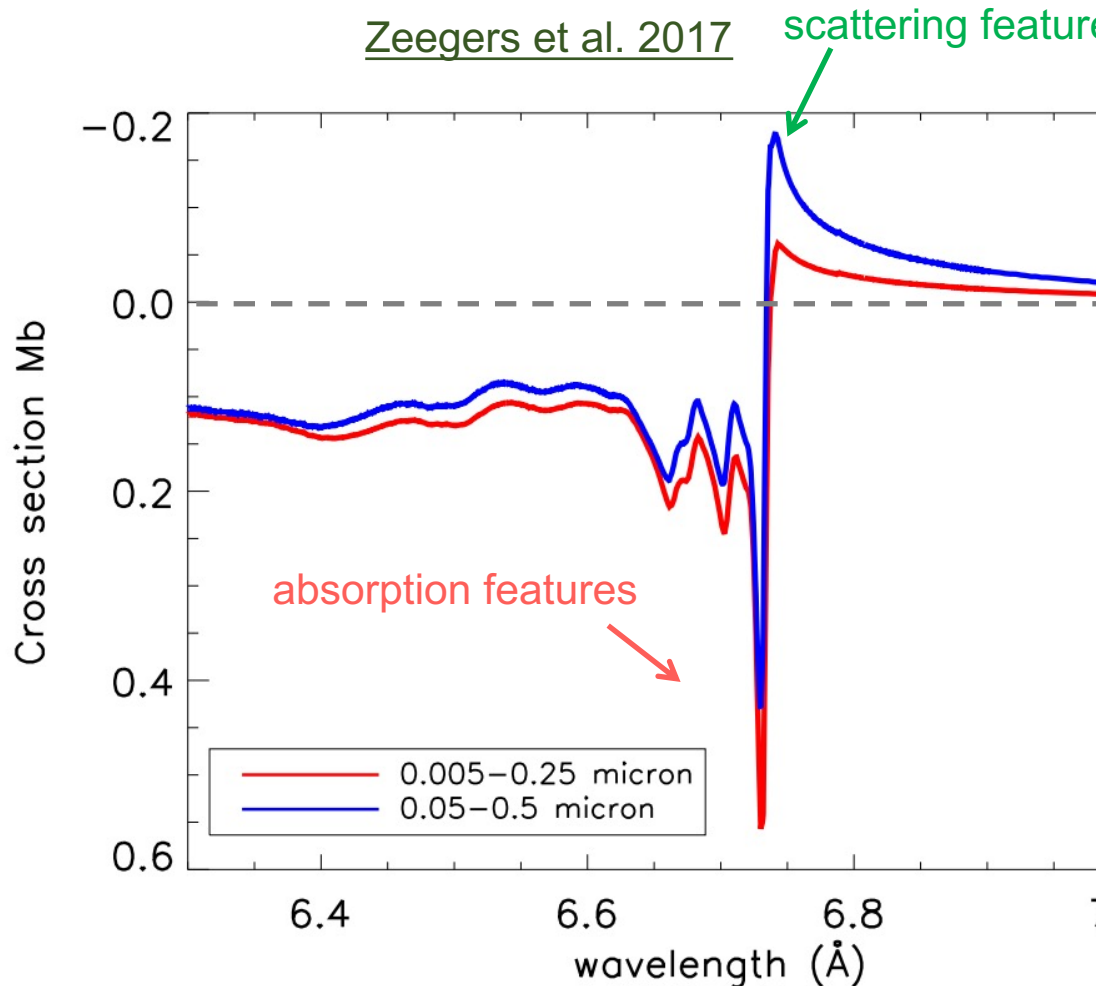
Ion	Edge	E (keV)
Fe I	3s	0.104
Si I	2p	0.106
Si I	2s	0.156
Si I	2p	0.170
Cl I	1s	0.291
O I	1s	0.543
Fe I	2s	0.857
Mg I	1s	1.311
Si I	1s	1.846
Si I	1s	2.477
Ca I	1s	4.043
Fe I	1s	7.124
Fe I	2p	7.240
Ni I	1s	8.348

Verner & Yakovlev (1995)



Dust X-ray extinction cross section

extinction = absorption + scattering



prev. sl.

Interstellar medium consists of gas and dust grains (solid-phase of material composed of metals).

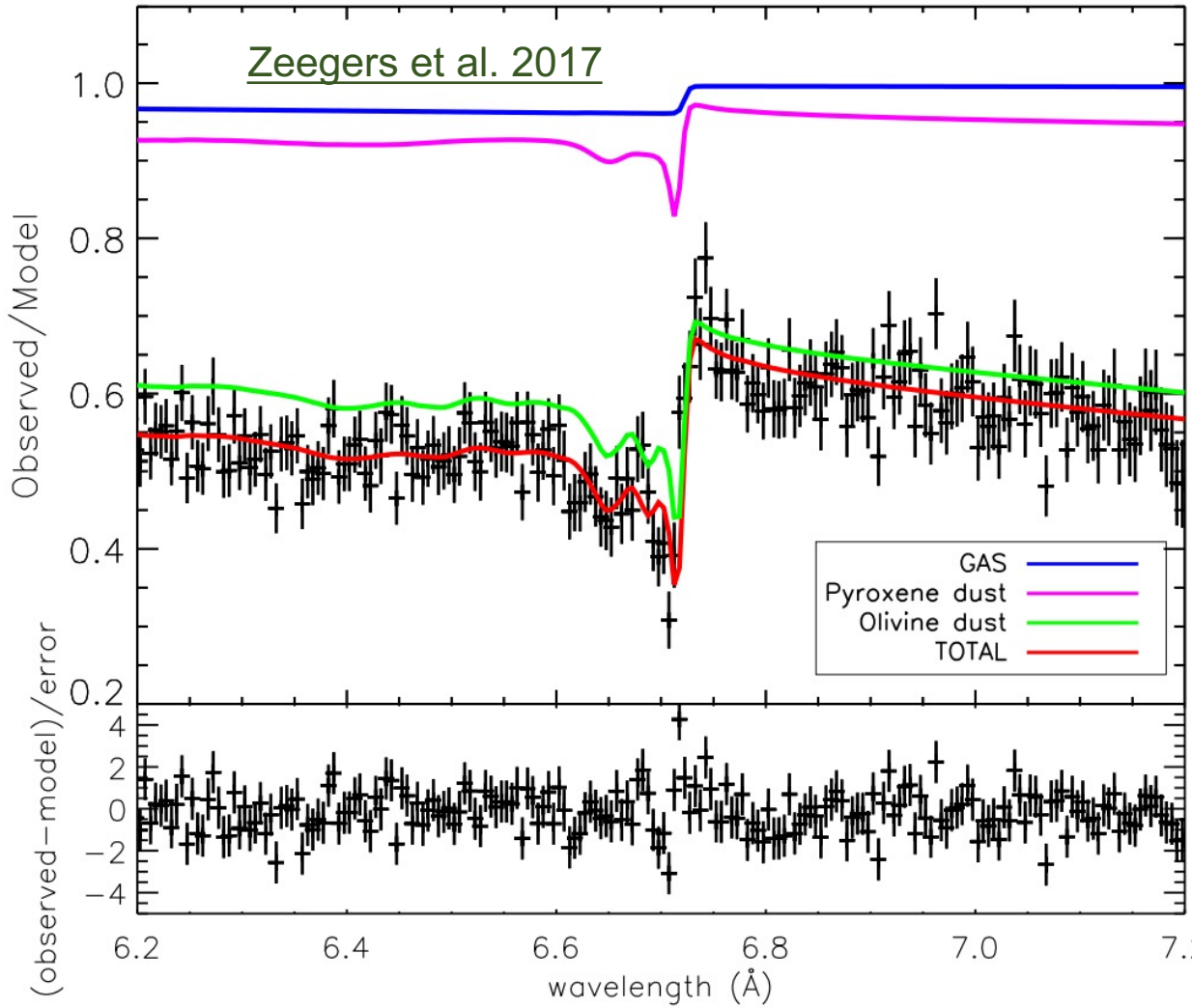
At the Si K-edge (6.7 Å), olivine dust grains following the MRN size distribution with different size range will have different extinction features

prev. sl.

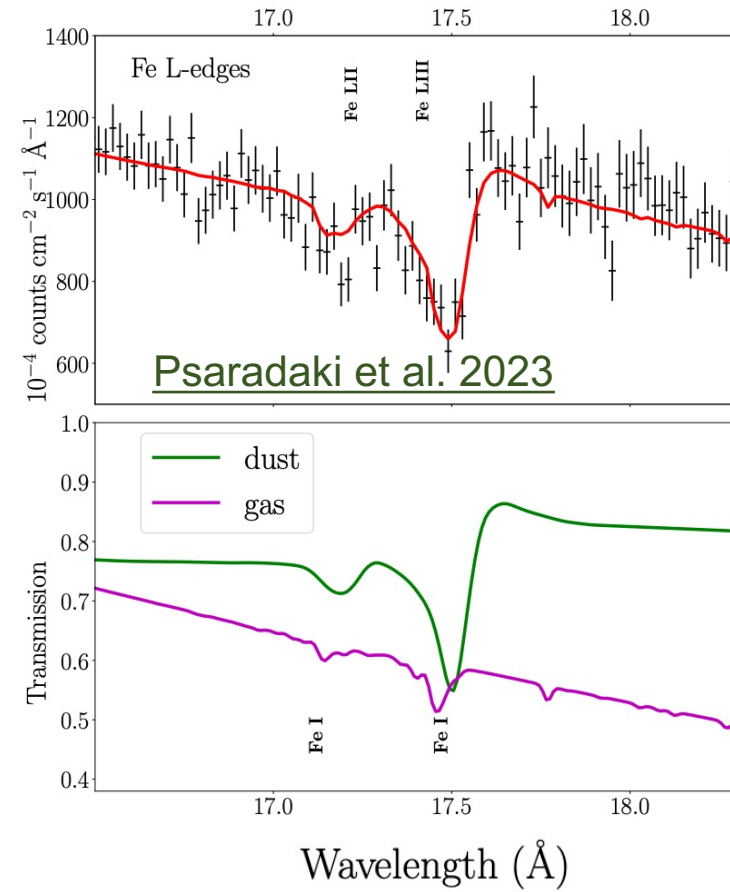
$$n(a) \propto a^{-3.5}$$

a_{\min} and a_{\max} might vary from paper to paper

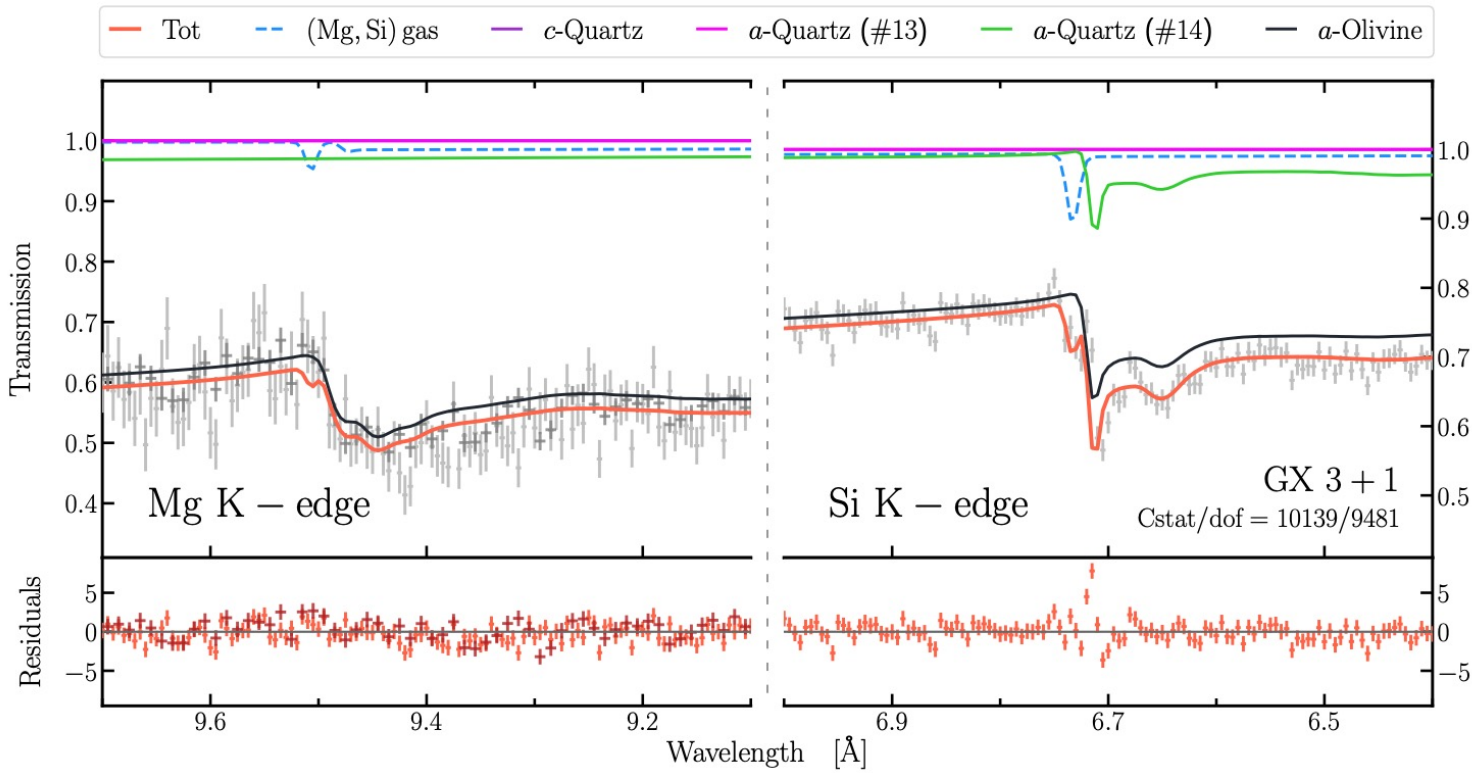
X-ray extinction effect



Name	Composition	Form
Olivine	$Mg_{1.56}Fe_{0.4}Si_{0.91}O_4$	crystalline
Pyroxene	$Mg_{0.9}Fe_{0.1}SiO_3$	crystalline
Pyroxene	$Mg_{0.9}Fe_{0.1}SiO_3$	amorphous

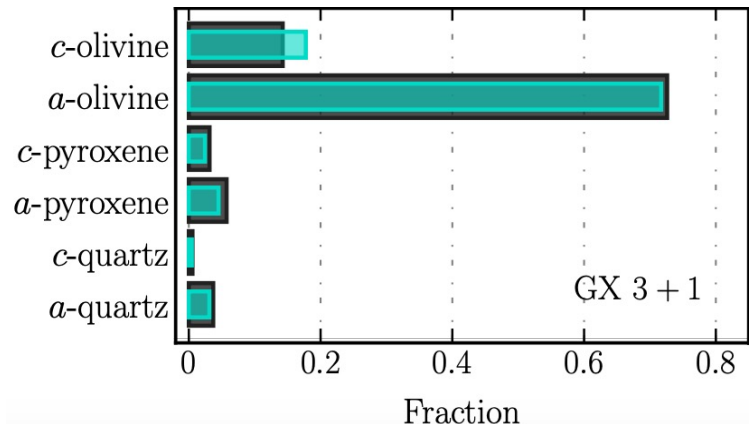


Constrain dust composition and form



Name	Composition	Form
c-Quartz	SiO_2	crystalline
a-Quartz	SiO_2	amorphous
Olivine	MgFeSiO_4	amorphous

Rogantini et al. 2020



Psaradaki et al. 2023

